Physical properties of copolymer layers

Stamouli, Amalia

PHYSICAL PROPERTIES OF COPOLYMER LAYERS

MORPHOLOGY, FORCES AND RHEOLOGY

AMALIA STAMOULI

Physical Properties of Copolymer Layers

Morphology, Forces and Rheology

Amalia Stamouli

Physical Properties of Copolymer Layers
Morphology, Forces and Rheology
A. Stamouli
Ph.D. Thesis
University of Groningen, The Netherlands
July 2000

This research was financially supported by the Dutch Organisation for Scientific Research (NWO)

Rijksuniversiteit Groningen

Physical Properties of Copolymer Layers

Morphology, Forces and Rheology

Proefschrift

ter verkrijging van het doctoraat in de
Wiskunde en Natuurwetenschappen
aan de Rijksuniversiteit Groningen
op gezag van de
Rector Magnificus, dr. D.F.J. Bosscher,
in het openbaar te verdedigen op
maandag 3 juli 2000
om 14.15 uur

door

Amalia Stamouli

geboren op 10 Augustus 1972
te Johannesburg

Promotor: Prof. dr. G. Hadziioannou

Beoordelingscommissie: Prof. dr. Ch. Toprakcioglu
Prof. dr. U. Steiner
Prof. dr. G. ten Brinke

ISBN-nummer: 90-367-1274-2

ACKNOWLEDGEMENTS

For this thesis I owe a lot to many people who gave their advice, time, encouragement or simply helping in making a pleasant environment to work in. I would like to express my sincere thanks to:

My supervisor, Professor Georges Hadziioannou, for offering me a Ph.D. position in his research group and making this work possible. Furthermore, for giving me the freedom to choose the direction of research.

The members of my reading committee, Professor Gerrit ten Brinke, Professor Ullrich Steiner and Professor Chris Toprakcioglu for carefully reading the manuscript and their insightful comments.

Dr. Paul van Hutten for carefully reading and correcting the manuscript and papers and for his helpful suggestions.

Gerald for teaching me how to use the Surface Forces Apparatus. Eric for his contribution in chapter 5 and sub chapter 3.II. Elena not only for very useful scientific discussions and the theoretical contributions in sub chapters 3.I and 3.III but also for reading parts of my thesis. Ute for assisting with the AFM force measurements in chapter 4. Christine and Lionel for their contribution in the new SFA. Mettler Toledo BV for proving their force sensor. The AFM team, Eric, Vasilis and Michiel. Our secretaries, Betty and Hilda. Nanno, Bert, Wieger, and Lucas from the electronic and mechanic workshops of the University, for proving me with the necessary electronics and mechanical constructions, for the SFA. Sjouke Kuindersman for assistance with the literature research.

Finally, the members of the research group: Victor, Vagelis, Richard, Diny, Geert, Valerie, Ulf, Henk, Bert, Sjoerd, Marten. I hope I did not forget anyone.

My friends that have supported me through all these years during my stay in Groningen: Giannis, Deanna, Stephania, Giannis, Vasilis, Vagelis, Makis, Tzenh. My friends in Greece.

My family, for their continuous support and encouragement. And finally, Hendrik-Jan not only for his scientific but also for his emotional help and of course Cassandra.

Amalia
April 2000

CONTENTS

CHAPTER 1

INTRODUCTION

Adsorbed polymer layers have important applications in different areas of technology such as steric stabilization of colloid particles suspended in solution[1], coatings, chromatography, biocompatibility of artificial organs[2], adhesion[3] lubrication and friction. Therefore, many experimental and theoretical studies have been devoted to the adsorption of various types of polymers at the solid–liquid interface.

A specific class in the field of polymers able to modify surfaces is *diblock copolymers*. The formation of a polymer monolayer is due to the amphiphilic nature of block copolymers. In selective solvents one block of the copolymer is well solvated and the other block is precipitated, forming unimers. At a concentration above the critical micelle concentration (cmc) the copolymers tend to self–assemble to form spherical polymolecular micelles (figure 1.1a). For a solution with a polymer concentration below the cmc the precipitated block can adsorb on a substrate, with the solvated block freely protruding into the solution without adsorption, forming an end–grafted polymer layer (figure 1.1b).

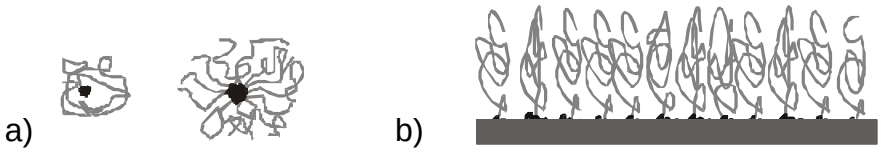

Figure 1.1: a) *Schematic representation of a diblock copolymer unimer and micelle;* b) *Model for the adsorption of diblock copolymers on a surface.*

From technological point of view the understanding of the normal and lateral interactions between end–grafted polymer layers is of major importance. The experimental method used for the study of the normal and lateral interactions between end–grafted polymer layers is the Surface Forces Apparatus (SFA) (figure 1.2a). The SFA is capable of measuring the normal forces between two surfaces as a function of the distance between them. Lateral forces can be measured using a modified SFA —adapted to operate as a rheometer at the near–molecular level. Although the normal forces have been extensively studied[4], measurements of the lateral forces between such layers are limited in number[5].

Since the relevant physical parameters (forces and rheological properties) depend strongly on the structure of these layers, the structure of end–grafted polymer layers normal to the surface has been studied extensively (density profile, monolayer thickness, etc.)[4, 6]. However, experimental measurements to determine the lateral structural properties of such layers are still lacking. With the invention of the Atomic Force

Microscopy (AFM) technique the structural properties of end–grafted polymer layers could be visualized. This technique is based on measuring the interacting forces between a sharp tip and a surface; proving information over the normal forces (figure 1.2b). Due to feedback systems the morphology of samples can be acquired.

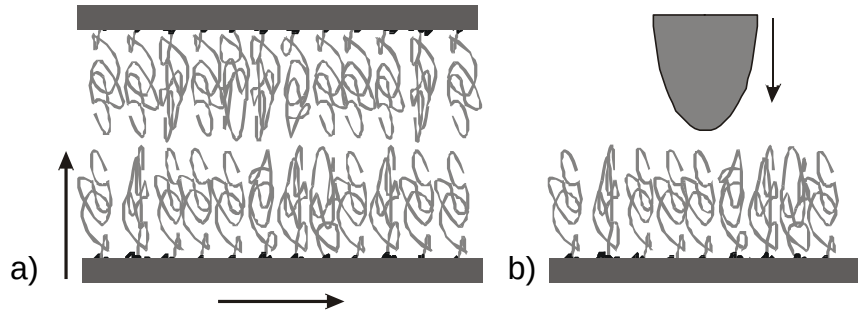

Figure 1.2: a) *Model for the determination of the normal and lateral interactions between two opposite layers with SFA;* b) *Model for the determination of the normal interactions between a tip and a layer with AFM.*

The aim of this thesis work was to get a better understanding of the normal and lateral interactions of adsorbed diblock copolymer monolayers in the presence of solvent at the near–molecular level. To attain this goal two different projects were pursued.

The first dealt with the construction of a novel Dynamic Feedback Surface Forces Apparatus, so that normal and lateral forces could be measured in real–time via a feedback system.

The second dealt with the utilization of the Atomic Force Microscopy technique. The AFM was utilized in order to *i)* measure the normal forces in the sub-nanometer regime and compare them with the data obtained from the SFA; *ii)* elaborate the structural properties of the adsorbed layers [influence of solvent quality and time] and *iii)* determine the adsorption properties of adsorbed diblock copolymer on a surface from a selective solvent [kinetics of adsorption and adsorption mechanisms].

Although, our primary intention was to study in more detail the lateral interactions between adsorbed diblock copolymer layers, due to difficulties encountered during its development/construction the largest part of this thesis is concentrated with the investigation of the structure of such systems.

This thesis has been organized as follows:

Chapter 2 presents briefly the experimental techniques used in this study: the Atomic Force Microscopy and the Surface Forces Apparatus. In addition the description of most successful feedback SFA is presented. This system is capable of measuring the normal forces, via a feedback system. The first attractive and repulsive force profiles are shown.

In *chapter 3*, the morphological evolution of adsorbed diblock copolymer monolayers is investigated with AFM as a function of solvent quality, adsorption time, nature of the substrate and polymer concentration. As it will be shown the structure of adsorbed diblock copolymer monolayers depends strongly on the presence of micelles in the solution. Therefor the first sub chapter is devoted to their visualization.

In *chapter 4*, the interaction between the adsorbed diblock copolymer monolayer and an AFM tip under various solvent conditions is shown. The results are discussed in terms of the structure of the adsorbed monolayer. Depending on the solvent quality different responses are obtained.

Chapter 5 discusses the process of shearing between adsorbed monolayers. A modified SFA to operate as a rheometer is presented. The complex shear modulus is measured and related via a model to the structure of the confined adsorbed monolayers.

REFERENCES

[1] Napper, D. *Polymeric Stabilization of Colloidal Dispersions*; Academic: London, **1983**

[2] Ruckenstein, E.; Chang, D.B. *J. Colloid Interface Sci*. **1988**, 123, 170

[3] Lee, L.H. *Adhesion and Adsorption of polymers*; Plenum Press: New York, **1980**

[4] see for example:

a) Belder, G. *Surface forces and nanorheological properties of adsorbed polymer monolayers* Ph.D. thesis, University of Groningen **1995**

b) Field, J.B.; Toprakcioglu, C.; Dai, L.; Hadziioannou, G.; Smith, G.; Hamilton W. *J. Phys. II France* **1992**, 2, 2221

c) Hadziioannou, G.; Patel, S.; Granick, S.; Tirrell, M. *J. Am. Chem. Soc.* **1986**, 108, 2869

[5] a) Pelletier, E.; Belder, G.F.; Subbotin, A.; Hadziioannou, G. *J. Phys. II (France)* **1997**, 7, 271

b) Cai, L.L. *"Nanorheoloy of polymer brushes"* Ph.D. thesis University of Illinois **1997**

c) Klein, J. *Colloids and Surfaces A* **1994**, 86, 63 d) Klein, J.; Kumacheva, E.; Mahalu, D.; Perahia, D.; Fetters. L.J. *Nature* **1994**, 370, 634

[6] a) Cosgrove, T. *J. Chem.Soc., Faraday Trans. I* **1990**, 86, 1323

b) Webber, R.M.; Anderson, J.L.; Jhon, M.S. *Macromolecules* **1990**, 23, 1026

c) Webber, R.M.; van der Linden, C.C; Anderson, J.A. *Langmuir* **1996**, 12, 1040

CHAPTER 2

EXPERIMENTAL TECHNIQUES AND DESCRIPTON OF A NEW FEEDBACK SURFACE FORCES APPARATUS

ABSTRACT

In this chapter the apparatuses used to investigate the subjects of this thesis will be reviewed: The Atomic Force Microscope (AFM) and the Surface Forces Apparatus (SFA). A brief description of the principle of operation of AFM is given, with emphasis on the modes of operation employed in the next chapters. The principle of operation of the classical SFA is reviewed, in order to primarily explain the necessity of a novel feedback SFA. The principle of operation, performance and first test experiments of the new SFA are presented.

2.1 ATOMIC FORCE MICROSCOPE (AFM)

The introduction of the Scanning Tunneling Microscope (STM) in 1982 by Binning and Rohrer[1] introduced a new method in the field of surface science. When a sharp tip is in close proximity to a surface so that the electron clouds of tip and surface atoms overlap, a tunnel current can be established when a voltage difference is applied between tip and surface. This current is extremely sensitive to tip-sample separation and is used to detect the topography of the surface. The use of STM is limited to (semi-) conductive materials since it is based on the tunneling current. In 1986, the major hindrance was overcome by the development of the Atomic Force Microscope (AFM)[2]. The AFM is based on the interaction forces present between a tip and a surface. These forces are measured by the motion of a very flexible cantilever spring, on which the tip is mounted. Since interatomic forces are always present when two bodies are in close proximity, the AFM is capable of probing (semi-) conducting surfaces as well as insulating. The key components in an AFM are the sensor for measuring the force on the tip, due to its interaction with the surfaces and the piezoscanners that scan the surface. A lever (with a sharp tip) with an extremely low spring constant is required for high vertical and lateral small force resolution.

2.1.1 PRINCIPLE OF OPERATION

In figure 2.1, a schematic drawing of an AFM is presented. A sample is mounted on a piezoelectric scanner tube, which consists of separate electrodes to precisely scan the surface in the X-Y plane in a raster pattern and to move the sample in the Z-direction. A sharp tip attached at the end of a cantilever is brought into contact with a surface, by means of the Z-piezo. A force F causes the cantilever to deflect, according to Hooke's law, $F = kD_z$, k is the spring constant and D_z is the vertical displacement of the cantilever. The cantilever's deflection is measured by a laser deflection technique. A laser beam from a diode laser is focused on the rear side of the cantilever and its reflection is directed to a position-sensitive detector (PSD), a photodiode split into two segments, Top and Bottom. When the cantilever deflection changes due to the interaction force between the tip and the surface, the intensities of the two segments change. The voltage difference of the two segments [(T-B)/(T+B)] provides the AFM signals which is a sensitive measure of the cantilever vertical deflection. Depending on the mode used, an electronic feedback circuit is used to keep the appropriate parameter (force, height) at a constant value and thus obtain the topography of the surface.

In the "*constant force" mode*, the PSD always adjusts the voltage directed to the Z-piezo of the sample in order to keep the cantilever deflection nearly constant — feedback loop — and the change in piezo voltage is collected by the system. The "voltage" values that are collected can be easily converted to "distances" via the piezo coefficients of the three piezos, which are obtained by scanning a standard sample.

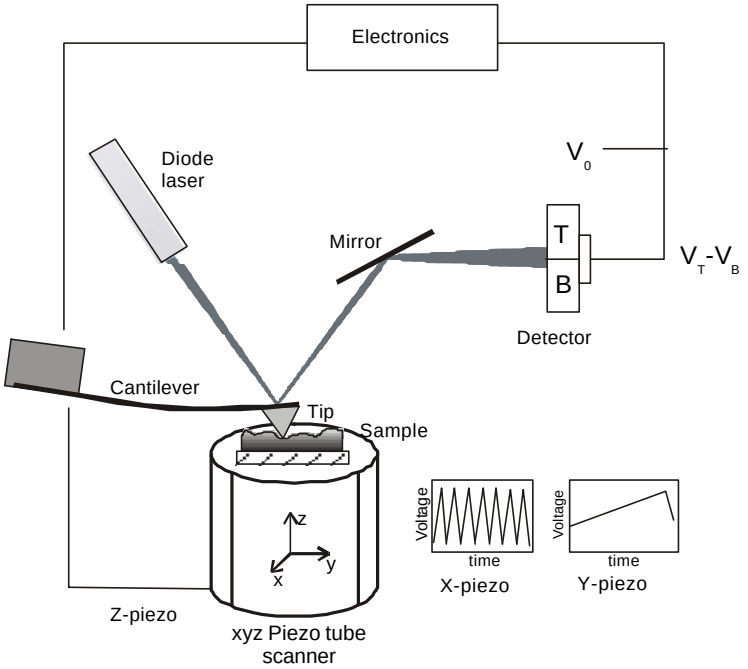

Figure 2.1: *Schematic drawing of AFM set-up.*

2.1.2 IMAGING OF POLYMER SURFACES

Atomic Force Microscopy was first applied to polymer surfaces in 1988, shortly after its invention[3]. Today, these studies range from relatively simple visualization of morphology to more advanced examination of polymer structures and properties on the nanometer scale. In contrast to imaging of surface crystalline lattices, the resolution of contact mode AFM for partially ordered morphological patterns is determined by the size of the tip-sample contact area. Low-force AFM imaging in contact mode and tapping mode allows observation of soft samples, such as polymers.

CONTACT MODE IN LIQUIDS¾ Using low-force AFM imaging in contact mode allows the imaging of polymer surfaces. The contact area can be reduced by minimizing the applied force, which helps to avoid surface deformation. To avoid capillary forces, which are common for ambient-condition measurements and which lead to increased forces, operation under liquid has been proposed[4]. When scanning in fluids, the overall forces in contact mode are lower than in ambient air: the fluid layer/meniscus, which is formed in air, is not present furthermore, electrostatic forces can be dissipated or screened.

TAPPING MODE¾ Tapping mode[5] imaging overcomes the limitations of the conventional scanning modes by alternately placing the tip in contact with the surface, to avoid dragging the tip across the surface. The cantilever is oscillated at frequencies

around 300 kHz, depending on the Si-cantilever (spring constant of 50 $N \cdot m^{-1}$, radius of curvature of 8-10 nm).

At these frequencies, viscoelastic surfaces become stiff and can more easily resist forces from the probe tip. This property further reduces the possibility of sample damage for extremely soft samples and causes less distortion of the sample due to tip forces. Another advantage of the tapping mode technique is that the vertical feedback system is highly stable, allowing routine reproducible sample measurements.

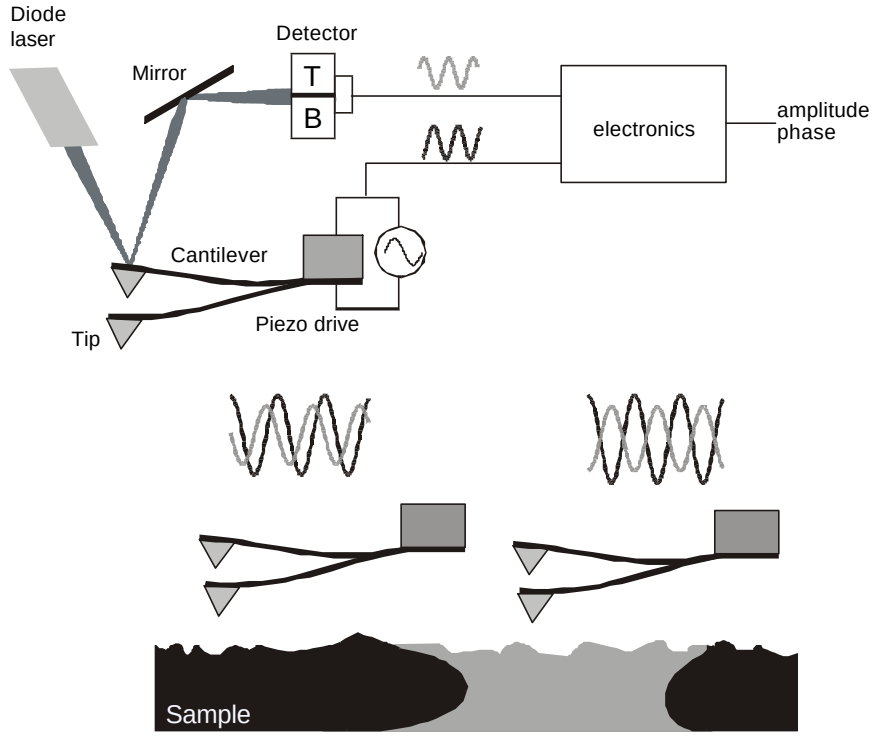

Figure 2.2: *Schematic drawing of tapping mode AFM.*

In tapping mode AFM, the cantilever is excited into resonance oscillation with a piezoelectric driver. The oscillation amplitude is used as a feedback signal to measure topographic variations of the sample. As the oscillating cantilever begins to intermittently contact the surface, the cantilever oscillation is necessarily reduced due to energy loss caused by the tip contacting the surface. The reduction in oscillation amplitude is used to identify and measure surface features. In phase imaging, the phase lag of the cantilever oscillation, relative to the signal sent to the cantilever's piezo driver, is simultaneously monitored. By mapping the phase of the cantilever oscillation during the tapping mode scan, variations in adhesion, friction, viscoelasticity, can be detected, although there is currently no simple correlation between phase contrast and a single material property.

Phase imaging can also act as a real-time contrast enhancement technique. Because phase imaging highlights edges and is not affected by large-scale height

differences, it provides clearer observation of fine features, such as grain edges, which can be obscured by rough topography.

2.2 SURFACE FORCES APPARATUS (SFA)

The Surface Forces Apparatus (SFA) was first developed by Tabor and Winterton[6] in 1969, in order to measure directly the van der Waals forces between two solid surfaces. As substrates muscovite mica surfaces were used. Due to the inherent smoothness of mica, for the first time measurement of forces at surface separations below 80 nm were made. Israelachvili[7] later developed a better design, in which forces between mica surfaces in liquid could be measured. This method was a major experimental breakthrough and was the basis of many experiments to follow. A couple of years later the SFA was used to measure forces between polymers, with a distance resolution of about 0.1 nm and a force sensitivity of about 10^{-7} N.

Several conditions are essential for meaningful surface force measurements. Firstly, the surfaces have to be smooth, in order to measure right down to surface contact. Secondly, the surface must be highly inert, it must not degrade during the course of the experiment which could lead to changes in the surface chemistry and consequently to changes in surface forces. Finally, the surface must also be hard so that the force being measured do not reflect the compression of the surface material.

The most common material for SFA measurements is mica ($K_2(AlSi_3)O_{10}(OH)_2$). Mica has a layered crystal structure consisting of aluminosilicate layers separated by layers of potassium ions held together by ionic bonds. By inserting a needle into a thick piece of mica, the crystal cleaves along the plane of the potassium ions, since these are the weakest bonds in the plane. Care has to be taken to cleave the mica sheet along its axis –the direction with the least resistance– so as not to contaminate the area with flakes of mica. Atomically smooth sheets with a thickness of 1–3 μm and an area of several square centimeters can be obtained by this procedure. Pieces of 1×1 cm^2 are then cut with a heated platinum wire and placed on a large mica sheet which has been freshly cleaved. Mica prepared in this way is ideal for measuring intermolecular forces because the surface is smooth, hard and chemically inert.

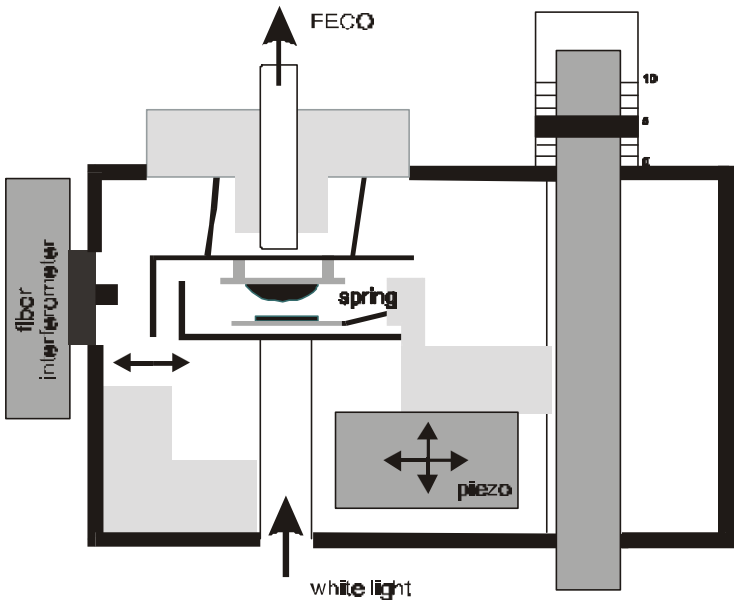

Figure 2.3: *Schematic drawing of SFA.*

Another important experimental consideration is choosing the geometry of the two surfaces. Most theories have been developed for surfaces of semi-infinite solids in a parallel-plate configuration. However, experimentally this geometry poses many problems –precise parallel alignment of the two surfaces, edge effects in the measured surface, only one contact position available for measurement. To overcome these problems the "crossed cylinder configuration" is used in practice. The Derjaguin approximation[8] can be used to compare the experimental results with theory. The force law *F(D)* between two curved surfaces is related to the interaction energy *E(D)* between two planar surfaces, under the assumption that the radii of the surfaces, R_1, R_2, are much larger than the distance, *D*.

$$F(D) = 2\pi\left(\frac{R_1 R_2}{R_1 + R_2}\right)E(D) \qquad [2.1]$$

2.2.1 DISTANCE MEASUREMENTS

The separation between the two surfaces from microns down to molecular contact can be measured by use of an optical technique[9] employing multiple beam interference fringes called Fringes of Equal Chromatic Order[10] (FECO). Here two transparent mica sheets are first coated with a semireflective layer of pure silver, prepared by evaporation before they are glued onto polished silica discs (R = 1 cm) with the silver sides down. The two mica surfaces separated by a medium form an optical cavity (figure 2.4).

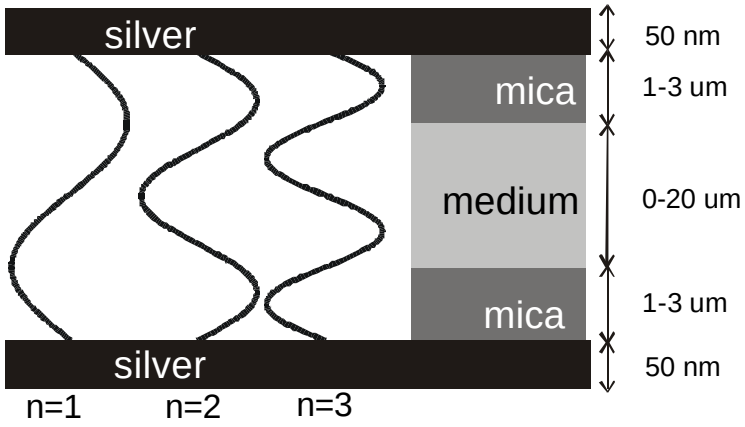

Figure 2.4: *Optical cavity formed by silver layers.*

Once in position in the apparatus, white light is passed vertically up through the two surfaces and the emerging light is then focused onto the slit of a grating spectrometer. The light consists of discrete wavelengths, which can be separated in the spectrogram as sharp fringes (FECO) (figure 2.5).

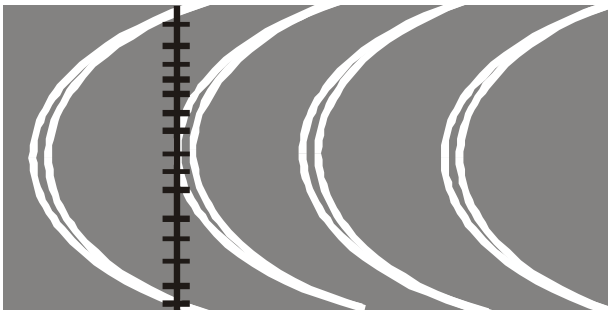

Figure 2.5: *Image in spectrograph.*

From the positions and shapes of the FECO the distance between the two surfaces can be measured. The positions can be converted to wavelengths by calibrating the spectrometer with the known wavelengths of a mercury lamp. When the two mica sheets are separated by a distance D then the fringes shift to longer wavelengths, l_n^0 to l_n^D. The distance between the two surfaces is given by the below formula:

$$\tan\left(\frac{2\pi n_1 D}{l_n}\right) = \frac{2n\sin\left[\pi\dfrac{1-l_n^o/l_n^D}{1-l_n^o/l_{n-1}^o}\right]}{(1+n^2)\cos\left[\pi\dfrac{1-l_n^o/l_n^D}{1-l_n^o/l_{n-1}^o}\right]\pm(n^2-1)} \qquad [2.2]$$

l_n^0 (n=1, 2, 3, …..) are the wavelengths in contact, (+) and (-) refer to an odd and even fringe, respectively, $n = n_1/n_2$, where n_1, is the refractive index of mica and n_2 the refractive index of the medium at l_n^D. In this way the distance and the index of the medium can be evaluated independently.

Note that the optical method for measuring the surface separation actually measures the distance between the two silvered layers on the reverse sides of the mica sheets. It has been shown[11] that no error greater than ±0.1 nm in the surface separation is caused by normal temperature variations (±0.5 ^oC) and applied pressures of the experiments.

The method for measuring D just described is recommended for distances up to 500–1000 nm. For larger distances on bringing the two surfaces in contact, and counting the number, x, of fringes that have passed one can readily obtain the surface separation $D = x\ l_n^0/2n_1$. This method is rapid and accurate to at least 1%.

2.2.2 FORCE MEASUREMENTS

The lower surface is mounted at the end of a horizontal leaf spring, which is used to measure the forces. The spring is connected to a small (10 ml) stainless steel liquid cell, which is placed on top of the translation stage, motor and piezoelectric block (figure 2.3). The distance is decreased in small steps by expanding the piezo. At each step the distance and the voltage given to the piezo to expand is noted. At distances beyond the range of forces the spring will be undeflected and there will be a linear relationship between the distance and the piezo voltage. In this regime the system is calibrated –this calibration is part of each experiment. Expanding the piezoelectric crystal further will bring the surfaces in the range of the force.

The force is measured by expanding the piezoelectric block by a known amount and then measuring optically how much the two surfaces have actually moved: any difference between the two values when multiplied by the spring constant of the measuring spring gives the force difference between the initial and final position. In this way, both attractive and repulsive forces can be measured and a full force profile can be obtained over any distance regime.

The method for determining the lateral forces is described in detail in the Experimental section of Chapter 5.

2.3 FEEDBACK SURFACE FORCES APPARATUS

As it was shown, the classical Surface Forces Apparatus uses an interferometry technique (FECO) to determine the separation between two crossed cylinders of molecularly smooth semi-transparent mica surfaces. The force is obtained by the deflection of a cantilever spring, with the aid of the FECO. Despite the enormous success of the apparatus, it suffers from a number of important restrictions. I) The number of surfaces

available for study is limited to transparent surfaces, because of the requirement of the interferometry technique. II) Studies equilibrium and dynamic surface forces are difficult to perform in real time, because of the complexity of the basic SFA. III) Apparatuses, such as the SFA, that are based on mechanical springs are prone to cantilever instabilities, because the force is not controlled independently of the displacement. These instabilities (jumps) occur when the distance derivative of an attractive force is greater than the spring constant of the force sensor. As a result, certain portions of the force profile are inaccessible.

The implementation of a servosystem, to control the position of the surface fixed on the position sensor, so that the surface separation is controlled, would allow us to eliminate many of the above–mentioned restrictions. Several apparatuses with a feedback system have been constructed. Steward and Parker[12] improved a Mark IV[13] SFA. A magnetic force transducer and a bimorph displacement sensor were connected in a servo loop. In this way, feedback measurements of surface forces could be obtained. Tonck et al.[14] introduced a feedback apparatus with capacitive displacement trasducers so that intermolecular forces and rheology could be measured continuously and simultaneously. Finally, a Magnetic Levitation Force Microscope has been constructed, by Gauthier-Manuel and Garnier[15], introducing a magnetic actuator, with a feedback system.

The following section describes a new feedback SFA; the principles of operation, the design considerations, the performance and the limitations. Finally, the first test-experiments are shown, the interaction of two mica surfaces in air and the forces exerted by a polymer melt sandwiched between two mica surfaces.

2.3.1 DESIGN AND PRINCIPLE OF OPERATION

A schematic drawing of the system is presented in figure 2.6. Surfaces are glued to cylindrical silica lenses. The lower lens is rigidly mounted in a cylindrically shaped liquid cell. The liquid cell is mounted onto a stage, which can be moved via a step motor or a piezo.

A flexible teflon-like bellow seals the chamber, but also allows the lower surface to be translated in all three directions (not shown in figure 2.6). The entire translation stage is supported by two perpendicular stages that can be moved manually in a horizontal plane and be locked securely in position. This allows changing the contact position between the surfaces, without the need for releasing any part that can increase the risk of contamination. The translating stage consists of a precise motor and a piezoelectric stage (P-915.856, Physik Instrumente). The piezoelectric stage has built-in capacitive sensors in the z-direction, with a total expansion range of 15 μm. The utilization of capacitive sensors, coupled to a feedback system, linearizes the motion and allows a resolution of about 1 Å.

The upper lens is connected to a force sensor-compensator (Mettler Toledo). A force acting on the upper surface causes the cantilever to deflect. This deflection is detected by means of a light source and a sensitive two-element photodiode (T and B). The voltage difference between the two elements is fed into a feedback system, with the objective to keep the voltage different constant and close to zero. The force compensator

operates according to the principle of electrodynamic force compensation. The acting force is compensated by an opposite force. The output of the feedback system is a current passing through the coil. The most important aspect of the design is that the current fed to the coil is proportional to the force.

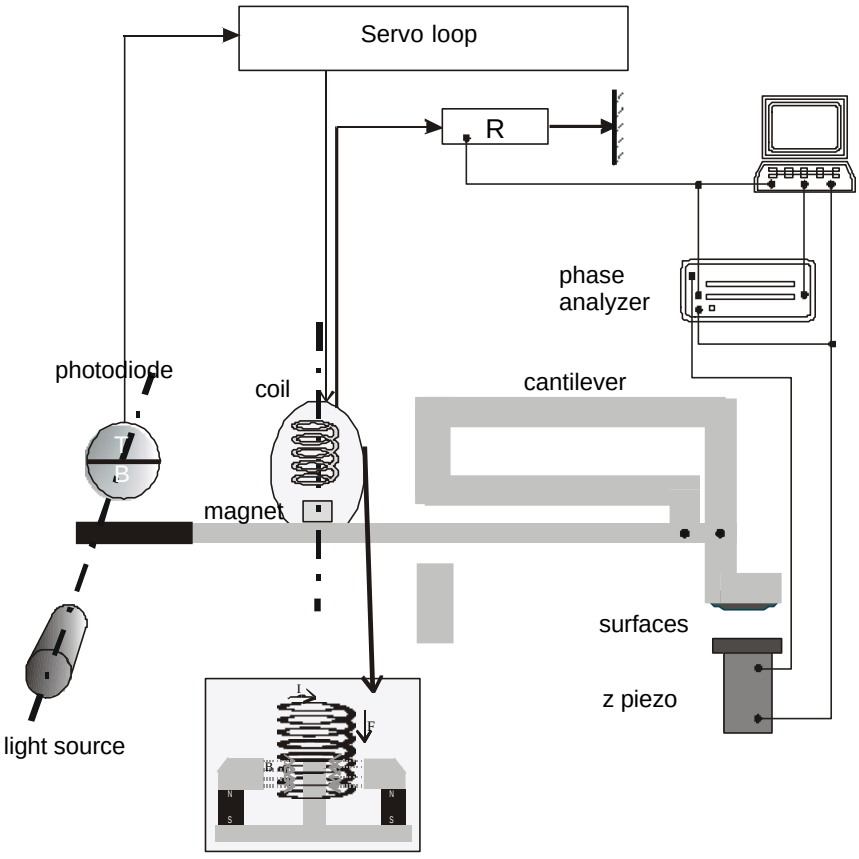

Figure 2.6: *Sketch of the apparatus. The movements of the cantilever are recorded by a photodiode and controlled by a magnetic force transducer, in such a way that there will be zero displacement. During operation the force exerted by the coils on the magnet acts to cancel the force between the surfaces, resulting in a surface separation controlled by the piezoelectric actuator. The surface forces are proportional to the current passing through the coils. The computer controls and records the movements of the piezo while recording the value of the current passing through the coil. For dynamic measurements, a dynamic phase analyzer is used. The insert displays the principle of electrodynamic force compensation.*

A computer program controls the parameters and the execution of the experiments. Basically, with a digital/analog converter the piezo stage translates in steps. During each step two signals are recorded, the current passing through the coil and the position of the piezo stage, with analog/digital converters. With an appropriate calibration, these two signals are transformed into Force versus Separation.

The force sensor has been constructed from one block of material. The advantage of such a construction is that it is less susceptible to thermal drifts, since there are no junctions between different materials, which can have different expansion coefficients.

Since magnetic forces are present, the apparatus is constructed entirely from non-magnetic stainless steel. However, temperature variations can influence the magnetic field of the permanent magnet and thus the current. To remendy, a temperature compensator is implemented in the force sensor and the laboratory room is temperature-controlled within 1°C.

For dynamic measurements, a dynamic phase analyzer (SI 1260, Solatron) is used (figure 2.6), coupled to the piezo stage and the force sensor. A built-in generator drives the piezo stage. The signals from the force sensor and the piezo movements are fed into the signal analyzer; a microprocessor creates an ASCII file, with the characteristics of the excitation signal, the amplitude of the response signal (voltage), and phase shift between the two signals.

2.3.2 PERFORMANCE OF THE APPARATUS

The sensor was calibrated, so that output voltage values were converted to force values. The noise, sensitivity, stability and response time were measured.

CALIBRATION¾ The purpose of the servosystem is to stabilize the deflection of the cantilever at a constant value, usually zero. This is done by changing the current passing through the coil, and is read as a voltage across a resistor. The first step is to calibrate the system, voltage has to be converted to force. This was done by placing known weight on the sensor and measuring the output voltage. Figure 2.7 shows a graph of the sensor's output voltage versus the masses of known weights. No averaging and filtering of the output signal was performed. It shows a linear relationship between the mass and the output voltage. Fitting the data points with a straight line gives the conversion factor. The Output Voltage/Force ratio is equal to 303 mV/N.

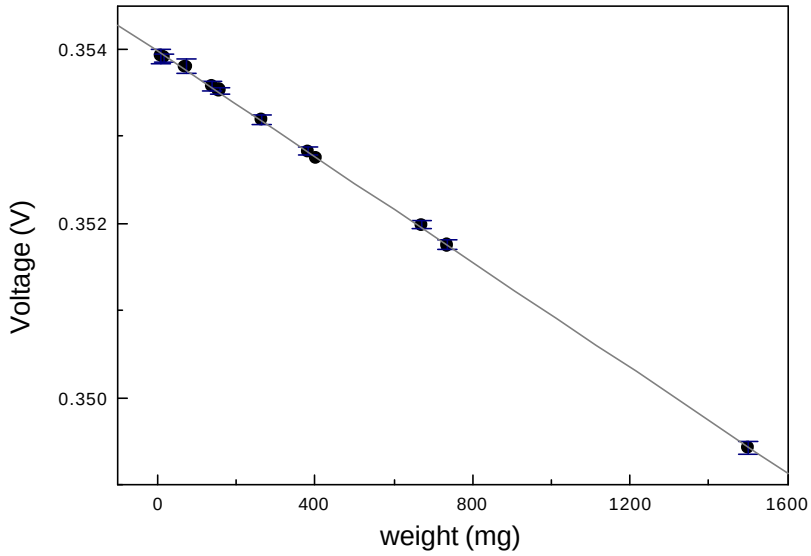

Figure 2.7: *Calibration of the force sensor with known weights.*

NOISE¾ One of the most important aspects of the system is its sensitivity. It depends on the inherent characteristics of the force sensor, basically the stiffness of the cantilever. However, this sensitivity is limited by the system's noise level. To reduce the noise levels a study of the origin of the different sources of noise was performed. A signal analyzer (3567 0A, Hewlett Packard) was used, to measure the output voltage of the sensor in the frequency regime. In the low-frequency regime, the noise is high due to magnetic fields radiated by transformers, which produce noise at 50 Hz and its multiple. To reduce this source of noise all apparatuses, which produce magnetic fields, were kept far away from our apparatus. Mechanical or acoustic perturbations can also increase the noise level. For this purpose the apparatus was placed on an antivibration table, which damps all transmissions from the floor. Another source of noise was found to be the laboratory lights (TL tubes). At 100 Hz and its multiples the noise level was high when the light was switched on. The insert of figure 2.8 shows the response of the system to laboratory light. With the lights off, the noise of the system is reduced, but there is also a voltage difference between the two states. The difference between lights on and lights off is 5 μV.

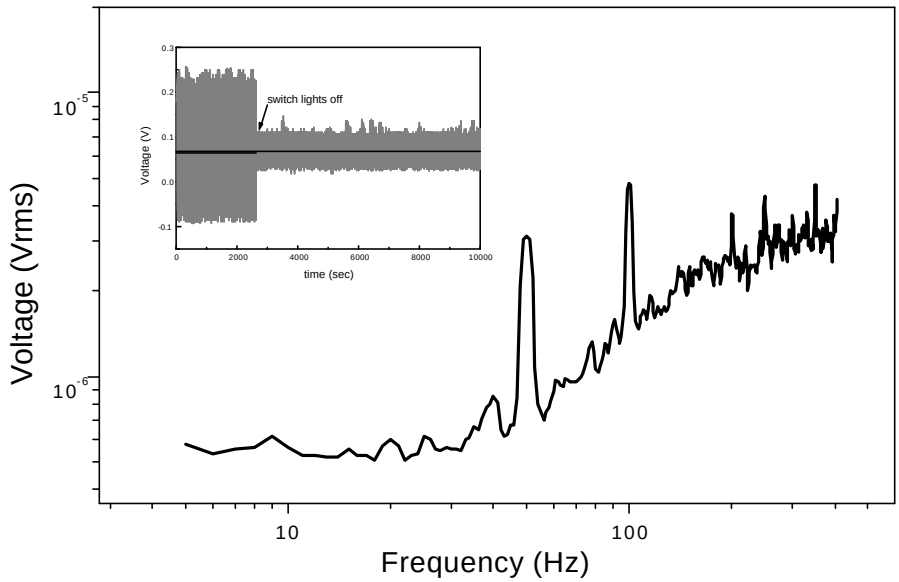

Figure 2.8: *Response of the sensor in the frequency regime. The insert shows the influence of the force sensor to light.*

Figure 2.8 shows the response of the sensor in the frequency regime, in the dark. The sensitivity of the prototype was calculated to be around 10^{-6} N. This sensitivity is low compared to the classical surface force apparatus, but it can be increased with the choice of a more sensitive sensor.

We have chosen an averaging method for reducing the noise of the output voltage, by means of a software program. The experiments were conducted using an analog input-output card (National Instruments) implemented in a PC computer and a software program written in a data acquisition package (Test Point).

DRIFT¾ In force measurements, the system has to be stable over the time scale of one force measurement. The use of an automated software acquisition program reduces this time. Figure 2.9 shows the output voltage of the sensor, recorded continuously over a period of 2 days. Every minute one data point was collected and added to the graph. A small drift is evident, as the linear fit to the data points shows. The slope is equal to $-10^{-9}\,\mathrm{V}\cdot\mathrm{min}^{-1}$. In the course of a 30 minutes experiments the error in the force value is equal to about 10^{-7} N. The error is one order of magnitude lower than the sensitivity of our apparatus, thus the stability of our system is quite good.

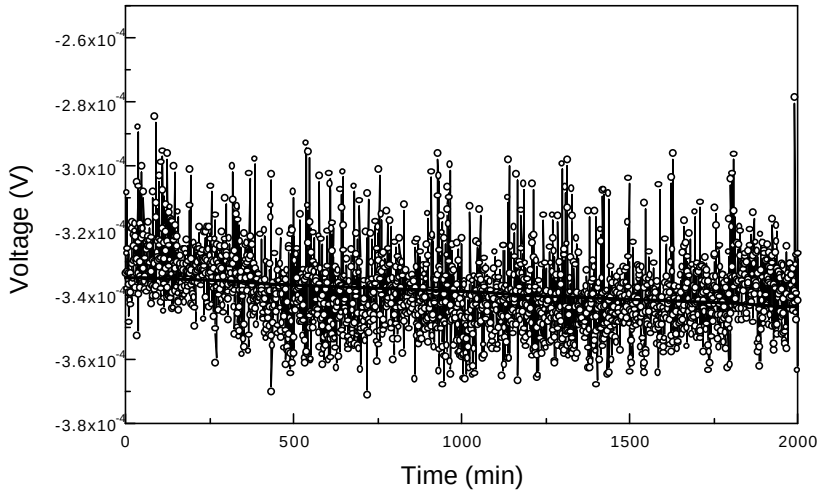

Figure 2.9: *Drift measurement. Output voltage of the sensor recorded continuously over a period of 2000 min.*

RESPONSE TIME¾ Apart from static measurements we also want to perform dynamic measurements with the apparatus.

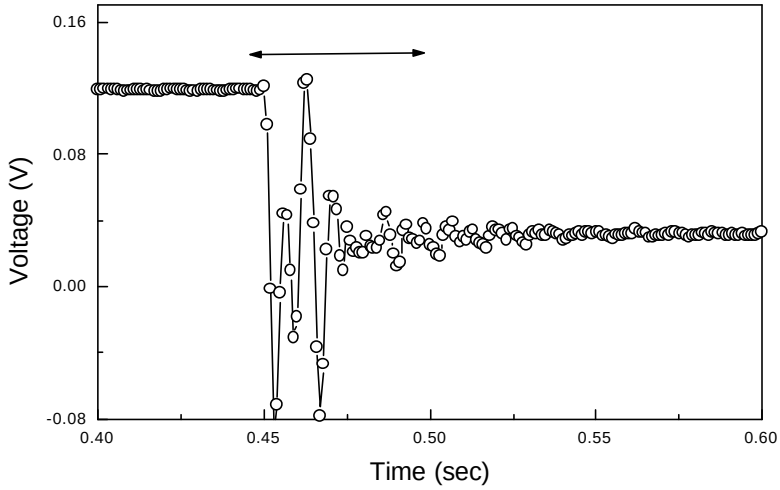

Figure 2.10: *Response time of the feedback system.*

Dynamic measurements can be performed by exciting the lower surface with a sinusoidal signal and measuring the response of the upper surface. Namely, the phase shift between the two signals and the ratio of their amplitudes as a function of the voltage or the excitation frequency. The response time of the device limits the frequency that can be employed. To measure the response time a weight was placed on the upper lens, while

the output of the sensor was recorded, figure 2.10. The response time was calculated to be 0.05 sec, thus limiting the frequency to around 20 Hz. The response time can be reduced by a better adjustment of the parameters of the feedback system (PID).

2.3.3 FORCE MEASUREMENTS

Attractive and repulsive interactions have been measured with the system. An attractive force profile is shown in figure 2.11. The interaction of two mica surfaces in crossed cylinder configuration, in an atmosphere of argon, is recorded. The experiment was performed without the use of the FECO technique.

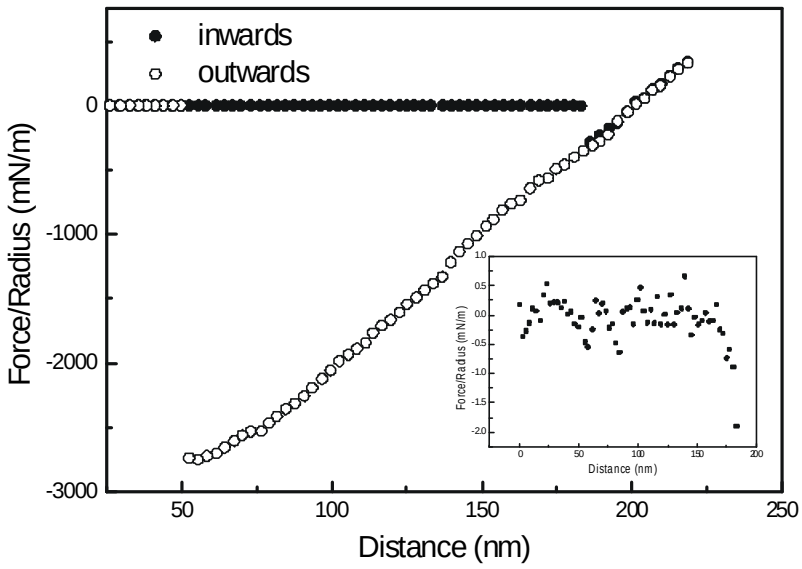

Figure 2.11: *Normalized force as a function of displacement for two mica surfaces in argon. The insert is a zoom of the inward curve before the jump to contact.*

The SFA –without the utilization of the fringe pattern– is much more user-friendly. Moreover, opaque substrates can also be used. Provided that the servo loop of the force sensor works, the separation between the two mica surfaces can be controlled and measured with the piezostage. The attractive force profile that was obtained shows a large jump in both the inwards and outwards curves, with no problems of hysteresis. This jump is basically due to the poor initialization of the parameters of the feedback system, discussed previously, but also due to the elasticity of the glue with which the mica surfaces were glued on the silica lenses[13].

Repulsive curves were obtained with a polymer melt, a perfluoropolyether (PFPE) with a linear structure, Fomblin Z60 (obtained from Montefluous). The average

molecular weight was 13 000 $gmol^{-1}$ with a polydispersity index of 1.5. The kinematic viscosity of the sample was 600 cSt.

$CF_3O\text{-}(CF_2CF_2O)_m\text{-}(CF_2)_n\text{-}CF_3$ m/n = 1.5

This system was chosen as a test sample for the following reasons. a) its' a liquid at room temperature; b) a considerable number of studies have been published on polymer melts with the Surface Forces Apparatus[16, 17, 18, 19, 20]; c) it exhibits a long-range monotonic repulsive force and d) drainage experiments can be performed.

It has been argued that polymer melts in thin films should not exhibit any long-range repulsive forces[19, 21, 22]. But, apparent repulsive forces can be observed experimentally, due to hydrodynamic forces[19]. Chan and Horn[23] have derived expressions for the rate of drainage of thin liquid films from between solid surfaces based on Reynolds' theory of hydrodynamic lubrication[24]. The hydrodynamic force, F_H, between crossed cylinders of radii R_1 and R_2 immersed in a liquid of viscosity h can be calculated. If the cylinders are separated by a distance D and one of them is moving along a line normal to the other surface, the other one experiences a force according to the equation:

$$F_H = -\frac{6\pi h R_H R_G}{D - 2D_s}\frac{dD}{dt} \qquad [2.3]$$

where $R_H = \left[\frac{1}{2}\left(1/R_1 + 1/R_2\right)\right]^{-1}$ and $R_G = \left(R_1 + R_2\right)^{1/2}$ are the harmonic mean and geometric mean of the cylinder radii, respectively. D_s is the position of the shear plane.

In figure 2.12, data are collected from three force runs during the same experiment. The only difference between them is the rate of approach of the lower surface with respect to the upper one. The velocity of the lower surface was $0.46\ \mathrm{nm \cdot s^{-1}}$, $1.3\ \mathrm{nm \cdot s^{-1}}$, and $2\ \mathrm{nm \cdot s^{-1}}$. The forces depend on the velocity of approach of the lower surface to the upper one, and hence they do not represent equilibrium forces. The fits on the curves (gray lines) follow equation [2.3], for the corresponding rates of approach. The forces measured experimentally can be entirely accounted by viscous drag forces.

An important assumption was that the shear plane is located at a position D_s = 5 nm. This is the only choice for the position of the shear plane that gives a good agreement between the measured forces and expression [2.3]. This distance is related to the thickness of the layer of polymer that is partially immobilized in the time scale of the experiments[17, 18, 19, 21]

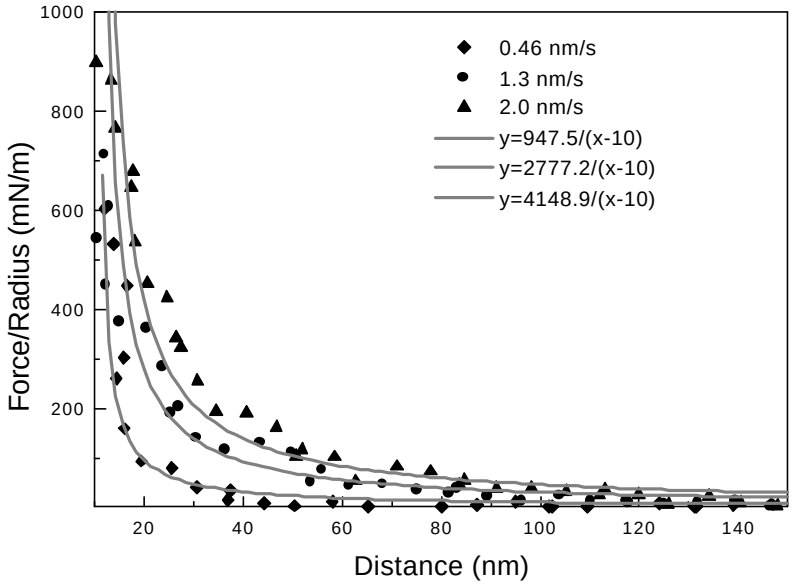

Figure 2.12: *Normalized forces as a function of displacement, for a polymer melt (PFPE) between two mica surfaces. Three force runs are illustrated having different rates of approaches (symbols). The gray lines represent equation [2.3], assuming a shear plane at D_s=5 nm from each surface.*

2.3.4 CONCLUSIONS AND FUTURE MODIFICATIONS

A Surface Forces Apparatus having a feedback force sensor that was originally designed for weight measurements, has been described. The main advantages that this setup offers are:

- A mono-bloc force sensor. This reduces thermal drifts.
- The introduction of a feedback loop in the SFA for measuring the forces. This could eliminate spring instabilities, when measuring attractive forces. In addition, the combination of this feedback loop with a piezo stage with its own feedback system allows accurate control and measurement of the separation between the surfaces.
- Automation of the measurements. This improves the reliability and reproducibility of the experiments.
- The range of driving speeds available with this apparatus makes it ideal for performing measurements of viscosity in thin films, drainage measurements.
- The FECO interferometry is not necessary, since the force can be measured independently from the distance. In such a case, other surfaces than mica become accessible for study. In classical SFA measurements, the FECO also allow the detection

of contamination. But since the force profiles are analyzed during the course of the measurement, depicted as a Force-Distance graph on the computer screen, contamination can be easily identified and the experiment can be aborted at an early stage.

The drawbacks of the system are it's low resolution and the poor initialization of the feedback-system's parameters. The later is easy modifiable, but the former problem needs the elaboration of a new force sensor. Nevertheless, the main objective of this work was to check if such a set-up had the potentials to work as a Surface Forces Apparatus. The forces measured with the apparatus are in good agreement with previous measurements.

The device can be eventually extended in the other two directions in space, by the realization of a three-dimensional sensor, so that lateral forces can also be experimentally accessible and coupled to the normal forces.

REFERENCES

[1] Binning, G.; Rohrer, H.; Gerber, Ch.; Weiibel, E. *Phys. Rev. Lett.* **1982** 49, 57
[2] Binning, G.; Quate, C.F.; Gerber, Ch. *Phys. Rev. Lett.* **1986**, 56, 930
[3] Albrecht, T.R.; Dovek, M.M.; Lang, C.A.; Grütter, P.; Quate, C.F.; Kuan, S.N.J.; Frank, C.W.R.F.; Pease, W. *J. Appl. Phys.* **1988**, 64, 1178
[4] Weisenhorn, A.L.; Hansma, P.K.; Albrecht, T.R.; Quate, C.F. *Appl. Phys. Lett.* **1989**, 54, 2651
[5] Zhong, Q.; Innis, D.; Kjoller, K.; Elings, V.B. *Surf. Sci. Lett.* **1993**, 290, L688
[6] Tabor, D.; Winterton, R.H.S. *Proc. Roy. Soc. London* **1969**, A312, 435,
[7] a) Israelachvili, J.N.; Tabor, D. *Proc. Roy. Soc. London* **1978**, A311, 19
b) Israelachvili, J.N.; Adams, G.A. *Nature* **1976**, 262, 774
c) Israelachvili, J.N.; Adams, G.A. *J. Chem. Soc. Faraday Trans.* **1978**, 74, 975
[8] Derjaguin, B.V. *Kolloid Z.* **1934**, 69, 155
[9] Israelachvili, J.N. J. *Colloid Interface Sci.* **1973**, 44, 259
[10] Tolansky, S. "*Multiple-beam Inteferometry of Surfaces and Films*" **1948** Oxford University Press, London
[11] Israelachvili, J.N. "*Surface Forces Apparatus Users' Manual*" September **1985** Anutech pty. Ltd.
[12] a) Stewart, A.M.; Parker, J.L. *Rev. Sci. Instrum.* **1992**, 63, 5626
b) Parker, J.L. *Langmuir* **1992**, 8, 551 c) Parker, J.L.; Stewart, A.M. *Prog. Colloid Polym. Sci.* **1992**, 88, 162
[13] a) Parker, J.L.; Christenson, H.K.; Ninham, B.W. *Rev. Sci. Instrum.* **1989**, 60, 3135
b) Stewart, A.M.; Christenson, H.K. *Meas. Sci. Technol.* **1990**, 1, 1301
[14] Tonck, A.; Georges, J.M.; Loubet, J.L. *J. Colloid and Interf. Sci.* **1988,** 126, 150
[15] Gauthier-Manuel B.; Garnier, L. *Rev. Sci. Instrum.* **1997**, 68, 2486
[16] Horn, R.G.; Israelachvili, J.N. *Macromolecules* **1988**,21, 2836
[17] Monfort, J.P.; Hadziioannou, G. *J. Chem. Phys.* **1988**, 88, 7187
[18] Israelachvili, J.N.; Kott, S.J. *J. Chem. Phys.* **1988**, 88, 7162
[19] a) Hirz, S.J. Ph.D. thesis **1991** University of Stanford

b) Hirz, S.J.; Homola, A.N.; Hadziioannou, G.; Frank, C.W. *Langmuir* **1992**, 8, 328
[20] Homola, A.M.; Nguyen, H.V.; Hadziiannou, G. *J. Chem. Phys.* **1991**, 94, 2346
[21] de Gennes, P.G. *C. R. Acad. Sci. Paris* **1987** 305, 1181
[22] ten Brinke, G.; Ausserre, D.; Hadziioannou, G. *J. Chem. Phys.* **1988**, 89, 4374
[23] Chan, D.Y.C.; Horn, R.G. *J. Chem.Phys.* **1985**, 83, 5311
[24] Reynolds, O. *Philos. Trans. R. Soc. London* **1886**, 177, 157

CHAPTER 3

BUILDING UP OF BLOCK COPOLYMER MONOLAYER

ABSTRACT

Atomic Force Microscopy (AFM) has been used to study the morphology of diblock poly(2-vinylpyridine)/polystyrene (P2VP/PS) copolymer films, adsorbed from a selective solvent ¾ toluene. In toluene the PS block is well solvated and the P2VP block is precipitated. Due to the selectivity of the solvent, the copolymer tends to self-assemble above a given concentration, the critical micelle concentration (cmc), to form spherical polymolecular micelles. If a substrate is immersed in a toluene solution of the diblock copolymer, the P2VP block adsorbs on the substrate and anchors the PS block, forming a monolayer.

The first section of the chapter concerns the organization (and visualization) of diblock copolymer micelles, deposited on an adsorbed diblock copolymer monolayer. The last three sections present the morphological evolution of diblock copolymer monolayers, formed via adsorption from toluene. The lateral structural characteristics have been investigated as a function of solvent quality, adsorption time, chemical nature of the substrate, and polymer concentration (presence of micelles in the solution). It will be shown that all variables affect the final structure of the adsorbed diblock copolymer monolayer. In addition, the adsorption properties (mechanisms and kinetics) have been determined.

3.I

ORGANIZATION OF NON-GRAFTED MICELLES ON DIBLOCK COPOLYMER MONOLAYER SURFACES DURING SOLVENT EVAPORATION

Thin films of P2VP/PS diblock copolymers formed on mica substrate were studied by means of an AFM, in tapping mode operation. The films were formed from P2VP/PS micellar toluene solutions by immersing the substrate in toluene solutions and after extraction allowing the solvent to evaporate. The AFM images of the films' morphology formed from the largest diblock copolymer micellar solutions revealed a multilayer structure consisting of an adsorbed monolayer (with the P2VP-block adsorbed on substrate and the PS-block anchored) underneath and spherical-like micelles on top. The size of the micelles turns out to be similar to that of P2VP/PS micelles in bulk. For solutions with concentrations below the cmc, ribbon and elliptic-like structures (without any spherical objects) were observed. The influence of the aggregation number of bulk micelles on the structure of the upper layer of the film was studied. With decreasing the size of P2VP-block and hence micelle aggregation number, monodisperse spherical micelles change into a worm-like structure and finally (for the smallest diblock copolymer) into a flattened layer with holes of equal height. Similar effects take place upon dissolution of the film, i.e. upon consequent addition of toluene. The increase of chain mobility is responsible for the phenomenon.

3.I.1 INTRODUCTION

Diblock copolymers are capable of forming self-assembled monolayers via selective adsorption on a substrate.[1] Recently[2, 3], it has been shown that block copolymers can be used in a rapidly growing area of technology, devoted to patterning surfaces and ultimately developing well-defined functionalized nanostructures, which can be used for molecular wires and switches. The scientific questions that are posed in this field concern the possible conformations adopted by the macromolecules, in different environments and various confinement configurations.

In the case of a sufficiently high molecular weight diblock copolymer, the two blocks tend to separate on a microscopic level, due to the incompatibility of the two blocks. In selective solvents, at a concentration above the critical micelle concentration

(cmc), the formation of spherical micelles is encountered,[4] with the insoluble block in the core of the micelle surrounded by the soluble block. The equilibrium structure of these micelles is defined by a balance between enthalpy (reduction of unfavourable interactions) and entropy (stretching of chains).

Block copolymers order themselves in structures in the bulk[5]. Highly ordered structures have also been observed in thin films. The symmetry, periodicity and orientation of the structures are influenced by the presence of boundary surfaces.[6] The strong interactions with the surface force the lamellae to orient parallel to the plane of the film. For films, where there is at least one interface with the air, the film thickness is quantized in terms of the bulk period, *L*, upon annealing. If the initial thickness does not satisfy this constraint, then an incomplete top layer, composed of islands or holes is formed.[7, 8, 9]

Atomic Force Microscope has been a useful tool to study self-organization of macromolecules on flat surfaces. It has been found[10] that the deposition of diblock copolymers from a selective solvent, followed by rapid solvent extraction, can lead to highly laterally ordered microdomain structures. Transmission Electron Microscopy[2] has been used to show that the structures are formed by micelles, consisting of a core of the insoluble block surrounded by a corona formed by the soluble block. Such structures (see for example figure 3.I.1), are produced by dipping a substrate into the polymer solution, taking it out and letting it dry. While the existence of such structures has been verified by various studies[2, 3, 10, 11, 12, 13, 14], the details of the process of the structure formation is under debate. It has been argued[11] that the surface structures are the result of the deposition of entire micelles, which collapse on the surface after solvent evaporation. However, it has also been suggested[12] that these structures are due to spontaneous self-ordering of diblock copolymers into a 2D superlattice.

The objective of the present study is to investigate the conformational behavior of diblock copolymer micelles deposited on top of an adsorbed monolayer, formed by the same diblock copolymers. Samples were prepared by immersing a mica surface in toluene solutions of diblock copolymers, at concentrations above and below cmc. After withdrawal of the surface from the solution, the samples were just let to dry, without removing molecules not strongly bound to the surface. Spherical structures were observed on top of the adsorbed monolayer, when a micellar solution of the largest diblock copolymer was used. It will be argued that these structures are due to direct deposition of whole micelles, which existed in the solution. The polymer solution with concentration below cmc does not produce any spherical objects on top of adsorbed monolayer. Four diblock copolymers consisting of the same PS block but with various molecular weights of the P2VP chains were employed to investigate the influence of micelle aggregation number on the structure of the upper layer of the polymer films. It will be shown that the conformation of the macromolecules forming an array of spherical micelles on an adsorbed monolayer, observed for the largest diblock copolymer, does not correspond to a thermodynamic equilibrium. A transformation, first from spherical structures into elliptic ones, then worm-like and finally into lamella-like structures, occurs when the films are exposed to toluene. The reasons for such transformations will be discussed.

3.I.2 EXPERIMENTAL SECTION

Details of the materials are given in Table 3.I.1. The block copolymers were dissolved in toluene (Merck). The selectivity of the solvent gives rise to micelle formation if the polymer concentration exceeds a certain value –the cmc. For the diblock copolymers used in this study, the exact cmc is not known, but an approximation can be made. Tang et al.[15], using light scattering, determined a cmc of 0.062 mg·ml^{-1} for the $P2VP_{76}PS_{577}$ diblock and 0.065 mg·ml^{-1} for the $P2VP_{60}PS_{60}$ diblock, in toluene. Sikora et al.[16] used block copolymers with larger PVP blocks and determined a cmc of the order of 3 mg·ml^{-1}. We expect therefore that the two solutions prepared for the $P2VP_{102}PS_{75}$, 0.05 mg·ml^{-1} and 0.5 mg·ml^{-1}, are below and above cmc, respectively. This estimation is also corroborated by experimental data presented here and elsewhere[17]. Toluene solutions with concentrations of 0.5 mg·ml^{-1} for the $P2VP_{68}PS_{75}$, $P2VP_{32}PS_{75}$ and $P2VP_{3.4}PS_{75}$ diblock copolymers are expected to be above the cmc.

Sample code	M^{P2VP} (g·mol^{-1})	M^{PS} (g·mol^{-1})	d	R^{core} (nm)	Q
$P2VP_{102}PS_{75}$	102000	75000	1.12	45	390
$P2VP_{68}PS_{75}$	68000	75000	1.09	28	150.4
$P2VP_{32}PS_{75}$	32000	75000	1.06	23	101.4
$P2VP_{3.4}PS_{75}$	3400	75000	1.04	9	15.6

Table 3.I.1: *Characteristics of the P2VP/PS diblock copolymer micelles. M^I: molecular weight of polymers; d: polydispersity; R^{core}: the radius of the core of the micelles, obtained from ref. 19 and Q: the aggregation number of micelles, evaluated according to ref. 18.*

Mica (clear ruby, grade 2) was obtained from Mica New York Corporation. Pieces of 1×1 cm^2 were cleaved in a laminar flow hood and placed in a polymer solution for a certain incubation time. For every mica sheet a fresh solution was used. The mica sheets were withdrawn from the polymer solution, and let to dry in a laminar flow hood, at room temperature. The presence of airflow can have an influence on the structure of the films. However, samples that were let to dry outside the laminar flow hood did not show any morphological difference. To obtain the surface topography, after drying, the samples were imaged with a Nanoscope III AFM (Digital Instruments Santa Barbara), operating in tapping mode. Measurements were performed under ambient conditions. For solutions above the cmc, several samples were made with incubation times ranging from a few seconds to several days. The topography of these films did not show any significant differences.

A series of samples were exposed to toluene. In the first exposure the film was placed in vapours of toluene for 10 min., subsequent exposures involved liquid toluene, by placing a droplet of toluene.

3.I.3 RESULTS AND DISCUSSION

3.I.3.1 BLOCK COPOLYMER MICELLES ON TOP OF ADSORBED MONOLAYERS

Figure 3.I.1 depicts the topography of a mica sheet immersed in the toluene solution of the $P2VP_{102}PS_{75}$ diblock copolymer, at a concentration above cmc. We observe that the coverage is incomplete, a two-phase region is revealed with domains of high polymer density separated from polymer-free areas. Furthermore also multilayers are formed.

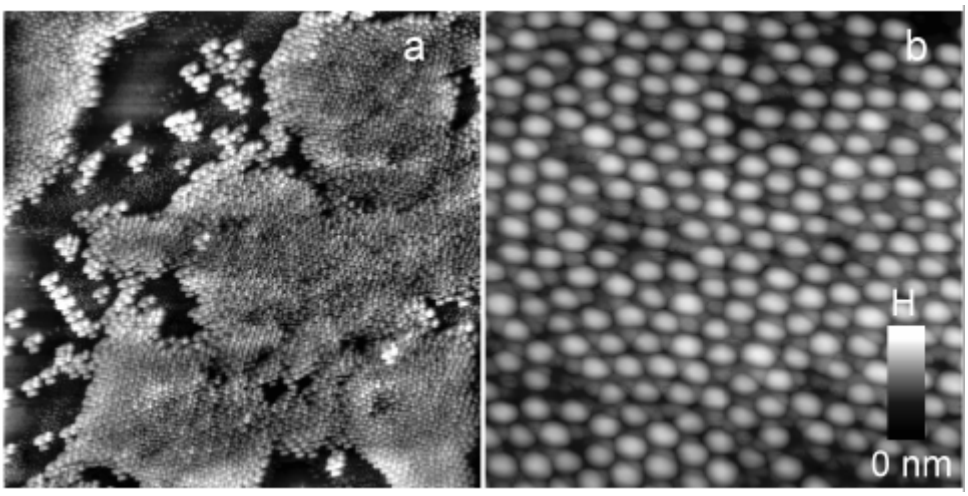

Figure 3.I.1: *AFM image of a freshly cleaved mica sheet after dipping in a toluene solution (0.5 mg/ml) solution of the $P2VP_{102}PS_{75}$ block copolymer. The gray scale represents the height of the features, H.* a) *A 6 ´ 6 mm² area (H = 35 nm);* b) *A 1 ´ 1 mm² area (H = 20 nm).*

For films prepared from solutions, it has been suggested[2] that a two-step mechanism exists. First a homogeneous copolymer monolayer is formed on the substrate, with the polar P2VP segments sticking to the polar substrate and thus grafting the PS, forming a dense layer. In the second step, micelles (with the P2VP block in the core of the micelle, and the PS block acting as a protective layer around the collapsed block, forming the corona of the micelle) will be deposited on the layer. Figure 3.I.2 is a schematic representation of the mechanism.

Figure 3.I.2: *Schematic representation of the process. A represents the substrate, B the adsorbed monolayer and C the layer of micelles. The black curves represent the P2VP blocks while the gray ones the PS blocks.*

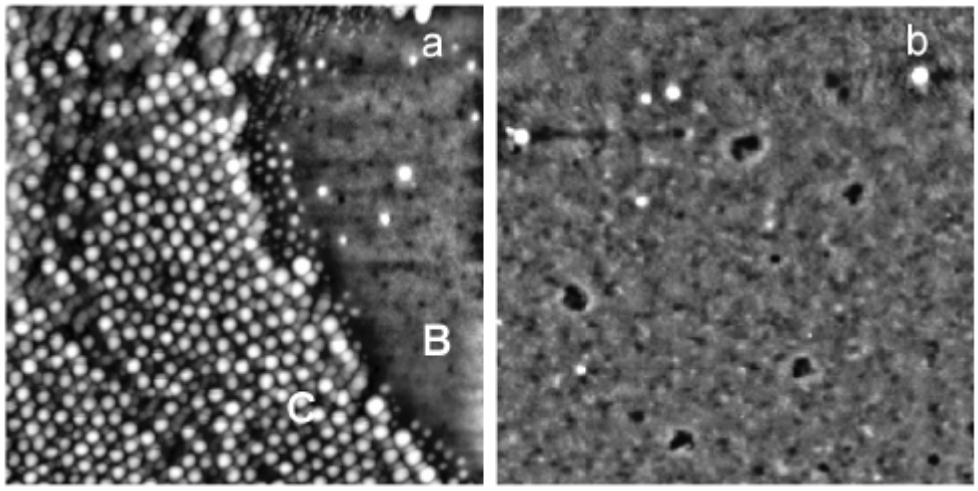

Figure 3.I.3: *2 ´ 2mm² scan of sample in figure 3.I.1 showing the proposed mechanism. a) In area B not covered with micelles, the adsorbed monolayer is visible; b) The remaining adsorbed monolayer after rinsing the sample with solvent and blowing it dry.*

Figure 3.I.3a is a $2 \times 2\ \mu m^2$ zoom of the sample shown in figure 3.I.1. In this area of the sample the underlying adsorbed monolayer is revealed. After rinsing the sample with pure solvent and drying it, under a stream of argon, only the diblock copolymers that are strongly attached on the substrate via the P2VP block remain (figure 3.I.3b).

It is known from other techniques[19] that diblock copolymer micelles have spherical shape in solution. The micelles deposited on the adsorbed monolayer are also globular but slightly elongated, figure 3.I.1. Reasons for the observed deformation will be discussed in detail in the section 3.I.3.4. The micelles in the polymer-rich domain tend to

order themselves in a hexagonal packing,[20] with the center-to-center distance between the micelles being 65 ± 5 nm.

The aggregation number, Q (number of unimers per micelle), can be estimated from the size of the spherical structures, measured from the AFM images using the volume condition (a = 25 ± 1 nm, b = 35 ± 0.35 nm, c = 30 ± 0.25 nm, where a, b and c are the principles semi-axes of the ellipsoid):

$$\rho_m = \frac{QM}{VN_a} \Leftrightarrow Q = \rho_m \frac{4/3 \pi abc}{M} N_a \qquad [3.I.1]$$

where N_a, is Avogadro's number and M the molecular weight of the diblock copolymer. The aggregation number of the observed collapsed micelles can be also calculated by:

$$\frac{4\pi}{3} abc = Q(N_{PS} + N_{P2VP})v \qquad [3.I.2]$$

where N_{PS} and N_{P2VP} are the polymerization index of the PS block and P2VP blocks respectively, and v is the volume occupied by a monomer (0.16 nm^3). Assuming that the micelle density, ρ_m, is similar to the bulk polymer density of PS and P2VP, $\rho_{PS} = \rho_{P2VP} =$ 1.06 g/cm^3, the aggregation number of 390 ± 20 can be found.

In a previous study[19], an aggregation number of 308 was found for the same diblock copolymer, by means of transmission electron microscopy. The aggregation number of the micelle was evaluated (using the Daoud–Cotton model[21]) from the size of the dense region (observed on TEM images), which was treated as a micelle core. It has to be noted that because of the convolution of the tip apex, there is also some uncertainty in the sizes found by evaluation of AFM images. Nevertheless, there is reasonable agreement between the aggregation number determined from AFM and the value estimated from TEM images, taking into account possible deviations of the density of the material in a thin film from its bulk density value (the possibility of toluene molecules trapped in the polymer chains cannot be excluded).

At this point, it can still be argued that the micelles observed on top of the adsorbed monolayer were formed during the evaporation process, while the polymer film was drying. Studies[22, 23, 24] have shown that the kinetics of micelle formation in solution to be relatively slow. The micellization kinetics of poly(α-methylstyrene)/poly(vinylphenethyl alcohol) diblock copolymers in selective solvent has been investigated[24] by performing temperature jumps within the micellar region. The characteristic time associated with the process of micelle re-equilibration was in the range of hours depending on polymer concentration and temperature. Although we have used a diblock copolymer with a different chemical structure, we can expect that the characteristic time for micelle formation on top of an adsorbed monolayer is of the same order of magnitude or even larger than that discussed in ref. 24, since we deal with a more dense polymer system. We can speculate that the time of toluene evaporation from

the film (which was in the range of seconds to a minute) has been too short to allow new micelle formation. Hence, the globular objects with aggregation numbers similar to those of bulk micelles, must be ordinary micelles formed in solution and carried away by the substrate during the withdrawal process.

3.I.3.2 SOLUTIONS BELOW THE CMC

If the conclusion discussed above is correct, the results of adsorption from a polymer solution with a concentration below cmc must be different, with no micelles present. Indeed, figure 3.I.4a depicts an AFM topography image of a mica surface immersed in a solution of $P2VP_{102}PS_{75}$ at a concentration below cmc (0.05 mg·ml^{-1}). In this case no ordered micelles are observed, but agglomerates of macromolecules, with an elliptic / ribbon-like shape. These structures have an anisotropic form, the ratio of the height to the width is small.

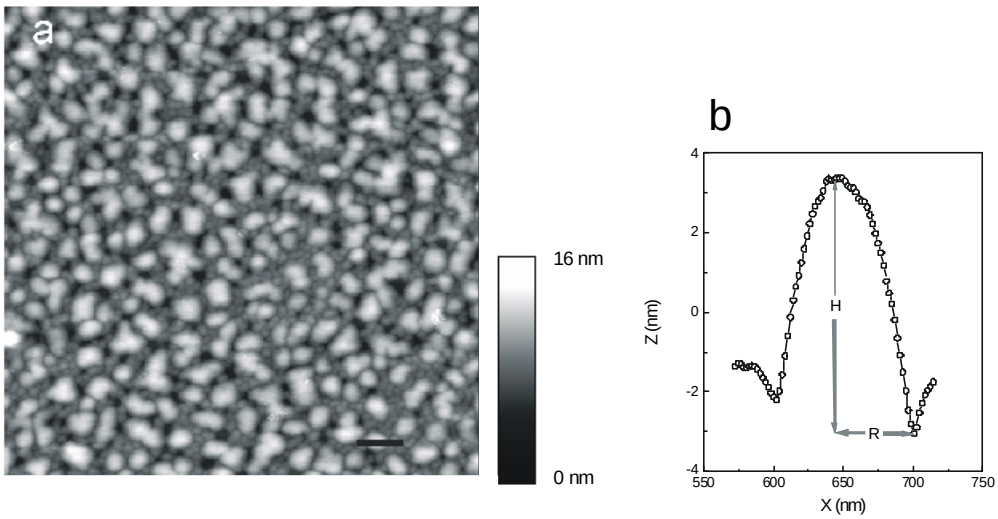

Figure 3.I.4: a) *2 ´ 2mm^2 AFM image of a freshly cleaved mica sheet after dipping in 0.05 mg/ml toluene solution of the $P2VP_{102}PS_{75}$ block copolymer for a few minutes, and subsequent drying in a laminar flow hood. The gray scale indicates the height, 16 nm;* b) *Cross-profile of a structure shown in the AFM image.*

The contact angle of the structures, *q*, can be measured from the AFM images as:

$$\tan\left(\frac{q}{2}\right)=\frac{H}{R} \qquad [3.I.3]$$

where H is the height of the structure and R is the averaged "radius" of the formations (figure 3.I.4b). θ is found to be equal to 11 ± 1.5 deg. The reasons for the formation of

structures with a characteristic contact angle could be due to dewetting mechanisms such as "autophobic" behavior; i.e., a liquid does not spread on its own monolayer[25, 26], or due to the segregation of diblock copolymers into flattened structures.

3.I.3.3 INFLUENCE OF MICELLE AGGREGATION NUMBER

As we discussed in the previous sections, the observed spherical structures on top of the adsorbed monolayer must be bulk micelles already existing in the solution of the $P2VP_{102}PS_{75}$ copolymer. If so, the structures emerging on top of the adsorbed monolayer should depend on the aggregation number of the bulk micelles. Figure 3.I.5 depicts the topography of the upper layer of mica substrates immersed in toluene solutions of the $P2VP_{68}PS_{75}$ (3.I.5a), $P2VP_{32}PS_{75}$ (3.I.5b) and $P2VP_{3.4}PS_{75}$ (3.I.5c) diblock copolymers, at concentrations above the cmc. The diblock copolymers have the same size of PS chain but varying P2VP sizes and hence aggregation numbers.

The $P2VP_{68}PS_{75}$ film exhibits some spherical structures with a diameter ranging from 10 nm to 57 nm, while on the background a vague worm-like structure can be distinguished. The worm-like structure is more evident for the upper layer of the $P2VP_{32}PS_{75}$ film, with a height of 3.5–4 nm. Spherical structures are not present there. For the smallest diblock copolymer, the $P2VP_{3.4}PS_{75}$, the worm-like structure is not pronounced. The structure is flattened and the film exhibits holes with a characteristic height of 7 nm (figure 3.I.5 c,d).

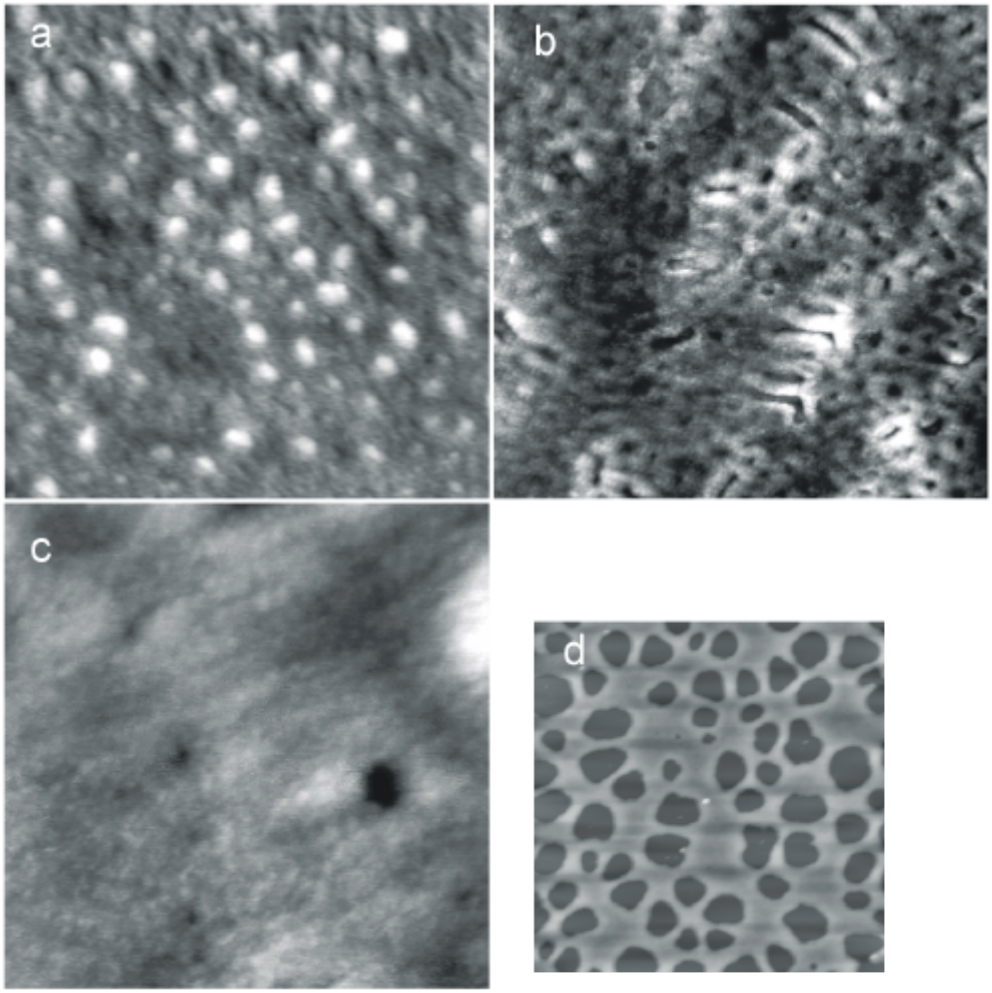

Figure 3.I.5: *AFM images of mica substrates after immersion in 0.5 mg·ml^{-1} toluene solutions of* a) *$P2VP_{68}PS_{75}$. The image covers a 1 ´ 1 mm^2 area and the height is 5 nm;* b) *$P2VP_{32}PS_{75}$. The image covers a 1 ´ 1 mm^2 area and the height is 3.4 nm;* c) *$P2VP_{3.4}PS_{75}$. The image covers a 0.6 ´ 0.6mm^2 area and the height is 5 nm;* d) *4 ´ 4mm^2 area of $P2VP_{3.4}PS_{75}$ and the height is 40 nm.*

It appears that the deposited micelles tend to lose their spherical shape with decreasing size of the P2VP block, and thus aggregation number (table 3.I.1). The micelles are not sufficiently stable to retain their original shape during the evaporation of the solvent, and a transformation into a more thermodynamically favored structure occurs. In a previous study[2], worm-like structures were observed when the polymer concentration of the solution was increased. Here, we observe a similar effect when the size of the P2VP block decreases (at constant polymer concentration).

The reason for this phenomenon can be the following. Firstly, for solutions of micelles with smaller aggregation number the amount of free unimers is also larger, i.e. the cmc is larger: $C_{cmc} \approx \exp\left(-Q^{5/6}\right)$ [27]. This increases the relative fraction of unimers in the solution.

Secondly, the final structural result depends also on the unimer expulsion rate from deposited micelles. The characteristic time for unimer expulsion from a micelle with aggregation number Q is of the order of[27]

$$t_{\exp}^{up}\Big|_{solution} \approx \frac{h_s v}{kT} N_{PS}^{9/5} Q \qquad [3.I.4]$$

$t_{\exp}^{up}$ increases with an increase of micelle aggregation number. Hence, it is natural to expect that adsorbed micelles with large aggregation number ($P2VP_{102}PS_{75}$ micelles) will "dissociate" into unimers more slowly than smaller micelles ($P2VP_{68}PS_{75}$ or $P2VP_{32}PS_{75}$ micelles). The process of micelle dissociation into unimers leading to flattening of the polymer layer depends also on the solvent evaporation time, which we will be discussed below.

3.I.3.4 EFFECT OF "DISSOLUTION"

A mica sheet was incubated, for a few seconds, in a toluene solution of $P2VP_{102}PS_{75}$, at a concentration above cmc. Micelles were observed on an adsorbed monolayer, figure 3.I.1. A droplet of toluene was then placed on the sample, let to dry, and the topography of the sample was recorded again. The topography of the sample showed only a small number of micelles, implying that the ones that disappeared were incorporated in the adsorbed monolayer. Since, the grafting density of the adsorbed monolayer is low, it is energetically favorable for the non-grafted polymer chains to enter the adsorbed monolayer and adsorb, due to the strong affinity of the P2VP block with mica.

Thus, in order to examine the influence of solvent on the stability of micelles deposited on an adsorbed monolayer, a monolayer with high grafting density should be used. Such adsorbed monolayers can be obtained either by using a diblock copolymer with a small P2VP block or by incubating the mica sheet in the polymer solution for a sufficiently long time. We have chosen the second approach. A mica sheet was incubated in a toluene solution of $P2VP_{102}PS_{75}$ at a concentration of 0.05 mg/ml[28] for 1 year. The sample was rinsed and dried under a stream of argon. To test if any non-grafted chains remained, the topography of the adsorbed monolayer was recorded. A homogeneous film was obtained. The sample was then dipped in the micellar solution of the same copolymer, for a few seconds, and let to dry. A similar image as in the case of a mica sheet incubated in micellar solutions followed by no rinsing was obtained.

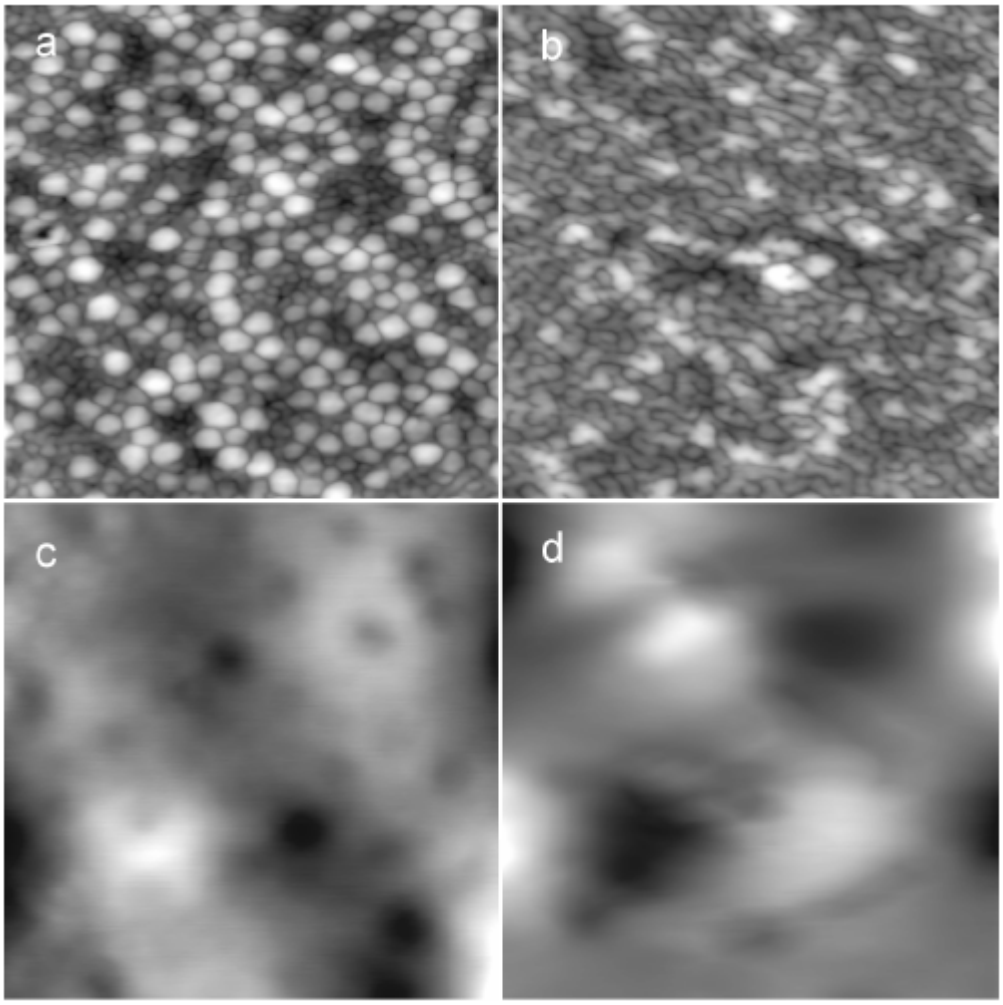

Figure 3.I.6: *AFM topographies of the same surface area after consecutive exposures to toluene, showing the evolution process of surface micelles of the* $P2VP_{102}PS_{75}$ *diblock copolymer.* a) *First (H=15nm);* b) *Second (H=15nm);* c) *Third (H=20nm) and* d) *Fifth exposure (H=70nm). Each image covers an area of 2 ´ 2mm*^{2}.

Figure 3.I.6 shows a series of AFM images of the "same" area[29] revealing the shape changes of $P2VP_{102}PS_{75}$ micelles cast on the adsorbed monolayer after five consecutive exposures to toluene. Figure 3.I.6a depicts the topography after the first exposure to toluene (see experimental section). On the top surface of the film agglomerates are observed with an average diameter, *D*, of 143.8 ± 5 nm and height[30], *H*, of 5.3 ± 0.15 nm. These structures have an anisotropic form, the ratio of the height to the diameter is small, H < D. The aggregation number found for these structures, Q = 408.5 ± 30, is close to the aggregation number found for the original spherical micelles

calculated from figure 3.I.1b. These are the bulk micelles observed before the exposure to toluene however, a transformation into an elliptic shape, with an axial symmetry within a plane parallel to the interface has occurred.

An exposure to toluene for a second time causes the structures to totally lose their spherical shape and transform into worm-like structures with a thickness of 73 ± 1 nm (figure 3.I.6b), as in the case of the film formed by the $P2VP_{32}PS_{75}$ block copolymer (figure 3.I.5b). A third exposure to toluene yields another transformation into an undefined structure with the appearance of holes with a height of 9 nm. Further exposures to toluene yield similar topographies with an increase of the height fluctuations; after the fifth exposure to toluene the height of the holes had increased to 30 nm.

The physical reasons for the changes observed can be explained along the following lines. In solution, the unfavorable interactions between PS and P2VP blocks (the Flory–Huggins parameter is $\chi_{PS/P2VP} = 0.11$[31]) and the selectivity of the solvent, lead to micelle formation, in which the minimal contact between PS-P2VP-blocks is achieved. When a substrate is immersed in the micelle solution, both unimers and micelles carried away when substrate is removed from the solution. After quick evaporation of solvent, the structure of the adsorbed polymer layers containing both unimers and micelles (possibly deformed) remains unchanged for a long time due to the slow kinetics of chain motion in melts. Indeed, the characteristic time for micelle diffusion in melts is exponentially large: $\tau \approx \exp(N_{PS})$. Moreover, even the characteristic time for unimer expulsion from a micelle is rather large[27]:

$$\tau_{\exp}^{up}\Big|_{melt} \approx \frac{\zeta}{kT}\frac{v^{4/3}}{a_{pr}^{2}}Q^{4/3}\left(N_{PS}+N_{P2VP}\right)^{7/3} \qquad [3.I.5]$$

where ζ is the monomer friction coefficient and a_{pr} is the step length of the primitive path in the reptation model[32].

As a result, the structure of adsorbed polymer/micelle layers (figure 3.I.7a) remains kinetically quenched in the absence of solvent even though this structure does not correspond to thermodynamic equilibrium, i.e. the free energy associated with the interfacial area between PS and P2VP blocks is larger than minimum, which is that of a lamella-like structure.

Upon solvent addition, polymer chains of the upper layer become mobile again. The characteristic time for unimer expulsion defined by eq [3.I.4] is considerably smaller than that in the melt (eq [3.I.5]). As a result, micelles of the upper layer start to transform and decompose (figure 3.I.7b). Released polymer chains tend to penetrate into the layers close to substrate however, the whole process requires the presence of solvent in those layers. So, multiple addition of solvent is required for the decomposition of all adsorbed polymer micelles (figure 3.I.7c). The first exposure to solvent “melts” the upper layer of the polymer/micelle structure, the second one “melts” some intermediate layer, which is

somewhat closer to the substrate, and so on till all adsorbed micelles will be dissolved and rearrange in an equilibrium ordered lamellar structure (figure 3.I.7c)

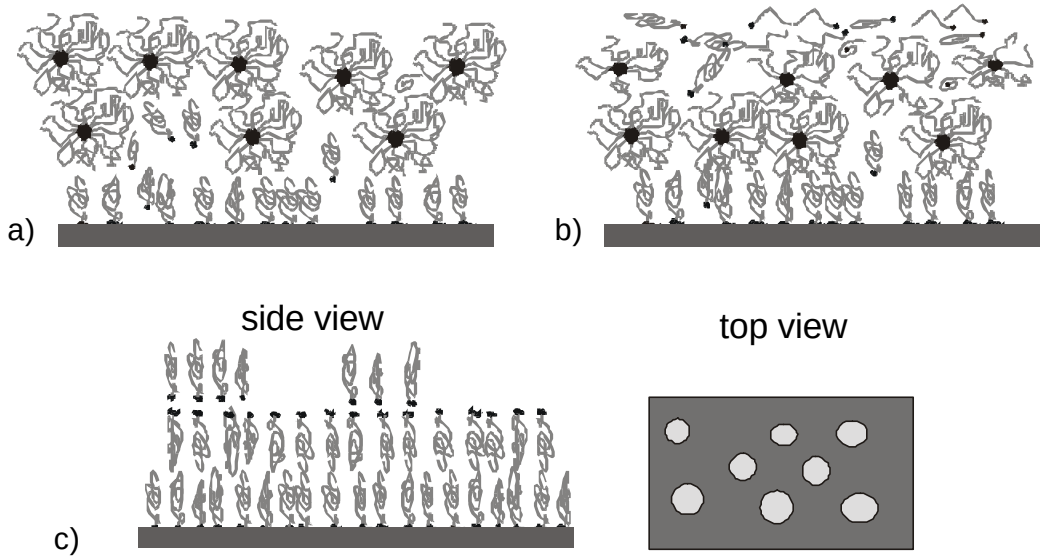

Figure 3.I.7: *Schematic representation of the proposed mechanism.* a) *Material deposited on the adsorbed monolayer, micelles and unimers;* b) *Decomposition of micelles into unimers;* c) *Ordering of unimers into lamella-like structures.*

It is worthwhile to compare the results of dissolution of polymer/micelle adsorbed layers with the polymer layers formed upon annealing of the sample. The sample shown in figure 3.I.8 was annealed at 183 °C for 1.5 hours, well above the glass transition temperature of the diblock, in order to observe the "equilibrium" structure of the film used in the experiment of figure 3.I.6. Formation of polymer islands on the substrate is evident. The PS blocks, having a lower surface energy than the P2VPs', will reside at the polymer/air interface, while the P2VP blocks will reside at the substrate/polymer interface, due to the affinity of these segments with mica.

In general, annealed thin films of nearly symmetric copolymers show a surface-induced ordering into a multilayer morphology parallel to the film surface.[6] It has been established that this orientation, in thin film geometry, was induced due to surface energy differences between the block components or the chemical affinity of one of the blocks on the one hand, the substrate and microphase separation of the block copolymers on the other. If L is the lamella periodicity of a symmetric diblock copolymer in the bulk, then this preferred orientation causes a quantization of the film thickness to $(n+1/2)L$, with n an integer. For films that do not satisfy this constraint, islands or holes with a step height of L will be formed on the surface. Three mechanisms have considered, individual process growth, coalescence and dissolution of the domains. The phenomenon of island

and hole formation of diblock copolymer film surfaces has been studied[33, 34, 35], and has been considered to be a signature of lamella formation.

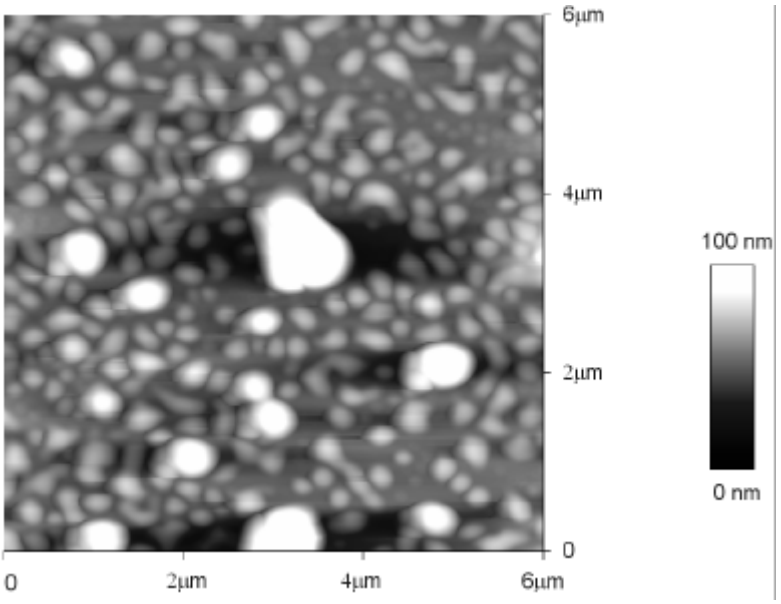

Figure 3.I.8: *AFM topography of the sample in figure 3.I.6, after annealing it at 183* °C *for 1.5 hours.*

For the $P2VP_{102}PS_{75}$ diblock copolymer, lamellar morphologies are observed,[36] –the lamella period is equal to 70 ± 5 nm[19]– upon annealing of the film well above the glass transition temperature of the blocks. The lamella period is larger than the height of the holes observed in the upper layers of the films of the $P2VP_{102}PS_{75}$ diblock copolymer (figure 3.I.5c and 3.I.6d), after the films were exposed to toluene, supporting the idea that some sort of lamella are formed at the polymer surface.

Concluding it can be remarked that the solvent exposure plays the same role as the annealing process however the kinetics of the two processes is different. With exposing the film to solvent the early stages of formation of an equilibrium structure can be assessed.

3.I.4 CONCLUSIONS

The organization of polymer chains, deposited in the form of micelles on a mica substrate from P2VP/PS micellar solutions was studied using the AFM technique. For $P2VP_{102}PS_{75}$ solutions at concentrations above the cmc, an array of monodisperse spherical micelles partially covering the adsorbed monolayer was observed. It was argued that it is highly

improbable that these assemblies were formed during the evaporation process. The size of the micelles observed was similar to that of $P2VP_{102}PS_{75}$ micelles in solution. Also, $P2VP_{102}PS_{75}$ solutions at concentrations below cmc provided layers with no traces of any spherical objects. This suggests that the observed spherical structures on top of the adsorbed monolayer are the micelles already existing in the solution and deposited on the film during the removal of the substrate from $P2VP_{102}PS_{75}$ micellar solutions.

The influence of micelle aggregation number, reflecting the size of the insoluble block, on the structure of the upper layer of the film was studied. With a decrease of micelle aggregation number the spherical objects deposited on top of the adsorbed monolayer start losing their shape and worm-like structures appear. For the smallest diblock copolymer, the structures were flattened with the appearance of holes, reminiscent of the formation of equilibrium lamellar structures. The reasons for such phenomena were discussed based on the difference in cmc (unimer amount) and unimer expulsion rates for the micelle solutions.

The transformations of adsorbed polymer/micelle layers upon stepwise dissolution were also studied. It was observed that the micelles deposited on the adsorbed monolayer tend to decompose upon dissolution, changing their shape from a spherical to an elliptical one. For larger degree, of dissolution, worm-like structures or lamella-like structures appear. Such structural transformations have been attributed to the "recovery" of the mobility of polymer chains upon addition of solvent. The structures observed upon dissolution were similar to ones formed in spin-cast thin films of diblock copolymers upon annealing. In both cases the kinetics of formation of an ordered structure depends on the mobility of the macromolecules, however the kinetics is different.

REFERENCES

[1] a) Hadziioannou, G.; Patel, S.; Granick, S.; Tirrell, M. *J. Am. Chem. Soc*. **1986**, 108, 2869
b) Parsonage, E.; Tirrell, M.; Watanabe, H.; Nuzzo, R. G. *Macromolecules* **1991**, 24, 1987
[2] Meiners, J.C.; Ritzi, A.; Rafailovich, M.H.; Sokolov, J.; Mlynek, J.; Krausch, G. *Appl. Phys.* **1995**, A61, 519
[3] Spatz, J.P.; Eibeck, P.; Möβmer, S.; Möller, M.; Herzog, T.; Ziemann, P. *Adv. Mater.* **1998**, 10, 11, 849
[4] Tuzar, Z.; Kratochvil, P. *Surface Colloid Sci.* **1993**, 15, 1
[5] Bates, F.S.; Fredrickson G.H. *Annu. Rev. Phys. Chem.* **1990**, 41, 525 and references therin
[6] a) Anastasadis, S.H.; Russell, T.P.; Satija, S.K.; Majkrzak, C.F. *Phys. Rev. Lett*. **1989**, 62, 1852
b) de Jeu, W.H.; Lambooy, P.; Hamley, I.W.; Vaknin, D.; Pederson, J.S.; Kjaer, K.; Seyger, R.; van Hutten, P.; Hadziioannou, G. *J. Phys. II (France)* **1993**, 3, 139
c) Henkee, C.S.; Thomas, E.L.; Fetters, L.J. *J. Mater. Sci.* **1988**, 23, 1685
d) Russell, T.P.; Coulon, G.; Deline, V.R.; Green, P.F. *Macromolecules* **1989**, 22, 4600

e) Anastasiadis, S.H.; Russell, T.P.; Satija, S.K.; Majkrzak, C.F. *J. Chem. Phys.* 1**990**, 92, 5677
[7] a) Coulon, G.; Collin, B.; Ausserre, D.; Chatenay, D.; Russel. T.P *J. Chem. Phys. (France)* **1990**, 52, 2801
b) Collin, B.; Chatenay, D.; Coulon, G.; Ausserre, D.; Gallot, Y. *Macromolecules* **1992**, 25, 1621
[8] Grim, P. C. M.; ten Brinke, G.; Hadziioannou, G.; Nyrkova, I.A.; Semenov, A.N. M*acromolecules* **1995**, 28, 7501
[9] Mayes, A.M.; Russell, T.P.; Bassereau, P.; Baker, S.M.; Smith, G.S. *Macromolecules* **1994**, 27, 749
[10] Spatz, J.P.; Sheiko, S.; Möller, M. *Macromolecules* **1996**, 29, 3220
[11] Meiners, J.C.; Quintel-Ritzi, A.; Mlynek, J.; Elbs, H.; Krausch, G. *Macromolecules* **1997**, 30, 4945
[12] Li, Z.; Zhao, W.; Liu, Y.; Rafailovich, M.H.; Sokolov, J.; Khougaz, K.; Eisenberg, A.; Lennox, R.B.; Krausch, G. *J. Am. Chem. Soc.* **1996**, 118, 10892
[13] Meiners, J.C.; Elbs, H.; Ritzi, A.; Mlynek, J.; Krausch, G. *J. Appl. Phys.* **1996**, 80, 2224
[14] Spatz, J.P.; Roescher, A.; Sheiko, S.; Krausch, G.; Möller, M. *Adv. Mater.* **1995**, 7, 731
[15] a) Tang, W.T. Ph.D. thesis, Stanford University, **1987**,
b) Tang, W.T.; Hadziioannou, G.; Cotts, P.M.; Smith, B.A. *Polymer preprints Am. Chem. Soc.* **1986,** 27, 107
[16] Sikora, A.; Tuzar, Z. *Makromol. Chem.* **1983**, 184, 2049
[17] Stamouli, A.; Pelletier, E.; Koutsos, V.; van der Vegte, E.; Hadziioannou, G. *Langmuir* **1996**, 12, 3221
[18] The micelle core depends on the aggregation number as $R_{core} \approx Q^{1/2}$ thus, by knowing the aggregation number and core radius for one micelle, we can estimate the aggregation number for the rest, assuming that their micelle radius core is known.
[19] Esselink, F.J. *Direct imaging of block copolymer structure in solution and neat state* Ph.D. thesis, University of Groningen, **1998**
[20] Dubochet, J.; Adrian, M.; Chang, J-J.; Homo, J-C.; Lepault, J.; McDowall, A.W.; Schultz, P. *Quart. Rev. Biophys.* **1988**, 21, 126
[21] Daoud, M.; Cotton, J. P. *J. Phys. (France)* **1982**, 25, 4967
[22] Esselink, F.J.; Dormidontova, E.; Hadziioannou, G. *Macromolecules* **1998**, 31, 2925
[23] Semenov, A. N. *Macromolecules* **1992**, 25, 4967
[24] a) Honda, C.; Hasegawa, Y.; Hirunuma, R.; Nose, T. *Macromolecules* **1994**, 27, 7660
b) Honda, C.; Abe, Y.; Hose, T. *Macromolecules* **1996**, 29, 6778
[25] Hare, E.F.; Zisman, W.A. *J. Phys. Chem.* **1955**, 59, 335; **1955**, 59, 1097
[26] a) Leibler, L.; Ajdari, A.; Mourran, A.; Coulon, G.; Chantenay, D. *Ordering in Macromolecular systems*; Teramonto, A.; Kobayashi, M.; Norisuie, T.; Eds., pringer-Verlag: Berlin, **1994**

b) Shull, K. *Faraday Discuss.* **1994**, 98, 203. d) Yerushalmi-Rozen, R.; Klein, J.; Fetters, L.J. *Science*, **1994**, 263, 793
e) Reiter, G.; Auroy, P.; Auvray, L. *Macromolecules* **1996**, 29, 2150
[27] Dormidontova, E.E. *Macromolecules*, **1999**, 32, 7630
[28] A polymer concentration below the cmc was preferred, due to complexity of the morphology of the samples that are incubated at concentrations above cmc for a long incubation time.
[29] The exact area can never be found back, due non linear effects of the piezo.
[30] The height was measured at isolated structures
[31] Shull, K.R.; Kramer, E.J.; Hadziioannou, G.; Tang, W. *Macromolecules* **1990**, 23, 4780
[32] Doi, M.; Edwards S.F. *The Theory of Polymer Dynamics;* Oxford University Press: New York, 1986.
[33] a) Coulon, G.; Collin, B.; Ausserre, D.; Chatenay, D.; Russel. T.P *J. Phys. (France)* **1990**, 52, 801
b) Collin, B.; Chatenay, D.; Coulon, G.; Ausserre, D.; Gallot, Y. *Macromolecules* **1992**, 25, 1621
[34] Grim, P.C.M.; ten Brinke, G.; Hadziioannou, G.; Nyrkova, I.A.; Semenov, A.N. *Macromolecules* **1995**, 28, 7501
[35] Mayes, A.M.; Russell, T.P.; Bassereau, P.; Baker, S.M.; Smith, G.S. *Macromolecules* **1994**, 27, 749
[36] $c_{PS/P2VP}N$=170

3.II

INFLUENCE OF SOLVENT QUALITY ON ADSORBED DIBLOCK COPOLYMER MONOLAYER. FORMATION OF SURFACE OCTOPUS "MICELLES"

Atomic Force Microscopy is used to study the conformation behavior of a diblock copolymer on a solid surface while the solvent quality is changed. In a first step, the copolymer P2VP/PS is adsorbed onto mica from a selective solvent (the PS block is well solvated and the P2VP is not solvated). In such a case, the P2VP block adsorbs preferentially on the substrate and anchors the PS block to the surface. In a second step, the solvent quality is reduced to such an extent that the PS block is no longer solvated. This procedure promotes the formation of surface octopus "micelles". The parameters characterizing this regime are measured using the AFM. In addition, a direct determination of the adsorbance is performed. It reveals that the PS blocks when immersed in good solvent do not overlap: a mushroom surface regime instead of a brush one is thus created at the surface.

3.II.1 INTRODUCTION

The conformation[1] of isolated polymer chains in solution is a function of the quality of the solvent. In the limit of high temperatures, *the good-solvent regime*, polymer chains can be described by self-avoiding walk statistics. In this case the polymer chains are swollen by the solvent, due to excluded volume interactions. As the temperature is lowered, one reaches the Θ temperature, defined as the temperature where the second virial coefficient vanishes. In this case the chains have Gaussian statistics, due to the effective cancellation of the attractive and repulsive interactions. For temperatures below Θ, *the poor-solvent regime*, the chains form collapsed structures in order to avoid contact with the solvent as much as possible. In polymer solutions there is a phase separation for temperatures below Θ into two phases, one that is almost pure solvent and one containing the polymer solution. It is interesting to observe how the changes in solvent quality affect the behavior of polymer molecules confined in a monolayer[2], that is polymer chains tethered on a surface by one of the ends of the polymer chain. It is clear that in the poor-solvent regime the system cannot undergo a macroscopic phase separation due to the strong bond of one end of the polymer chain to the surface.

Therefore, the tendency of the molecules to avoid the solvent will not be completely satisfied, resulting in the formation of spatial domains of large concentration of polymer segments while others will be almost free of solvent.

The stretching of isolated chains in 3D in a bad solvent was studied originally by Halperin and Zhulina[3]. It was argued that at weak extensions the globule deforms into an ellipse and then into a cylinder. At a critical extension, the polymer chain undergoes a sharp first-order transition into a "ball and chain" configuration. This transition is a demonstration of a Rayleigh instability for a liquid cylinder (i.e. the polymer can decrease its surface energy by breaking up into a ball and a thin filament). This instability has consequences for chains grafted to non-adsorbing surfaces. In this case the chains fuse to form octopus surface "micelles" or pinned micelles (figure 3.II.2)

The behavior of tethered chains in poor-solvent conditions has been addressed theoretically by scaling,[4, 5] analytical[6] and numerical[7] self-consistent field (SCF) methods. These approaches assumed lateral uniformity within the layer, and studied the variations of the free energy and the segment concentration profile normal to the surface. While the collapse of tethered chains in the mushroom regime was found to be analogous to the collapse of free chains in dilute solutions, at high surface coverage the density profiles become more step-like with the decrease of the temperature, due to interchain interactions.

Various theoretical studies have addressed the lateral structure as well as the contraction normal to the surface[8-14]. Ross and Pincus[8] examined the conformations of collapsed polymer layers, in the high brush regime, using the Alexander approach and random-phase approximation (RPA) and found that the brushes are stable to lateral fluctuations. Later, Yeung, Balazs and Jasnow[9] looked at the same problem using the RPA and SCF approach. It was found that there is a regime of surface coverages for which the homogeneous layer is unstable and there is formation of clusters on the surface. The contradiction was resolved by Tang and Szleifer[10] who showed that with extending the RPA approach to the low surface coverage regime one finds three regimes. It was shown that at very low surface coverage mushrooms are stable, that this is followed by clusters and that at high surface coverage the homogeneous layer becomes stable. Further numerical SCF analysis[11] Monte Carlo[12] and Molecular Dynamics simulations[13] showed the existence of these three regimes. A scaling analysis has been developed, by Williams[14], based on comparing the free energy of a homogeneous brush with that of the cluster-like structure. In particular octopus surface "micelles" were predicted for a sudden decrease of solvent quality and sufficiently high molecular weight. Finally, Soga et al.[15] using simulations of the Edwards Hamiltonian predicted clusters at the intermediate surface coverages.

The case of polymer chains having tethered ends that are mobile has also been addressed.[16, 11] A lateral phase separation into polymer-rich and polymer-poor phases is predicted. Isotherms and phase diagrams including regions of metastability have been calculated.

Atomic Force Microscope has proven a very successful technique for observing the changes in conformation of grafted polymer layers. O'Shea et al.[17] used PEO/PS diblock copolymers adsorbed on mica and observed "agglomeration" of molecules in solvents of different quality. Zhao et al.[18] studied the lateral structure of PS chains end-grafted on Si substrates by a small reactive end group, whereas in another study[19] the PS was grafted via a short block, PEO, much shorter than the PS block. Both studies confirmed[9] the transition occurring, in poor solvent, from dimples to isolated islands when the grafting density is decreased. Siquera et al.[20] using end-functionalized diblock copolymers observed the three theoretically predicted regimes. Finally, Koutsos et al.[21] used end-functionalized PS chains end-grafted on a gold surface. The experimental data fitted well in a diagram of states which was deduced by scaling arguments.

Auroy at al.[22] examined PDMS chains end-grafted onto silica particles by neutron scattering, over a wide range of surface density and in various solvent conditions. They reported a linear variation of thickness of the polymer layer with temperature. A step-like profile was used to model the experimental data. Karim et al.[23] used PS chains end-grafted onto silicon and immersed in cyclohexane. They found a good agreement with the analytical SCF profile predicted by Zhulina et al.[6] at Θ. Finally, Kent et al.[24] employed Langmuir monolayers formed by asymmetric PDMS/PS diblock copolymers as a function of the temperature. The thickness of the layers, measured by neutron reflectivity, for several temperatures was determined as a function of grafting density and molecular weight, and compared to scaling laws.

In this sub chapter we investigate the conformations of PS chains adsorbed via a P2VP block, when the solvent quality is decreased. The images obtained with AFM show that each polymer chain does not collapse individually but that the PS blocks fuse to form surface octopus "micelles". Although the change of the solvent quality alters the conformation of the PS segments, it does not change the adsorbance[25]. The number of P2VP blocks that are adsorbed onto the substrate remains the same. Thus, information about the chain conformation in good solvent can be obtained.

3.II.2 EXPERIMENTAL SECTION

Poly(2-vinylpyridine)/Polystyrene diblock copolymer ($M_{w,P2VP}$ = 102 000 g·mole^{-1}, $M_{w,PS}$ = 75 000 g·mole^{-1} with an index of polydispersity of 1.12) is used. The size of a polystyrene monomer unit is comparable with the dimension of that of a poly(2-vinylpyridine) one — a_{PS} = 5.46 Å and a_{P2VP} = 5.32 Å: these values were obtained from their bulk densities, ρ_{PS} = 1.06 g/ml and ρ_{P2VP} = 1.17 g/ml[26]. The block copolymer is dissolved in toluene (Merck) at a concentration of 0.05 mg/ml, below the critical micelle concentration (see sub chapter 3.I). Data for the radius of gyration of PS in toluene have been reported[27]: $R_{PS} = 1.86\ N_{PS}^{0.595}$ = 8.9 nm.

Mica sheets (clear ruby, grade 2) are cleaved in a laminar flow hood and immediately immersed in the polymer solution. Toluene is a selective solvent for the

P2VP/PS diblock copolymer, the P2VP block is not solvated and adsorbs on the surface while at the same time the PS block is well solvated and stretches away from the surface. After an appropriate incubation time — presented in Table 3.II.1 —, the mica sheets are taken out, rinsed with toluene and dried under a stream of argon. A commercially available AFM (Topometrix, type Explorer) was employed with microfabricated Si_3N_4 cantilevers — having a spring constant of 0.036 $N \cdot m^{-1}$. The imaging was performed in demineralized water. Several samples were made for each incubation time and each sample was imaged at different areas. Similar images were obtained, demonstrating the reproducibility of the results.

3.II.3 THEORETICAL BACKGROUND

Marques et al.[28] have theoretically studied the adsorption of A-B diblock copolymers onto a solid plane immersed in a highly selective solvent. The A part is in a poor solvent and forms a molten layer on the solid wall where the solvent does not penetrate. The B part is in a good solvent and forms a brush grafted layer on this molten layer. Various adsorption regimes are found depending on the asymmetry between the two parts of the copolymer which is measured by b. This parameter[29] is defined as the ratio of the respective molecular dimensions of the diblock copolymer - $b = \frac{R_{F,B}}{R_{G,A}}$. Assuming that the segment lengths of the A and B blocks are equal, $b = N_B^{6/5} / N_A^{2/3}$.

Three regimes[30] have been found as a function of the value of b. Copolymers with $b > N_A^{1/2}$ can be identified as highly asymmetric, those with $1 < b < N_A^{1/2}$ as moderately asymmetric, and those with $b < 1$ as symmetric.

The overlap coverage, s_o, of the PS blocks onto the P2VP layer adsorbed onto the solid surface can be defined as:

$$s_o = (p R_{PS}^{\ 2})^{-1} \qquad [3.II.1]$$

3.II.4 RESULTS AND DISCUSSION

A typical image of an AFM scanning performed on a moderately asymmetric — $b \cong 25$ — diblock copolymer P2VP/PS adsorbed on mica is presented in Figure 3.II.1.

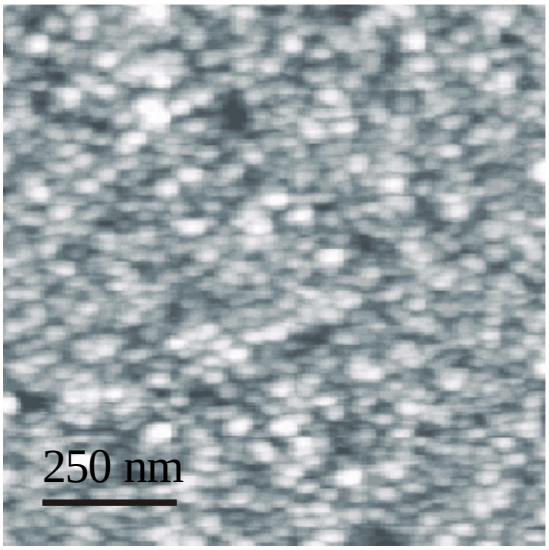

Figure 3.II.1: *AFM image of an adsorbed layer of P2VP/PS diblock taken in water after adsorption from a toluene solution. The mica sheet was immersed in the polymer solution for 224 min.*

An array of close–packed spherical features are observed on the substrate. The grey-scale indicates the height of the features, ranging from 0 (black) to 14 nm (white). From the AFM images we are able to measure the following parameters :

- $\boldsymbol{x}$, number of spherical features within a scanned area.
- $\boldsymbol{D_{half}}$, half the distance between the centres of two neighboring features.

These parameters are presented in Table 3.II.1.

In good solvent the PS blocks are swollen — Figure 3.II.2a — with radius equal to R_{PS} = 8.9 nm[31]. If some overlapping occurs, they can be slightly stretched away from the surface depending on the lateral confinement. When the solvent quality is reduced slowly from good to a worse-than-Θ solvent, each PS block can individually collapse to form its own globule. Its size is given by ~a_{PS} $N_{PS}^{1/3}$ = 4.77 nm. If the PS blocks in good solvent are slightly interpenetrated, *n* PS–blocks fuse together to form a surface octopus "micelle", when the solvent quality is reduced to below Θ — Figure 3.II.2b.

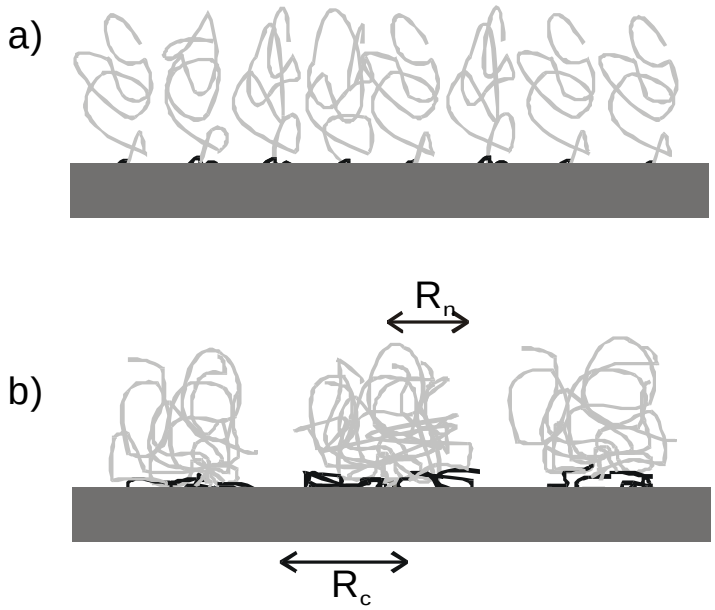

Figure 3.II.2: *Scheme of the diblock copolymer as a function of the solvent quality.* a) *Conformation of an adsorbed layer of P2VP/PS on a mica surface immersed in a good solvent - toluene. The P2VP block is not solvated by toluene and anchors the PS block to the mica surface. The PS block does not adsorb onto mica and dangles in the solution.* b) *the solvent quality has been reduced from good (toluene) to worse-than-Q (water) for the PS block. The PS segments have fused to form octopus "micelles". R_n is the globule radius and R_c is the "corona" radius of a micelle.*

Williams[14] has theoretically studied the formation of surface octopus "micelles" of grafted polymers, when immersed in a bath of solvent of which the quality is changed. The transition from a good solvent to one that is worse-than-Θ solvent for polymer chains which are irreversibly grafted to a surface has been studied. Depending on the grafting density three different regimes can be found. At high grafting densities a uniform collapsed layer occurs[9], at low grafting densities each chain forms its own globule and in the intermediate regime octopus surface "micelles" are formed, see figure 3.II.1. It has to be noted that these have nothing to do with the micelles observed in bulk copolymer systems[32]. Two opposite effects play a role in their formation: they want to minimize the contact area with the solvent, but this is opposed by the stretching energy of the chains which form the micelles.

The characteristic radius of a surface "micelle" should be $R_n \sim a_{PS}(n\ N_{PS})^{1/3}$, which can be determined, using scaling laws, from the minimization of the free energy[14]. Let all the chains in a circle of radius R_c collapse to form a globule of radius R_n, then:

$$R_c \approx a_{PS} N_{PS}^{9/15} \qquad [3.II.2a]$$

$$n \approx N_{PS}^{2/3} \qquad [3.II.2b]$$

$$\frac{R_n}{R_c} \approx N_{PS}^{-1/15} \qquad [3.II.2c]$$

Theoretically, therefore, 14 PS blocks have fused to form one micelle with dimension: R_c ~18.64 nm, and R_n ~ *12* nm.

The numerical prefactors in the above expressions are of order unity, so a semi-quantitative comparison between theory and experimental results can be done. According to the model, half the distance between neighboring globular features, D_{half}, can be equated to R_c. The comparison of the theoretical value of R_c with the values of D_{half} = 24 ± 4 nm (Table 3.II.1) shows a good agreement. This demonstrates that the PS blocks have fused to form surface octopus "micelles" at the mica surface.

Parameters such as the number of chains per unit surface area, σ, and the mass coverage, *G*, can be determined using the AFM. The number, *x*, of features within the surface area covered (S = 500 × 500 nm^2) is counted. As *n* diblock copolymers are involved in the formation of one feature, σ is given by the relation :

$$\sigma = \frac{nx}{S} \qquad [3.II.3]$$

From σ, the mass coverage *G* of polymer onto the mica surface is directly calculated :

$$\Gamma = \frac{(M_{w,PS} + M_{w,P2VP})}{N_a} \sigma \qquad [3.II.4]$$

where N_a is the Avogadro number.

An additional parameter, which will allow a comparison with results obtained with different techniques by other groups, is the grafting density σ^*, which can be calculated as:

$$\sigma^* = \sigma \left(\frac{M_{w,PS}}{M_{w,PS} + M_{w,P2VP}} \right) \qquad [3.II.5]$$

The results are presented in table 3.II.1 as a function of the incubation time of the mica surface within the toluene solution. The mass coverage values are consistent with

published data determined by means of the Surface Forces Apparatus[33], showing the validity of the technique of measurement.

Time (min)	x	D_{half} (nm)	G (mg/m^2)	s (10^{-16} m^{-2})	s^* (10^{-16} m^{-2})	N (10^{-12} moles cm^{-2})
9	92	27.67	1.525	0.519	0.219	0.862
76	98	24.85	1.624	0.553	0.234	0.918
224	113	23.50	1.889	0.643	0.271	1.066
5760	150	20.20	2.486	0.846	0.358	1.405

Table 3.II.1: *Parameters measured from AFM pictures, x: number of features within a scanned area of 500 ´ 500 nm^2, D_{half}: half the distance between the centers of two neighboring features, s: the number of chains per unit surface area, G: the mass coverage, s^*: the grafting density, and N: the number of adsorbed molecules per unit surface area.*

Equation 3.II.1 gives the grafting density value at which the PS blocks just start to overlap, $s_o = 0.3654\ 10^{-16}$ m^{-2}. It is about equal to the value that we have obtained for the highest incubation time (4 days). This shows that the PS blocks in good solvent are closer to a mushroom regime than to a brush regime. However, the PS blocks have to overlap slightly to allow the formation of surface octopus "micelles" when the solvent is changed.

Such a process is supported by results obtained with neutron reflectivity by Field et al.[34]. These authors found that the polymer density profile for the block copolymers with large P2VP blocks was better described by the mushroom-type profile rather than by a brush-type profile. By reducing the size of the adsorbing block they found a soft crossover from mushrooms to brushes. The same conclusion was also reached by other studies[33, 24].

All measurements dealing with the adsorption of block copolymers reveal that the adsorbed amount of polymer increases with time until it reaches a first plateau value. Figure 3.II.3 shows the number of adsorbed molecules, N (moles/cm^2) —calculated from the values of s — as a function of the incubation time of the mica sheets in the polymer solution.

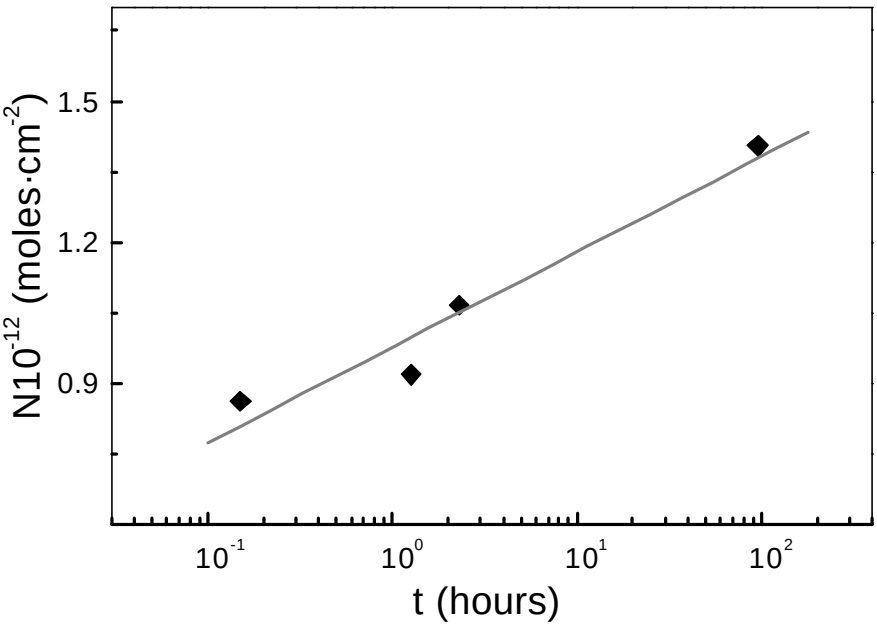

Figure 3.II.3: *Plot of the number of adsorbed molecules, N, as a function of the incubation time of the P2VP/PS layer within the toluene solution. It shows that N varies linearly with log t. The slope of the line corresponds to an adsorption rate of 2.032 10^{-13} moles/h.*

Assuming that the adsorption energy depends only on the thermodynamic characteristics of the diblock layers we can use the Arrhenius relation for describing the adsorption rate:

$$\frac{dN}{dt} = \frac{k}{t} \qquad [3.II.6]$$

where k denotes the average number of adsorbed molecules per hour. From the slope of Figure 3.II.3 we obtain k = 2.032 10^{-13} moles/hour.

3.II.5 CONCLUSIONS

We have presented an AFM study of an adsorbed P2VP/PS copolymer layer. The polymer was adsorbed from a selective solvent in such a way that the P2VP was the anchor block and the PS formed the tails extending from the surface into the solution. The reduction of the solvent quality — from toluene to water — changed the conformation of the PS chains, which fused to create surface octopus "micelles". The AFM images furnish a direct way to measure their sizes and time-dependent adsorption parameters such as the number of chains per unit surface area, the mass coverage or the

grafting density. The mass coverage data are in agreement with independent measurements performed with SFA. In addition, the results confirm previously reported data on similar systems showing that a mushroom regime can be expected, in good-solvent, rather than a brush one.

REFERENCES

[1] Flory, P. J. "*Principles of Polymer Chemistry*" **1953** Cornell University Press (Ithaca N. Y.)
[2] for a review Szleifer, I.; Carignano, M. A. "*Advances in Chemical Physics: Polymeric Systems*" **1996**, Volume XCIV, edited by Prigogine, I.; Rice, S. A. John Wiley & Sons, Inc.
[3] Halperin, A.; Zhulina, E. B. *Europhys. Lett.* **1991**, 15, 417
[4] Halperin, A. *J. Phys. (France)* **1988**, 49, 547
[5] Shim, D. F. K.; Cates, M. E. *J Phys. II (France)* **1980**, 50, 3535
[6] Zhulina, E. B.; Borisov, O. V.; Priamitsyn, V. A. J. *Macromolecules*, **1991**, 24, 140
[7] Huang, K.; Balaza, A. *Macromolecules* **1993**, 26, 4736
[8] Ross, A. S.; Pincus, P. *Europhys. Lett.* **1992**, 19, 79
[9] Yeung, C.; Balazs, A. C.; Jasnow, D. *Macromolecules* **1993**, 26, 1914
[10] Tang, H.; Szleifer, *Europhys. Lett.* **1994**, 28, 19
[11] Carignano, M. A.; Szleifier, I. *J. Chem. Phys.* **1994**, 100, 3210
[12] a) Lai P.-Y.; Binder K. *J. Chem. Phys*. **1992**, 97, 586
b) Weinhold, J. D.; Kumar, S. *J. Chem. Phys.* **1994**, 101, 4312
c) Lai P.-Y. *Comput. Polymer. Sci.* **1992**, 2, 157
[13] a) Grest G. S.; Murat M. *Macromolecules* **1993**, 26, 3108
b) Grest G. S. *Macromolecules*, **1994**, 27, 418
[14] Williams, D.R.M. *J. Phys. II (France)* **1993**, 3, 1313
[15] Soga, K. G.; Guo, H.; Zuckermann, M. J. *Europhys. Lett.* 1995, 28, 531
[16] a) Szleifer, I. *Adv. Chem. Phys.* **1996**, 94, 165
b) Tang, H.; Carignano, M. A.; Szleifier, I. *J. Chem. Phys.* **1995**, 102, 3404
[17] O'Shea, S.J.; Welland, M.E.; Rayment, T. *Langmuir* **1993**, 9, 1826
[18] Zhao, W.; Krausch, G.; Rafailovich, M.N.; Sokolov, J. *Macromolecules* **1994**, 27, 2933
[19] Takahashi, A.; Kawaguchi, M.; Hirota, H.; Kato, T. *Macromolecules* **1980** 13, 884
[20] Siquera, D. F.; Köhler, K.; Stamm, M. *Langmuir* **1995** 11, 3092
[21] Koutsos, V.; van der Vegte, E. W.; Pelletier, E.; Stamouli, A. Hadziioannou, G. *Macromolecules* **1997**, 30, 4719
[22] a) Auroy, P.; Auvray, L.; Leger, L. *Macromolecules* **1991**, 24, 2523
b) Auroy, P.; Auvray, L.; Leger, L. *Macromolecules* **1992**, 25, 4134

[23] a) Karim, A.; Satja, S. k.; Douglas, J. F.; Anker, J. F. Fetters, L. *J. Phys. Rev. Lett.* **1994**, 3, 3407
b) Karim, A.; Douglas, J. F.; Horkay, F.; Fetters, L.; Satja, S. K. *Physica B* **1996**, 221, 331
[24] Kent, M. S.; Majewski, J.; Smith, G. S.; Lee, L. T.; Satija, S. *J. Chem. Phys.* **1999**, 110, 3553
[25] In order to investigate the influence of water on the conformation of the adsorbed layer, a sample that was kept in water for a longer period of time than the time scale of the experiments. A significant difference was observed only after a time scale of 7 days. So, in the time scale of the experiments conformational changes, due to the influence of water can be neglected due to the big size of the molecules.
[26] Webber, R.M.; Anderson, J.L. *Langmuir* **1994**, 10, 3156
[27] Higo, Y.; Ueno, N.; Noda, I. *Polymer J.* **1983**, 15, 367
[28] Marques, C.; Joanny, J.F.; Leibler, L. *Macromolecules* **1988**, 21, 1051
[29] a) Parsonage, E.; Tirrell, M.; Watanabe, H.; Nuzzo, R.G. *Macromolecules* **1991**, 24, 1987 b) Tirrell, M.; Parsonage, E.; Watanabe, H.; Dhoot, S. *Polym. J.* **1991**, 23, 641
[30] Guzonas, D.A.; Boils, D.; Tripp, C.D.; Hair, M.L. *Macromolecules* **1992**, 25, 2434
[31] Higo, Y.; Ueno, N.; Noda, I. *Polymer J.* **1983**, 15, 367
[32] a) Tang, W.T. Ph.D. thesis, Stanford University, **1987**
b) Sikora, A.; Tuzar, Z. *Makromol. Chem*. **1983**, 184, 2049
[33] Belder, G.F.; ten Brinke, G.; Hadziioannou, G. *Langmuir* **1977**, 13, 4104
[34] Field, J.B.; Toprakcioglu, C.; Dai, L.; Hadziioannou, G.; Smith, G.; Hamilton, W. *J. Phys. II France* **1992**, 2, 2221

3.III

ADSORPTION MECHANISMS OF DIBLOCK COPOLYMERS ON VARIOUS SURFACES FROM A SELECTIVE SOLVENT EVIDENCE OF MICELLE ADSORPTION

The adsorption of P2VP/PS diblock copolymers from toluene solutions, on different surfaces is investigated. Adsorbing properties of gold surfaces were varied by treatment with Self-Assembling Monolayers. CH_3-modified surfaces have strong affinity for both blocks, so adsorption of micelles and unimers was easily observed. Substrates with carboxylic acid functionality, as well as mica substrates, are attractive only for P2VP-blocks, forming the micelle core, but not for PS-blocks. The evidence that micelles adsorb on a mica surface with no chemical affinity for the solvated block will be presented. In order to visualize adsorbed micelles, the number of adsorbing sites of mica was reduced, by using a mixed solution of a homopolymer poly(4-vinyl pyridine) and the diblock copolymer. It was observed by Atomic Force Microscopy that the number of spherical structures, with a size similar to micelles in bulk, linearly increases with an increase of adsorption time. The mechanism of micelle adsorption through the rearrangement (deformation) of the corona of PS-chains, allowing the direct contact of P2VP blocks of the micelle core with the substrate, is discussed. Mixed solutions with a concentration of diblock copolymers below cmc do not provide any spherical objects adsorbed on the substrate.

3.III.1 INTRODUCTION

The adsorption behavior of block copolymers depends on many variables: the solvent quality, the adsorption ability of a substrate, the copolymer composition and the concentration of the solution. In the present study we will study the influence of substrate on the adsorption of diblock copolymers from a selective solvent.

In selective solvents, when one block of the copolymer is well solvated and the other is collapsed, the copolymer tends to self-assemble above a given concentration, the critical micelle concentration or cmc, forming well-defined micellar structures. The possible adsorption mechanisms of diblock copolymers from a micellar solution are depicted in figure 3.III.1. If only the insoluble block has affinity for a surface then a thick polymer brush can be achieved, by adsorption of both unimers [1] and micelles [2]. If

we have the opposite situation, when only the solvated block adsorbs, then a polymer chain or a micelle can be adsorbed via the corona [3], with minor changes for the blocks forming the core. Lastly, when both blocks adsorb on a substrate, the polymer layer formed is rather thin since both blocks of unimer [4] or micelle [5] prefer to have as much contact with the substrate as possible.

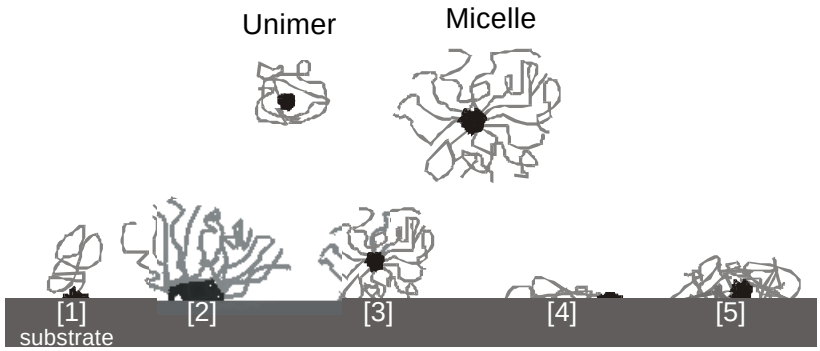

Figure 3.III.1: *Possible adsorption mechanisms of a diblock copolymer, as unimer or micelle, from a selective solvent.*

Tassin at al.[1] investigated the kinetics of adsorption of P2VP/PS diblock copolymers from toluene solutions onto silver surfaces, by measuring changes in the surface plasmon resonance. They studied the influence of the length of both blocks on the adsorption rate and found that the larger the block length the slower the adsorption. In addition, they found that micelle solutions can provide much higher surface coverage, at relatively short times, than solutions with concentrations below cmc. Munch and Gast[2] studied the kinetics of adsorption of polystyrene/poly(ethylene oxide) (PS/PEO) diblock copolymers on glass and sapphire substrates, from cyclopentane. They found different adsorption rate dependency below and above the cmc, but no significant difference between the two surfaces. It was suggested that the diblock copolymer micelles would first adsorb on the substrate and subsequently unfold, so that the nonsolvated block would come into contact with the substrate. Similar suggestions have been made by Awan et al.[3], who investigated by means of ellipsometry polystyrene/polybutadiene copolymers adsorbed from hexane onto silicon wafers and polystyrene surfaces. A strong dependence of the adsorption rate on the bulk concentration of the solution and on the chemical nature of the substrate was observed. Hong et al.[4] studied by means of surface-enhanced raman scattering the adsorption of diblock copolymers of P2VP/PS, from toluene solutions below and above cmc onto silver surfaces. The spectra showed a strong dependence of the adsorption time on polymer concentration. For solutions above cmc it was concluded that initially micelles adsorbed from solutions by the PS chains but with time the micelles unfolded on the silver surface and the P2VP chains (which have larger adsorption energy) gradually adsorb. Huguenard and Pefferkorn[5] concluded (using chromatographic separation based on surface area exclusion) that unimers and micelles of P2VP/PS copolymers adsorb on a silica surface through the P2VP blocks. It was argued

that although the corona of the micelle is in good solvent, the micelles behave as if they are in poor solvent and can adsorb to a surface, similar to unimers.

Monte Carlo simulations were employed to study the adsorption of diblock copolymers from micellar solutions.[6] Three different regimes were distinguished. Below the cmc, the adsorption occurs from free chains. Just above the cmc, micelles have little contribution to the adsorption and the adsorption occurs from free chains. At higher concentrations, the adsorption occurs at the expense of free chains and micelles. The latter emit unimers to obey the cmc amount. Furthermore, it was argued that as more chains adsorb they begin to self-assemble to form surface micelles. Direct micelle adsorption has been reported by others[7] studying the adsorption of PS/PEO diblock copolymers from aqueous solutions on polystyrene latex particles.

On the other hand, Johner and Joanny[8], based on thermodynamic considerations, argued that for copolymers in a selective solvent the potential barrier for direct adsorption of micelles is extremely high and only unimers can adsorb on a surface having no affinity for either block. However, the equilibrium situation changes due to the reduction of the amount of unimers in the solution, through their adsorption. And thus micelles emit unimers to obey the cmc amount. Hence micelles can serve as a source of non-associated chains, rather than to participate in adsorption.[10] Bijsterbosch et al.[9] measured the adsorption kinetics of diblock copolymers of poly(dimethyl siloxane)/poly(2-ethyl-2-oxazoline) from micellar aqueous solutions on silica and titania substrates. Titania has affinity for only the nonsolvated block and silica has an affinity for both blocks. It was suggested that micelles do not adsorb directly on titania, but break up into unimers. On silica a mixed adsorbed layer is formed from unimers and micelles if the polymer chains are long enough. Micelles formed by small copolymers would have enough time to break up into unimers before reaching the surface, so a smooth polymer layer is formed in this case.

All the above interpretations of the experimental data and the theoretical predictions agree that the bulk copolymer concentration drastically affects the kinetics of adsorption. However, different mechanisms of micelle adsorption have been proposed. Three models have been suggested for the adsorption of micelles of diblock copolymers onto a surface. (i) If both blocks are capable of adsorption, micelles directly adsorb through their corona on a surface with possible further rearrangements of their structure. If only the insoluble block may adsorb then (ii) diblock copolymer micelles do not adsorb on a surface (but they can emit unimers or break up into unimers in the vicinity of the surface) or (iii) micelles adsorb by their core chains, through a rearrangement of their corona chains.

The goal of this study is to provide some insight into the mechanisms of adsorption of diblock copolymers, P2VP/PS, from a micelle solution. The role of the substrate will be discussed. Two substrates different in chemical nature were prepared, by using Self-Assembling Monolayers chemisorbed on gold surfaces. AFM was employed to visualize the morphology of the films adsorbed from micelle solutions. As will be shown, the structure of the adsorbed monolayer strongly depends on the substrate's surface energy. One of the substrates studied has affinity for both blocks, the others only for the insoluble block. Our main objective is to study whether micelle adsorption is

possible when only the insoluble block may adsorb. To visualize micelle adsorption, the grafting density of the adsorbed diblock copolymers was reduced by instantaneous addition of homopolymer in the solution. The experimental data suggest that adsorption of both species in the copolymer solution, unimers and micelles, occurs. The mechanism of micelle adsorption will be discussed.

3.III.2 EXPERIMENTAL SECTION

MATERIALS AND SOLUTIONS¾ The materials used in this study are listed in Table 3.III.1, including their molecular weights, the solvents used to prepare the solutions and contact angles of films. Diblock copolymers were dissolved in toluene (Merck) at concentrations above and below cmc, 0.5 $mg \cdot ml^{-1}$ and 0.05 $mg \cdot ml^{-1}$ respectively.[10] Toluene was also used to prepare two solutions of PS- and P4VP-homopolymers with concentrations of 0.5 $mg \cdot ml^{-1}$ each. The toluene solution of the homopolymer P4VP exhibited traces of white precipitates at the bottom of the vial, even after placing it in an oven for several hours at 45 °C. Several milliliters of the clear saturated solution was taken from the vial and were further used. The two-component solutions of P4VP and P2VP/PS were prepared by mixing equal quantities of each solution and stirring for a while. This procedure was done just prior to the immersion of the substrates in the solution.

Material	Water contact angle (deg)	Type of molecule	Molecular weight (g/mol^{-1})	Solvent
P2VP/PS	-	Diblock copolymer	102k/75k	Toluene
PS	93 ± 3	Homopolymer	100k	Toluene
P2VP	55 ± 4	Homopolymer	80k	Methanol
P4VP	-	Homopolymer	50k	Toluene
COOH	<10[11]	$HS(CH_2)_{12}COOH$	256	Ethanol
CH_3	114[11]	$HS(CH_2)_{12}CH_3$	216	Ethanol
Mica	3.7[12]	-	-	-

Table 3.III.1: *Characteristics of materials.*

In order to estimate the adsorption behavior of PS- and P2VP-homopolymers with different substrates, contact angle measurements were performed. Pure PS and P2VP films were prepared by spin coating 2% (w/w) toluene and methanol solutions of the homopolymers, respectively, on glass plates. Contact angle measurements were performed with a home-built apparatus[13]. A method to obtain the film's surface energy is to measure static water contact angles. This gives a qualitative characterization of the

film.[14] In table 3.III.1, the contact angles for various substrates and films are listed. A CH_3 surface exhibits the highest contact angle, a COOH and a mica surface the lowest.

PREPARATION OF SUBSTRATES¾ Mica was cleaved in a laminar flow hood and placed in the vacuum chamber of a, diffusion pumped, thermal evaporator (Edwards Auto 306). The mica sheets were heated to 400 °C. Gold wire -99.99% pure- (Schöne Edelmentlen) was evaporated from a resistively heated molybdenum boat at pressures below 8×10^{-7} mbar. The thickness of the gold layer was monitored with a quartz crystal oscillator; 30 nm were deposited with a rate of less than 0.1 $nm\cdot s^{-1}$. The gold substrates were left at 400 °C for a couple of hours, and then let to cool down at room temperature overnight.

Self Assembling Monolayers (SAM) of ω-functional η-alkanethiol compounds on gold (111) surfaces are extensively used nowadays to modify substrates[15]. A molecule with typically 10–20 methylene units, is given a head group with a strong preferential adsorption to the substrate. The thiol molecules adsorb readily from solution onto a noble metal, creating a dense monolayer with the tail group exposed at the air interface. By employing thiol molecules with different tail groups, the resulting chemical surface functionality can be varied within wide ranges. Even though a self-assembled monolayer forms very rapidly on the substrate, it is necessary to use adsorption times of 15 h or more to obtain well-ordered, defect-free SAMs. Multilayers do not form, and adsorption times of two to three days are optimal in forming highest-quality monolayers. Gold substrates were placed in a 1–3 mM ethanol solutions of the desired thiol in ethanol for at least 2 days. Samples were taken out of the solution, rinsed with ethanol and dried in a stream of prepurified argon gas.[16] In such as way -CH_3 and -COOH modified gold substrates were prepared.

SAMPLE PREPARATION AND IMAGING— To investigate the ability of polymer chains and micelles to adsorb on substrates, several samples were prepared by exposing the substrates to toluene solutions of the desired polymer concentration for various incubation times. After the elapse of the adsorption time, the samples were removed from the solutions and immediately rinsed exhaustively with fresh toluene and dried under a stream of argon.

The films were imaged with a Nanoscope III AFM, (Digital Instruments, Santa Barbara), operating in tapping mode, in ambient conditions.

3.III.3 RESULTS AND DISCUSSION

-CH_3 SUBSTRATE

Figure 3.III.2a (left) depicts the topography of a P2VP/PS diblock copolymer film adsorbed from a toluene solution onto a gold surface modified with CH_3 groups. A solution below cmc was used. The films were formed by immersing the substrate in the solution for a few seconds. Figure 3.III.2a (right) shows the corresponding phase image.

Individual, atomically flat Au terraces[17] separated by steps and deep channels are observed. On top of these terraces, collapsed polymer islands are evident. We measured the dimensions of the well-separated islands and found an average height and width of 3.2 nm and 20 nm, respectively. The average volume of the objects corresponds to 320 nm^3. Such a characteristic object represents a single P2VP/PS chain adsorbed. The volume, U, of the collapsed chain must be about 280 nm^3 according to:

$$U = \frac{M}{\rho N_a} \qquad [3.III.1]$$

where M is the molecular weight of the diblock copolymer, N_a is Avogadro's number and ρ the density of the diblock copolymer. We assume that the density of the adsorbed chain is approximately equal to the bulk density for polystyrene (1.06 $g \cdot cm^{-3}$).

The calculated volume is close to the value found experimentally. Hence, we believe that the objects observed in figure 3.III.2a are isolated unimers of diblock copolymers adsorbed onto the CH_3 surface.

In figure 3.III.2b a film formed from a solution of the same diblock copolymer but with a concentration above the cmc, is shown. The procedure was the same as described above. Micellar solutions provide a higher amount of adsorbed polymers (figure 3.III.2b), compared to films formed by non-micellar solutions (i.e. below cmc) (figure 3.III.2a), in agreement with other studies[1, 2]. Films prepared with longer adsorption times fully cover the surfaces. The height of the layer shown in figure 3.III.2b, 3.7 nm, is similar to the height of the isolated structures observed for films formed from the non-micellar solution (figure 3.III.2a). Furthermore, spherical structures protrude from the adsorbed layer, with an average height and width of 23 nm and 52 nm, respectively. Their average measured volume, 45×10^3 nm^3, is much higher than the volume calculated for the collapsed unimer, 280 nm^3, but is of the same order of magnitude as the volume of the "collapsed" micelle -i.e. the micelle with the same aggregation number as in solution, but with collapsed PS blocks-, 80×10^3 nm^3, (obtained by multiplying eq.3.III.1 with an aggregation number of 309[18]). Although the large spherical objects are visible (figure 3.III.2b), we cannot distinguish clearly their full size, due to the close packing of adsorbed unimers. Hence, the volume of the objects experimentally measured can be easily underestimated.

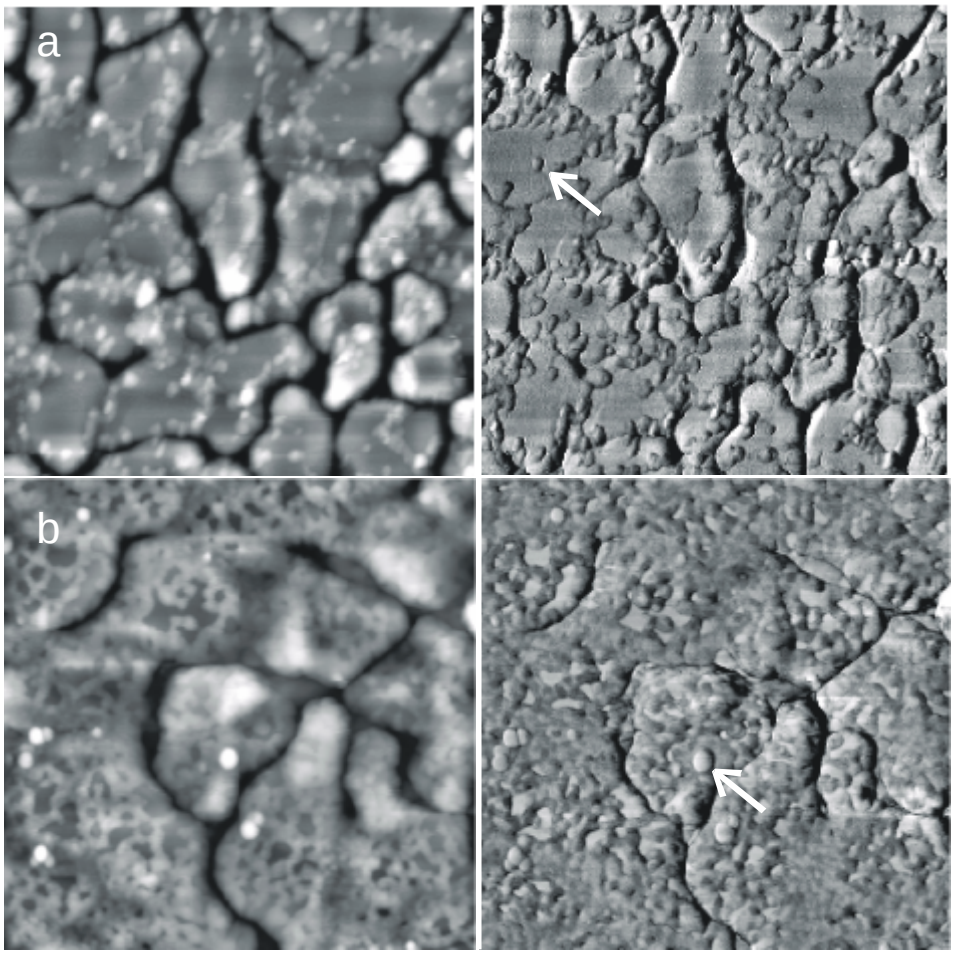

Figure 3.III.2: *Adsorption of the diblock copolymer on a -CH_3 substrate, from toluene solutions. The left-hand images correspond to topography and the right-hand ones to the corresponding phase images. a) solution below cmc (H = 40 nm). b) solution above cmc (H = 40 nm). The images cover an area 1 ´ 1 mm^2. In the height images, H corresponds to the maximum measured height (white).*

The phase images (figure 3.III.2b right), which were simultaneously recorded, provide a better contrast between the polymer islands and the substrate: the substrate looks "brighter" than the polymer islands, although the polymer islands lie on the gold terraces. This contrast is the result of different elastic behavior of the two materials (a gold surface[19] has a higher Young's modulus -E_{Au} = 80 GPa-, than the polymer islands -E_{PS} = 4 GPa[20]), although, the color contrast is also enhanced by the height differences. The phase images clearly show the height and shape difference between the substrate, an adsorbed polymer layer (or single chains adsorbed as in figure 3.III.2a) and large

spherical objects. The latter are likely the bulk micelles adsorbed from the solution, according to the measured volume of the objects.

Our estimations of the characteristic volume per collapsed diblock copolymer chain and "collapsed" micelles were based on the assumption that both blocks adsorb on the substrate. Indeed, toluene is a poor solvent for the P2VP block and it is reasonable to expect that the P2VP-block would prefer to have a contact with the substrate rather than with toluene, with the PS-block protruding in the solution. But, for the PS-block toluene is a good solvent and it is not evident whether PS-blocks adsorb on the surface. It has been found that polystyrene chains adsorb onto chromium from carbon tetrachloride[21] and on graphite from toluene solutions[22]. To check whether polystyrene can adsorb on a CH_3-modified substrate from a toluene solution, a solution of PS-homopolymer was prepared. A substrate was then immersed in the solution for a few minutes, rinsed from the excess material and dried. The topography was visualized with AFM. The surface was covered with molecules, showing the ability of polystyrene to adsorb on the substrate, from good-solvent conditions. Hence, our assumption about the adsorption of both blocks of diblock copolymers from toluene solutions was correct and we observed the direct adsorption of polymer chains (micelles) on CH_3-modified substrates.

-COOH/MICA SUBSTRATE

A film obtained from a micelle solution of the diblock copolymer adsorbed on a COOH-modified substrate is shown in figure 3.III.3a. The adsorption time was a few seconds. As is seen from figure 3.III.3a, the polymer film fully covers the carboxylic acid-modified gold surface, implying very quick adsorption. The same morphology was observed when mica sheets were exposed in the micelle solution of the diblock copolymer (figure 3.III.3b). Protrusions appear with a diameter around 15–20 nm (see sub chapter 3.II).

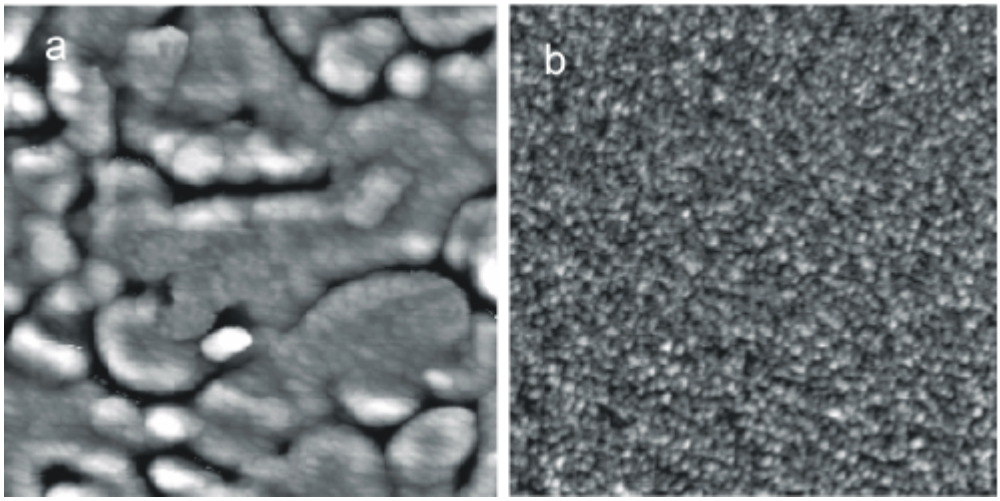

Figure 3.III.3: a) *Adsorption of the diblock copolymer on a COOH substrate (H= 32 nm), from a micellar solution.* b) *Adsorption of the diblock copolymer on a mica substrate (H = 5 nm), from a micellar solution. The images cover an area of 1 ´ 1 mm*^{2}.

Mica sheets were practically immediately fully covered by adsorbed polymer chains. We note that a COOH-surface and a mica surface exhibit somewhat similar surface energies (table 3.III.1). Therefore, it is reasonable to expect the adsorption mechanisms to be the same for both COOH and mica surfaces. Since it has been found that PS does not adsorb from a toluene solution on a mica surface[23] (and likely not on a COOH-substrate either) we expect that for both films depicted in figures 3.III.3a and 3.III.3b, PS-blocks are anchored to the surfaces via the P2VP-blocks. It was found that the morphology of the films does not change with the concentration of the solution: when the adsorption was carried out from solutions below the cmc, the morphology of the films was similar to the images in figure 3.III.3.

We summarize our findings. For films formed on the methyl-modified gold surface, the direct adsorption of both unimers and micelles is observed (figure 3.III.2) since both, PS and P2VP blocks adsorb. Thus, in this case the processes [4] and [5] schematically shown in figure 3.III.1 are active. For the mica surface (or carboxylic acid-modified gold surface) a polymer brush is formed, with the P2VP-block adsorbed on the surface, grafting the PS-block. In this case also (indirect) adsorption of both unimers and micelles (described by processes [1] and [2] shown in figure 3.III.1) is possible, in principle. However, to distinguish whether both unimer and micelle adsorption occurs or only unimer adsorption takes place is rather a formidable task, since the rate of adsorption on the mica surface (or carboxylic acid-modified gold surface) is incomparably larger than that for the methyl-modified gold surface. High degree of coverage on mica surfaces (or carboxylic acid-modified gold surfaces) prevents the observation of isolated

structures, so special modification of the experiment is required to clarify the adsorption behavior. This issue will be discussed in detail in the following section.

ADSORPTION OF MICELLES ON A MICA SUBSTRATE

As was discussed in the previous section, the adsorption on a mica (or COOH-modified) surface is very quick, making it impossible to image isolated structures and distinguish adsorbed micelles. In principle, in order to visualize separate objects on the surface, the concentration of the solution cannot be decreased, since then no micelles are present in the solution. The alternative idea was to reduce the number of adsorption sites on the mica surface available for diblock copolymer chains. In this way, if micelles would adsorb, they could be distinguished as spherical clusters, having the dimensions of micelles observed in solution. Mica surfaces will be used, because they are molecularly smooth. It has been well established that adsorption of a P2VP/PS diblock copolymer on mica, from a selective solvent, yields films with the P2VP binding strongly on mica, whereas the PS chains are stretched away from the surface.

The idea was realized by coadsorbing a homopolymer together with a block copolymer, forming a mixed monolayer. (This concept is similar to other experimental tricks to create isolated polymer chains on a substrate, with the use of two-component solutions of end-functionalized polymer chains and dodecanethiols adsorbing on gold[24]).

The solution mixture of poly(4-vinyl pyridine) (P4VP) and diblock copolymer P2VP/PS was chosen, after the following considerations.

i) To ensure a higher adsorption rate of the homopolymer compared to the diblock copolymer, we employed a homopolymer with a lower molecular weight. We expect the homopolymer to be more mobile, since it does not "carry" a PS chain. The molecular weight of the homopolymer was chosen to be half of the molecular weight of the diblock copolymer. Thus, we expect that the homopolymer will reach the surface quicker and adsorb.

ii) P4VP is known to have a slighter higher affinity for mica than P2VP.

iii) To minimize the possibility for P4VP homopolymer to be incorporated into the micelles of the diblock copolymer (to reduce unfavorable interactions with solvent), the solution of P4VP was mixed with the micelle solution of P2VP/PS just prior to the experiments (see experimental section).

iv) Due to incompatibility between PS and P4VP, the grafted PS chains will tend to be far away from the substrate.

The schematic picture of adsorption from the solution containing homopolymers, diblock copolymer micelles and unimers is shown in figure 3.III.4. As we discussed above, we expect the homopolymer to have the largest adsorption rate and hence to occupy a considerable space of the substrate. Diblock copolymer unimers and micelles can adsorb either on vacant places of the substrate or they may replace adsorbed homopolymers.

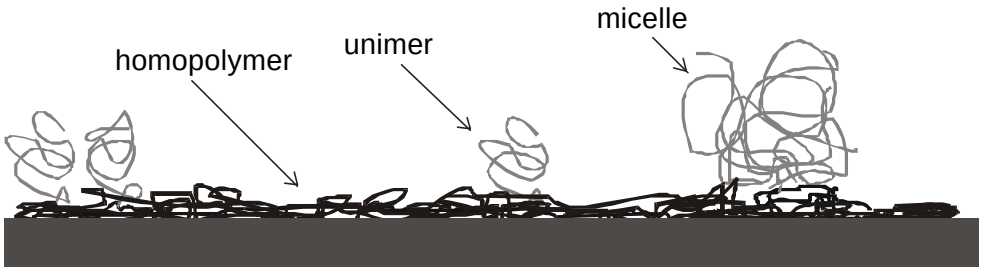

Figure 3.III.4: *Schematic representation of a mixed monolayer formed from a two-component solution, containing a diblock copolymer (P2VP/PS) and a homopolymer (P4VP). The homopolymer reduces the available adsorption sites on the substrate, thus increasing the distance between neighboring grafted diblocks.*

Figure 3.III.5 shows AFM topography images of mica substrates exposed to a two-component solution of P2VP/PS diblock copolymer and P4VP homopolymer in toluene. The concentration of the initial solution of diblock copolymer (before mixing with homopolymer solution) was above cmc. The mica sheet was immersed in the mixed solution for different incubation times, ranging from a few seconds to 4 days.

For an incubation time of a few seconds a network-like structure is observed (figure 3.III.5a). The same pattern was reproducible over the whole area of the sample. The material that covered the mica substrate forms two layers. The first layer has a height of 1.3 nm and the other has a height of 2.2 nm. (The height is measured with respect to the surface of the mica substrate[25]). The polymer layers do not cover the whole surface of the substrate: there are holes in the lower layer. With an increase of the incubation time, the degree of coverage of the substrate by polymers increases (figure 3.III.5b). The average height of the adsorbed layer increases, indicating the increase of the amount of adsorbed diblock copolymers (PS-blocks anchored to the substrate assume a more stretched conformation when the concentration of adsorbed diblock copolymer chains increases).

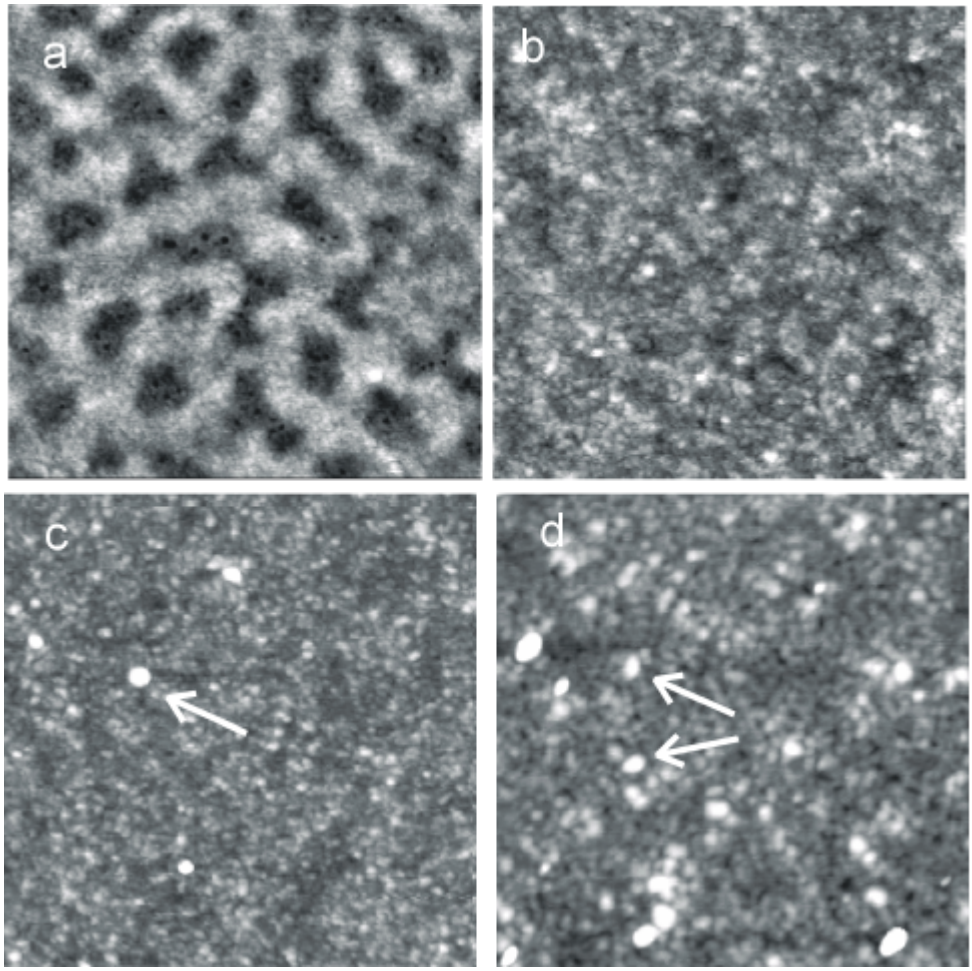

Figure 3.III.5: *Monolayers formed from a two-component solution of diblock copolymer, at a concentration above the cmc, and homopolymer for various adsorption times.* a) *30 seconds (H = 4.5 nm);* b) *10 min (H = 10 nm);* c) *45 min (H = 7 nm);* d) *55 min (H = 8 nm). The images cover an area of 1 ´ 1 mm*^{2}.

When the incubation time approaches 45 min, spherical structures (protrusions) are observed on the film (figure 3.III.5c). The average size of these structures is 60 nm in diameter and 6 nm in height. The corresponding volume is around 20×10^3 nm^3, close to the dimensions of solution micelles with collapsed PS chains. Actually, the measured height of the structures is lower than the real one since it was measured with respect to the underlying polymer layers, rather than with respect to substrate surface; hence the actual volume is surely larger. Figure 3.III.6 is a frequency histogram of the diameters of the spherical structures visible in a sample incubated in the solution for 1 hour.

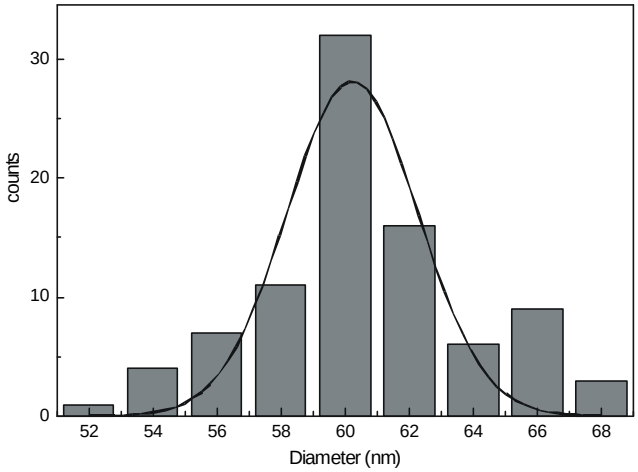

Figure 3.III.6: *Histogram showing the size distribution of spherical structures, corresponding to a sample immersed in the mixed solution for 1 hour.*

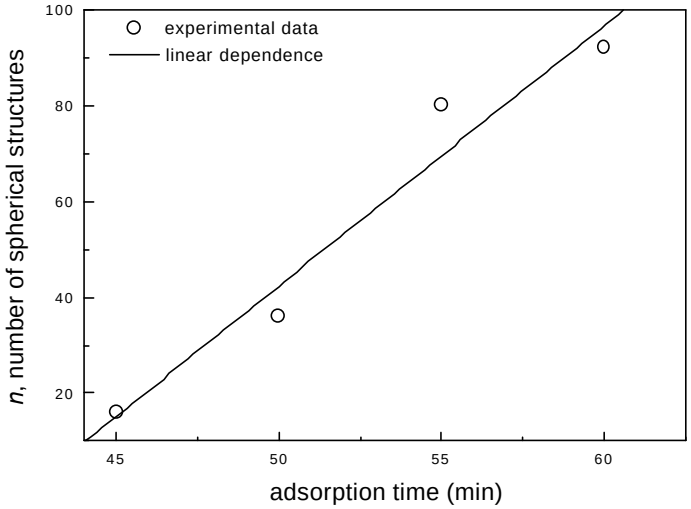

Figure 3.III.7: *Number of spherical structures of a diameter 60 ± 8 nm, measured from the AFM images over a 2 ´ 2mm² area, as a function of the time that the mica surface was immersed in the solution. The experimental data are fitted by a linear dependence.*

The number of spherical structures (figure 3.III.5c, d) observed on the film increases with an increase of adsorption time. The number of spherical structures counted from $2 \times 2\ \mu m^2$ area obtained for different adsorption times is presented in figure 3.III.7.

For longer adsorption times spherical protrusions are no longer really evident. These spherical structures become completely indistinguishable in the polymer films.

Furthermore, the general morphology of the adsorbed monolayers seems to remain unchanged for adsorption times of 1 day and 4 days.

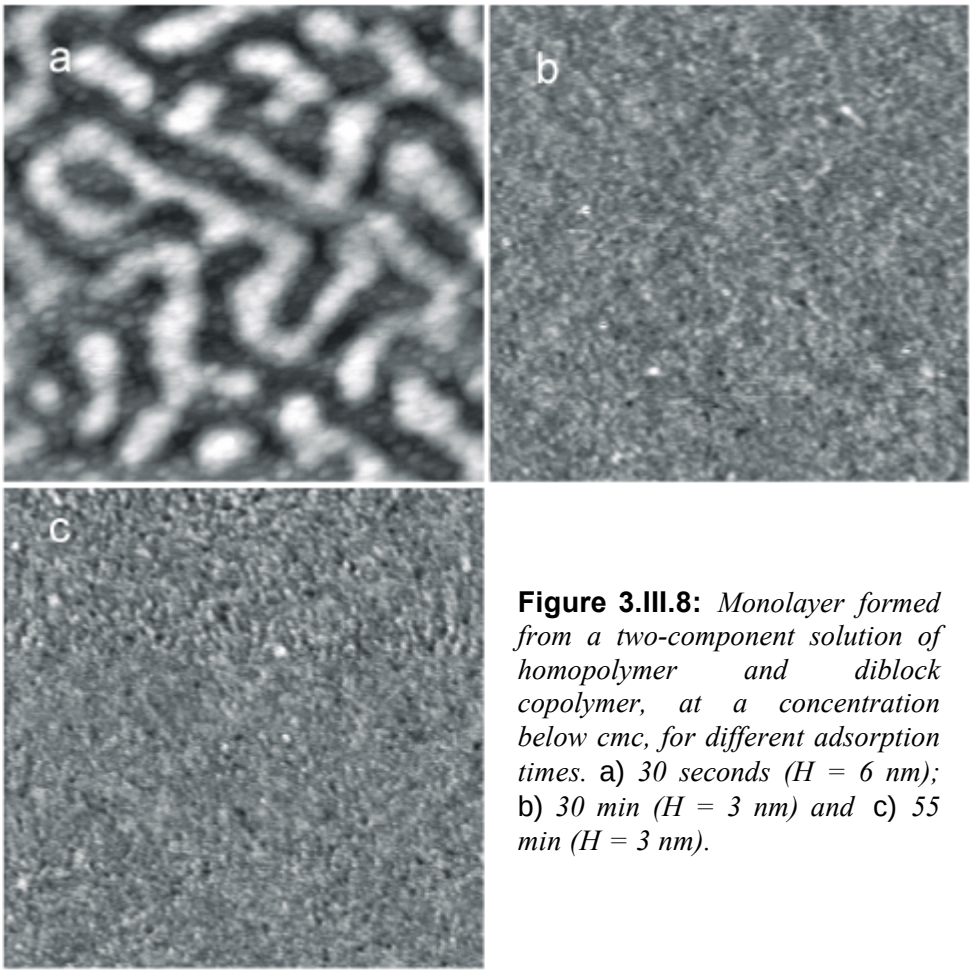

Figure 3.III.8: *Monolayer formed from a two-component solution of homopolymer and diblock copolymer, at a concentration below cmc, for different adsorption times.* a) *30 seconds (H = 6 nm);* b) *30 min (H = 3 nm) and* c) *55 min (H = 3 nm).*

The spherical objects observed on polymer films at intermediate time of adsorption (45 min – 1 hour) might be the bulk micelles adsorbed from the solution, according to the size of the spherical objects. This would mean that the adsorption of micelles having corona blocks non-adsorbing on the substrate takes place. On the other hand, we cannot exclude the possibility that these spherical structures were the result of self-organization of unimers adsorbed on the surface. In order to check this, the set of experiments with different adsorption times was repeated for the two-component solution of the homopolymer and the diblock copolymer at a concentration below the cmc (0.05 $mg \cdot ml^{-1}$). The resulting films are shown in figure 3.III.8. The film that was adsorbed for a few seconds in the solution (figure 3.III.8a) exhibits the same pattern morphology as the film obtained (for the same adsorption time) from a micellar solution of the diblock

copolymer (figure 3.III.5a). The height difference between the two layers corresponds to 2.5 nm (figure 3.III.8a), and is larger than that for the film shown in figure 3.III.5a. For longer adsorption times, the film becomes featureless, with no spherical protrusions of the dimensions of bulk solution micelles (figure 3.III.8b,c). No spherical structures appear on the films obtained for even much longer adsorption times. Hence, we can conclude that the spherical objects observed on the films obtained from micelle solutions (figure 3.III.5c) do not appear as a result of self-organization of adsorbed unimers but are the micelles adsorbed from the solution.

THEORETICAL CONSIDERATIONS

Comparing the AFM images obtained from the diblock copolymer solutions below (figure 3.III.8a) and above cmc (figure 3.III.5a), for an adsorption time of a few seconds, we observe that the adsorption is practically independent of the concentration of the solution. A two-layer network-like structure was observed in both cases. The lower layer is formed by the adsorbed homopolymer. The adsorption rate of the homopolymer depends on its diffusion coefficient[26]

$$D_{\mathrm{hom}opolymer} \cong \frac{kT}{\eta_s (N_{P4VP} v)^{1/3}} \qquad [3.III.2]$$

where k is Boltzmann's constant, T is the temperature, η_s is the viscosity of the solvent (0.59 cp[27]), v is the average volume occupied by a monomer (0.16 nm^3); N_{P4VP} is the polymerization index of the homopolymer.

The upper layer is formed by the diblock copolymer chains with the P2VP adsorbed on mica. The diffusion coefficient of a diblock copolymer, which primarily determines the adsorption rate for unimers is[26]

$$D_{unimer} \cong \frac{kT}{\eta_s v^{1/3} N_{PS}^{3/5}} \qquad [3.III.3]$$

where N_{PS} is the polymerization index of the PS block of the diblock copolymer.

Of course, in general the adsorption rates depend on many factors such as the interaction energy between the polymer chain and substrate, the concentration of the polymer in solution, the diffusion coefficient of the chain and other factors. The concentration of diblock copolymer is slightly larger than the concentration of homopolymer chains in solution (experimental section). Employing eqs 3.III.2 and 3.III.3 it is found that the diffusion coefficient for homopolymer is larger than that for diblock copolymer and also the adsorption energy for P4VP is larger than for P2VP, as we discussed above. Hence, it comes as no surprise that the fraction of adsorbed homopolymer chains is rather large at the small adsorption times but not to such an extent that diblock copolymers cannot adsorb.

For concentrations above cmc, there are polymer micelles in solution, which can adsorb on the substrate as well. It is hard to estimate the adsorption energy for micelles, however; it is evident that the interaction between a micelle and substrate will be screened by the corona of PS-blocks, which has no affinity with the mica. Also, the diffusion coefficient for a micelle[28] is much smaller than that for diblock copolymer or homopolymer:

$$D_{micelle} \cong \frac{kT}{\eta_s v^{1/3} N_{PS}^{3/5} Q^{1/5}} \qquad [3.III.4]$$

where Q is the aggregation number of the micelle.

Hence, we can expect to observe the following qualitative time order of adsorption of different components of the solution. Since the adsorption energy and the diffusion coefficient are the largest for homopolymer, we would expect that the homopolymer will have the shortest adsorption time and the fraction of adsorbed homopolymer will be large at short time of adsorption. At longer adsorption times unimers of diblock copolymer start to adsorb as well and their fraction in adsorbed material will increase with time, as they will replace homopolymers. This tendency is clearly seen from figures 3.III.5a, b and figure 3.III.7.

At even longer adsorption times micelle adsorption can become possible. As we discussed above, we believe that spherical objects observed on the films incubated for more than 45 min (figure 3.III.5) are the bulk micelles adsorbed on the substrate. In figure 3.III.7 we presented a graph of the number of spherical structures (of the dimension of bulk micelles) versus the adsorption time. The micelles were measured over an area of 2×2 μm^2. The number of micelles increases linearly with the adsorption time, t. We find a slope of 9×10^{-2} sec^{-1}.

The number of micelles adsorbed can be estimated as

$$n = \frac{t}{\tau_{mic}} \qquad [3.III.5]$$

where τ_{mic} is the characteristic time per micelle adsorption. Hence, the slope found from the experimental data of figure 3.III.7 must correspond to $1/\tau_{mic}$.

The characteristic time for micelle adsorption can be estimated from the following considerations. First, a micelle has to approach the surfaces of the substrate. If we estimate the characteristic distance for a micelle to diffuse as being equal to the average distance between micelles in solution we get:[28]

$$\tau_{diffusion} \cong \frac{\eta_s v}{kT} N_{PS}^{3/5} Q^{13/15} \left(\frac{N_{PS} + N_{P2VP}}{cv} \right)^{2/3} \qquad [3.III.6]$$

where *cv* is the volume fraction of the micelles in solution (equal to the volume fraction of diblock copolymer less cmc).

When a micelle has approached the substrate surface, the next step should be the micelle adsorption (possibly with replacement of some homopolymer adsorbed). Since polystyrene does not adsorb from toluene solutions on mica, the adsorption of micelles would involve the rearrangement of the PS chains in the corona, in order for the P2VP groups to be adsorbed on the surface. This rearrangement is somewhat similar to corona "deformation" accompanying micelle fusion. So, we can estimate the characteristic time for micelle adsorption as the time for corona deformation:[28]

$$\tau_{deformation} \cong \frac{\eta_s v}{kT} N_{PS}^{9/5} Q^{13/15} \qquad [3.III.7]$$

The total time for micelle diffusion and micelle adsorption is $\tau_{mic} = \tau_{diffusion} + \tau_{deformation}$. Since, $\tau_{diffusion} << \tau_{deformation}$ we can consider only the deformation time, i.e. $\tau_{mic} \cong \tau_{deformation}$. Then, for the polymer system under consideration we get that $1/\tau_{mic}$ is of the order of 5×10^{-2} sec^{-1}. This is very close (taking into account the scaling character of the calculations) to the value obtained from the experimental data presented in figure 3.III.7.

When copolymers were adsorbed from a micellar solution on a substrate having a chemical affinity for the corona of the micelle (-CH_3 surface), micelles were evident on the substrate at the early stages of adsorption. However, on a substrate with chemical affinity only to the core of the micelle (mica surface), micelles were observed at longer time scales. This time difference can be partly attributed to the different mechanisms of adsorption. To adsorb on a CH_3 surface, micelles only have to diffuse to the surface, while, to adsorb on a mica surface, the micelle corona has to be rearranged to allow contact between P2VP-block and substrate after a micelle approached the surface. This process of corona deformation is rather slow, increasing the characteristic time for micelle adsorption.

The spherical structures were evident only at intermediate adsorption times (figures 3.III.5). For longer adsorption times, micelles were indistinguishable and the morphology of the film remained principally the same with an increase of adsorption time, although the roughness of the films slightly increases. The increase of adsorption time can lead to some reorganization of the adsorbed layers. For instance, the process of replacement of P4VP homopolymer by diblock copolymer will proceed further. At longer adsorption times, diblock copolymer chains adsorbed will form a brush, which will screen the influence of the surface on polymer chains in solution. In order to adsorb on the surface, newly arriving molecules have to penetrate through the dense brush. This is a formidable task especially for micelles since P2VP blocks forming the core of a micelle are separated from the substrate by both the brush of adsorbed chains and the corona of PS-blocks. Hence, only unimers will contribute to the adsorption, at later times.

3.III.4 CONCLUSIONS

The influence of the chemical nature of the substrate on the adsorption of polymer micelles and unimers from P2VP/PS solution was analyzed using the AFM imaging technique. Monolayers with CH_3 and COOH functionalities, modifying the substrate to an extremely hydrophobic one and a completely hydrophilic one, respectively, were studied. It was observed that in the case of the CH_3-modified surface both, PS and P2VP, blocks adsorb on the substrate. The direct adsorption of both, unimers and micelles is evidenced. For mica (or COOH-modified surface) only the P2VP block adsorbs, leading to the formation of a polymer brush. The rate of adsorption is much higher for mica or a COOH-modified surface than for a CH_3 surface.

In order to investigate micelle adsorption on mica, the number of adsorption sites of the substrate was reduced by mixing the P2VP/PS micelle solution with a solution of P4VP homopolymer capable of adsorbing on the surface. The process of polymer adsorption from the mixed solution was studied as a function of adsorption time. In a window of adsorption times spherical structures were adsorbed on the surface. The number of spherical objects linearly increased with an increase of adsorption time till some critical time after which the adsorbed layer became too dense to distinguish separate objects. Solutions with the concentration of diblock copolymers less than cmc did not provide any spherical objects on the surface regardless of the adsorption time. Hence, the adsorbed spherical objects with a size similar to the size of bulk micelles could not be the result of self-organization of adsorbed chains, and were evidence of adsorption of bulk micelles on mica. The mechanism of micelle adsorption through the rearrangement (deformation) of the corona of PS-chains to allow the direct contact of P2VP blocks of the micelle core with the substrate is proposed.

REFERENCES

[1] Tassin, J. F.; Siemens, R.L.; Tang, W.T.; Hadziioannou, G.; Swalen, J.D.; Smith, B.A. *J. Phys. Chem.* **1989**, 93, 2106

[2] a) Munch, M.R.; Gast, A.P. *Macromolecules* **1990**, 23, 2313

b) Munch, M.R.; Gast, A.P. *J. Chem. Soc. Faraday Trans.* **1990**, 86, 1341

[3] Awan, M.A.; Dimonie, V.L.; Filippov, L.K.; El-Aasser, M.S. *Langmuir* **1997**, 13, 130

[4] Hong, P.P.; Boerio, F.J.; Tirrell, M.; Dhoot, S.; Guenoun, P. *Macromolecules* **1993**, 26, 3953

[5] a) Huguenard, C.; Pefferkorn, E. *Macromolecules* **1994**, 27, 5271

b) Huguenard, C.; Elaisssari, A.; Pefferkorn, E. *Macromolecules* **1994**, 27, 5277

[6] Zhan, Y.; Mattice, W.L. *Macromolecules* **1994**, 27, 683

[7] Xu, R.; D'Unger, G.; Winnik, M.A.; Marthinho, J.M.G.; d'Oliveira, J.M.R. *Langmuir* **1994**, 10, 2977

[8] Johner, A.; Joanny, J.-F. *Macromolecules* **1990**, 23, 5299

[9] Bijsterbosch, H.D.; Cohen Stuart, M.A.; Fleer, G.J. *Macromolecules* **1998**, 31, 9281

[10] a) sub chapter 3.II b) sub chapter 3.I
[11] Troughton, E.B.; Bain, C.D.; Whitesides, G.M.; Nuzzo, R.G.; Allara, D.L.; Porter, M.D. *Langmuir* **1988**, 4, 365
[12] Gaines G.L. *Colloid and Interface Sci.* **1960,** 15, 321,
[13] van der Mei, H.C.; Rosenberg, M.; Busscher, H.J. *Microbial Cell Surface Analysis*; VCH Publishers: New York, **1991**, 261
[14] Young's Dupré equation: $\gamma_{sl} = \gamma_{sv} - \gamma_{lv}\cos\theta$, where γ_{sl} denotes the surface energy of the surface-liquid interface, γ_{lv} the surface-vacuum interface, γ_{lv} the liquid-vacuum interface and θ represents the contact angle between the liquid and the surface.
[15] Nuzzo, R.G.; Allara, D.L. *J. Am. Chem. Soc.* **1983**, 105, 4481
[16] van der Vegte, E.W. *Chemical and Physical Surface Properties Studied with Scanning Force microscopy*; Ph.D. thesis State University of Groningen, **1998**
[17] Zheng, X.-Y.; Youzhen, D.; Bottomley, L. *J. Vac. Sci. Technol. B.* **1995**, 13, 1320
[18] Esselink, F.J. *Direct imaging of block copolymer structure in solution and neat state* Ph.D. thesis, University of Groningen, **1998**
[19] The existence of SAM's chemiadsorb onto the gold surface does not change significant the elastic behavior of solids. Thomas, R.S.; Houston, J.E.; Michalske, T.A.; Crooks, R.M. *Science* **1993**, 259, 1883
[20] *Polymer Handbook*; **1989**, third edition, edited by Brandrup, J.; Immergut, E.H.; Wiley: New York.
[21] Kawaguchi, M.; Hayakawa, K.; Takahashi, A. *Macromolecules* **1983**, 16, 631
[22] Dunn, V.K.; Vold, R.D. *Adsorption at interfaces*; ACS symposium series, xii, 1975 p290 edited by Mittal, K.L.
[23] Marra, J.; Hair,M.L. *Macromolecules* **1998**, 21, 2349
[24] Grim, K. *Direct view of thin Polymer Films with Scanning Force Microscopy* Ph.D. thesis, University of Groningen, **1996**
[25] Some holes are evident on the AFM images. The phase image, which was acquired simultaneously, revealed that these holes end up at the hard substrate.
[26] Doi, M.; Edwards S.F. *The Theory of Polymer Dynamics;* Oxford University Press: New York, 1986.
[27] *Handbook of Chemistry and Physics* **1986**, 66th edition, edited by Weast, R.C. CRC Press, Boca Raton, Florida
[28] Dormidontova, E.E. *Macromolecules*, **1999**, 32, 7630

3.IV

EQUILIBRIUM MORPHOLOGIES OF ADSORBED DIBLOCK COPOLYMER MONOLAYERS

The conformations of an adsorbed diblock copolymer —P2VP/PS— monolayer are investigated. Mica sheets were exposed to toluene solutions of the copolymer for a series of long incubation times. Adsorption was performed from solutions below and above the cmc. The evolving film was characterized by means of an Atomic Force Microscope. Distinct morphologies were found depending on the incubation time and the concentration. For long adsorption times, films formed from a micellar solution developed a surface pattern similar to spinodal decomposition in the bulk.

3.IV.1 INTRODUCTION

Polymer structures and physical properties are, in general, time- and temperature-dependent. Because of the relatively large size of synthetic polymer molecules, most polymeric structures rarely achieve true equilibrium. This situation is well-known in bulk polymer properties, and has been recognized in polymer surface chemistry and physics.

When polymer molecules are concentrated within an adsorbed surface layer, or confined within a thin layer between two surfaces, their motions and relaxations can be different from the motions observed in the bulk due to different environmental, boundary and concentration constraints. Furthermore, their molecular relaxation times can be many orders of magnitude higher than in the bulk. Consequently, experimental measurements are made often far from equilibrium, exhibiting time-dependent and history-dependent effects, and thus performed in a so-called "restricted equilibrium".[1]

The objective of this study is to investigate the conformations of adsorbed diblock copolymer monolayers as a function of time. Most of the studies dealing with polymer chains on surfaces, have only involved measurements on the early stages of adsorption. Sub chapter 3.II describes a kinetic study, by means of an AFM, which show that the grafting density increases with incubation time. The regime that was investigated comprised up to 4 days. However, Huguenard et al.[2], who studied the kinetics of adsorption of P2VP/PS with large P2VP blocks from toluene solutions on silica, found that even after a period of 2 months equilibrium was never reached.

3.IV.2 EXPERIMENTAL SECTION

MATERIALS¾ Freshly cleaved muscovite mica is used as a substrate for the experiments. The P2VP/PS block copolymer employed has a molecular weight of 75 000 $g \cdot mol^{-1}$ and 102 000 $g \cdot mol^{-1}$ for the PS and P2VP block, respectively. Diblock copolymers were dissolved in analytic toluene at concentrations above and below cmc, 0.5 $mg \cdot ml^{-1}$ and 0.05 $mg \cdot ml^{-1}$ respectively.[3]

MEASUREMENTS PERFORMED IN AIR¾ An average number of three samples were prepared by exposing mica substrates to toluene solutions of the desired concentration, for various incubation times. After the elapse of the incubation time, the samples were removed from the solutions and immediately rinsed exhaustively with fresh toluene and dried under a stream of argon. To obtain the topography, the samples were imaged with a Nanoscope III AFM (Digital Instruments, Santa Barbara), operating in tapping mode.

MEASUREMENTS PERFORMED IN TOLUENE¾ The sample's surface topography was obtained using a commercial Atomic Force Microscope (Molecular Imaging), in contact mode. The experimental set-up employs a closed cell that protects the sensitive parts of the apparatus from hazardous solvents. Commercially available V-shaped Si_3N_4 cantilevers (Park Scientific) with pyramidal probe tips (radius of curvature of 30 nm; spring constant of 0.1 $N \cdot m^{-1}$) were used. A piece of mica 1×1 cm^2 was cleaved and immediately placed in the liquid cell. The polymeric solution (0.5 $mg \cdot ml^{-1}$) was then injected and incubated for two hours, during which adsorption of the polymer on the mica sheet took place. The solution was then replaced with pure toluene, and the topography was recorded continuously, using the movie option of the software.

3.IV.3 RESULTS

Figure 3.IV.1 shows samples that were immersed in the micellar (above cmc) solution of the $P2VP_{102}PS_{75}$ diblock copolymer, for various incubation times. Distinct morphologies are evident.

For short adsorption times (figure 3.IV.1a) the coverage is rather homogenous in the plane of the layer. Small globules, with a width of 15 nm and a height of 4 nm, protrude from the layer underneath. With increasing incubation time a different pattern is observed (figure 3.IV.1b). Large globules, with a width of 78 nm and a height of 8 nm are evident. A rough estimate, one finds that around 10 smaller globules have fused to form a bigger one. This morphology is only evident for a period of ~3 days.

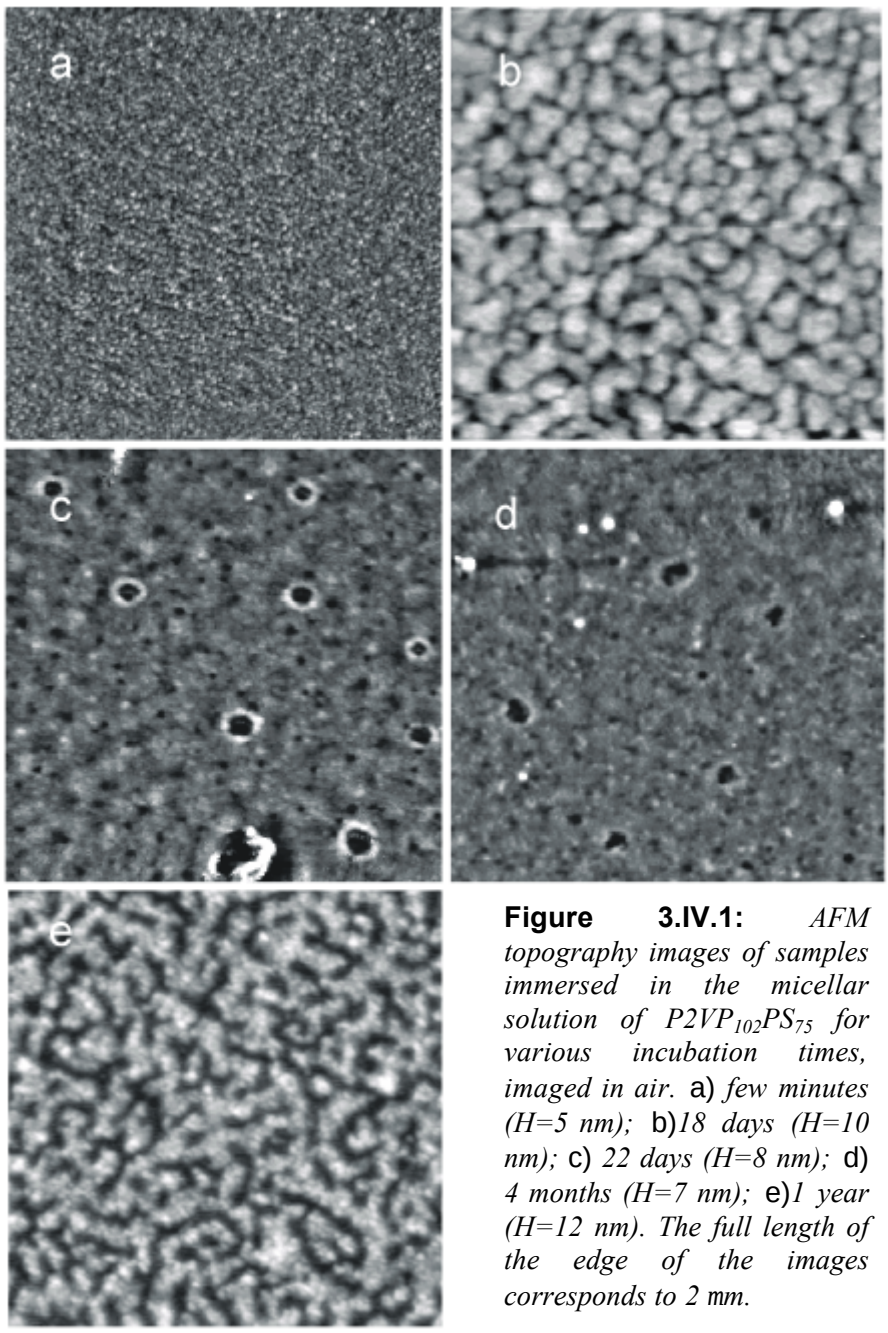

Figure 3.IV.1: *AFM topography images of samples immersed in the micellar solution of $P2VP_{102}PS_{75}$ for various incubation times, imaged in air.* a) *few minutes (H=5 nm);* b)*18 days (H=10 nm);* c) *22 days (H=8 nm);* d) *4 months (H=7 nm);* e)*1 year (H=12 nm). The full length of the edge of the images corresponds to 2 mm.*

The structure (figure 3.IV.1c) changes again, now into a homogeneous film with holes with a diameter around 130 nm and a height of 3.2 ± 0.3 nm. The holes are covered with a rim having a height around 2 nm. The rim disappears with time (figure

3.IV.1d). For the largest adsorption time, 1 year (figure 3.IV.1e) a spinodal-like pattern is formed, with a characteristic wavelength corresponding to the maximum scattering intensity of q = 0.2 μm.

Samples that were immersed in the non-micellar (below cmc) solution of the $P2VP_{102}PS_{75}$ diblock copolymer, for various incubation times, had morphologies similar to the one formed from the micellar solution figure 3.IV.1a. Even after a period of 1 year the morphology of the monolayer was unchanged.

3.IV.4 DISCUSSION

Variations in the surface morphology, which arise when increasing the time the substrate was kept in the polymer solution, were observed. In addition, the morphologies depended on the concentration of the solution, whether a micellar or non-micellar solution was employed. In this section the physical mechanisms responsible for the formation of heterogeneous morphologies will be discussed.

Due to experimental limitations, the visualization of the films' morphology was performed in ambient conditions —the films were blown dry, prior to investigation with AFM. Hence, the morphology of the films can be considered to be the result of structural changes that happened in the toluene environment and changes that happened during the drying.

We shall start with considering the influence of solvent quality on the adsorbed monolayer. In sub chapter 3.II, it was shown that the reduction of the solvent quality from a good solvent to a poor solvent for the PS chains causes the PS chains to fuse and form surface octopus "micelles". It has been well established[4] that surface octopus "micelles" exist only at intermediate grafting densities. At lower grafting densities each chain will collapse on itself, while at higher grafting densities a uniform layer will be the result. The films formed from the micellar solution do not exhibit the expected features at intermediate and large incubation times. For short adsorption times, surface octopus "micelles" are indeed evident. However, the large globules on the surface and the spinodal-like patterns cannot be explained as a result of fusion of grafted PS chains due to the reduction of solvent quality.

Hence, the conformational changes observed in figure 3.IV.1 most probably happened during the adsorption process. Toluene is a selective solvent for P2VP/PS, since it is a non-solvent for the P2VP and a good solvent for PS. The P2VP block is driven to the surface by its incompatibility with toluene (lyophobic effect), while the PS prefers to be solvated. Thus, when a substrate is immersed in the solution, the P2VP block will act as the anchor and the PS as the buoy. Surface Force Measurements[5] of diblock copolymer layers reveal purely long-range repulsive forces starting at distances much higher than the radius of gyration of the PS chains, revealing that the PS chains are stretched in the direction normal to the surface. Some models consider that the P2VP blocks form thin disks on the surface. Because of the high adsorption energy, the disks try to fill the surface as much as possible. This forces the buoy blocks to come closer and

leads to overlap between the neighboring buoy chains. The unfavorable osmotic interactions, resulting from lateral overlap, can be diminished by stretching of the buoy blocks away from the surface. The entropy associated with the stretching is overcome by the adsorption energy of the anchor blocks. The resulting structure is called a "polymer brush".

The structure of adsorbed copolymer monolayer will be a balance between osmotic repulsive forces between neighboring PS chains, attractive forces between neighboring P2VP chains and attractive interactions of the P2VP chains with the substrate. The structure of the polymer brush will be sensitive to the relative size of the two blocks of the copolymer, the adsorption energy of the P2VP block on mica and the grafting density.

Although a lot of studies have investigated the structure of the PS layer, only few have dealt with the P2VP layer. For diblock copolymers with $N_{PS} < N_{P2VP}$ it has been found that the buoy chains do not significantly overlap and the structure is better described as a mushroom-like rather than a brush-like type. A neutron reflectivity study has been performed, by Field et al.[6], on adsorbed diblock copolymer layers, using diblock copolymers having the same size PS block but different sizes of the P2VP block. It was found that the P2VP blocks can be considered to be lying on the surface as disks, with a radius r and a thickness h. Increasing the size of the P2VP block increases r, but h remains constant. The volume fraction of polymer in the PVP layer was calculated to be 0.75. A volume fraction of 0.4 was found from an adsorption kinetics study performed by SFA.[7] Both values are close to the one obtained from a phase diagram determined by Parsonage et al.[8] on PVP/toluene systems. These authors report that for high molecular weights of the PVP block ($> 30 \times 10^3$), the PVP precipitates out of solution and the PVP-rich phase contains up to about 50% toluene. Hence, the adsorbed P2VP layer cannot be considered as a dense thin "pancake", since it is plasticized by the solvent.

The optimum configuration of the adsorbed P2VP chains, is usually not reached in experimental conditions. When a polymer solution comes into contact with a substrate at low coverages, the polymer chain can adsorb preferentially on the substrate. However, at high coverages, the "late-comers" find few empty adsorbing sites. Thus, equilibrium has not been reached since the adsorbed chains have to rearrange their configuration. In the case of adsorbed diblock copolymer monolayers formed by micellar solutions, where the adsorbed layer is formed by micelles and unimers, the situation is more complicated. The film is inhomogeneous and the P2VP core of the micelle is adsorbed as a dense coil, with few monomer units adsorbed on the surface.

It is clear that concerning the P2VP layer the structure is not an equilibrium one initially. The question then arises whether the adsorbed polymer chains are able to optimize their configuration by adsorption/desorption mechanisms. Recently, the question of the conformation of strongly adsorbed chains on a surface in poor-solvent conditions has been addressed. The main question is whether adsorbed chains are still in a fluid state or glassy.[9] Thin films of polymer melt, have been investigated by Monte Carlo simulations.[9] It was found that even strongly adsorbed polymer layers are not completely frozen, and slow lateral diffusion, corresponding to reorganization of the adsorbed layer, can still occur.

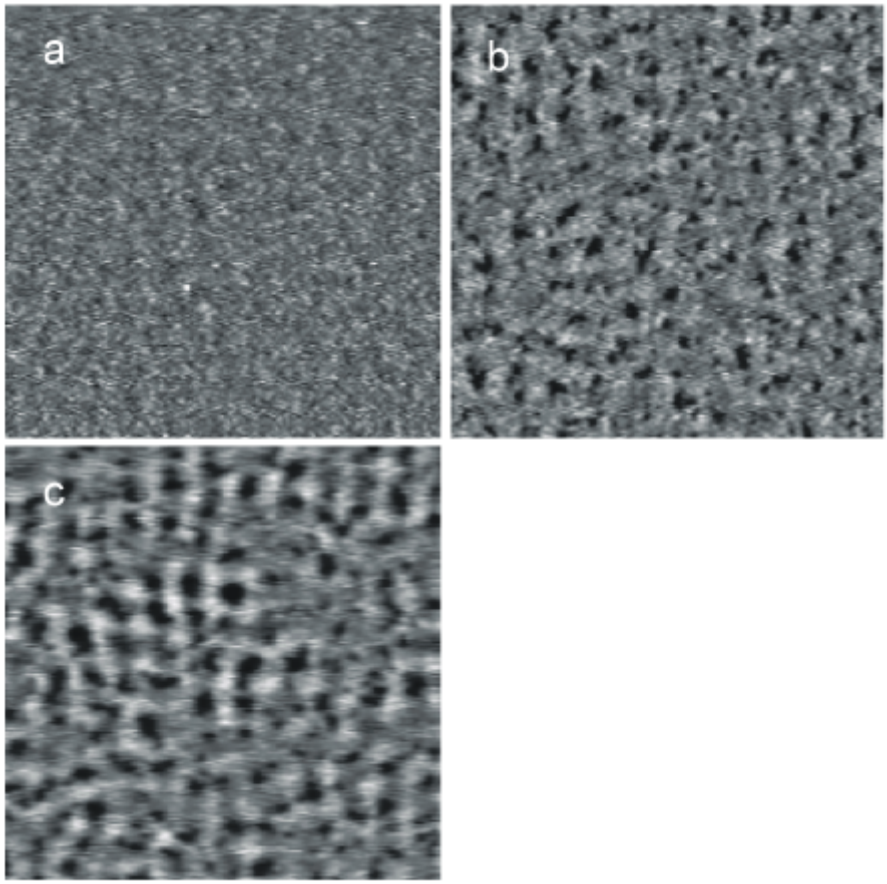

Figure 3.IV.2: *AFM images of films covered with adsorbed diblock copolymer $P2VP_{102}PS_{75}$ imaged in a toluene environment.* a) *2 hours after injection of the polymer solution (H= 6 nm);* b) *2 hours after replacing the polymer solution with pure toluene (H= 6 nm);* c) *3 hours after replacing the polymer solution with pure toluene (H= 6 nm). The images cover a 1 ´ 1 mm^2 area.*

In view of such considerations, we conducted the following experiment to observe to what extent diblock copolymer layers are reversibly adsorbed on the substrate. A mica surface was placed in the liquid cell of the AFM head and a polymer solution of the diblock copolymer was injected. During adsorption of the polymer on the mica surface AFM images were collected, which show that the film was homogeneous in the plane of the surface. After an adsorption time of 2 hours the polymer solution was replaced with pure solvent, and the morphology of the film was visualized as a function of time (figure 3.IV.2).

The snapshots of the morphology shown in figure 3.IV.2 show that the adsorbed diblock copolymer is not strongly adsorbed on the surface and P2VP chains can desorb

from the surface in order obtain the conformation, which minimizes the total free energy. In figure 3.IV.3 the bearing ratio (percentage of uncovered mica surface) measured from the AFM images is plotted as a function of the incubation time. The data are fitted to a straight line of gradient close to ¼.

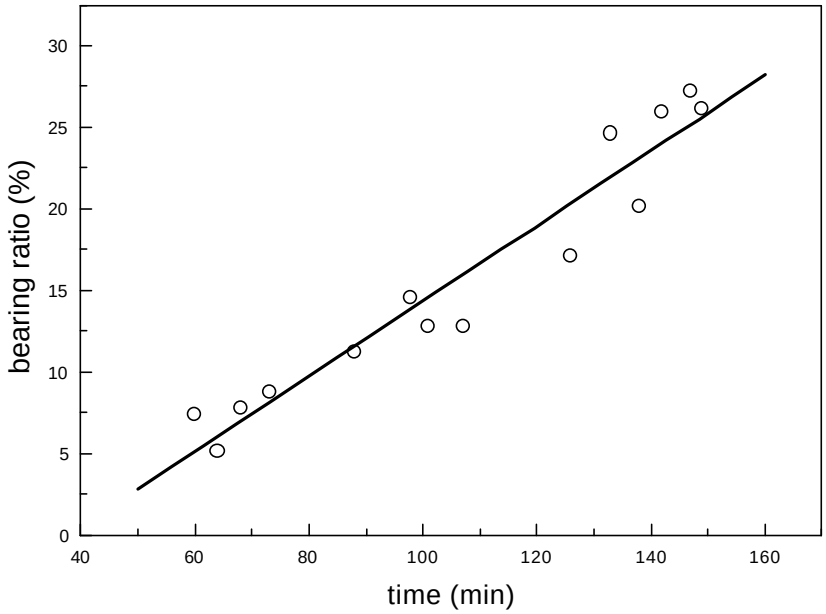

Figure 3.IV.3: *Plot of bearing ratio as a function of time. The straight line is a least-squares fit with a gradient of 0.23.*

The above measurements not only show the ability of desorption but also the segregation of the copolymer by lateral diffusion, forming dense coils on the surface. The experimental data presented in the previous section can only be explained by assuming segregation of the P2VP chains on the surface, due to strong polymer−polymer interactions. This conclusion is also corroborated by the similarity of the morphologies we obtained with the morphologies reported for grafted polymer chains in poor−solvent conditions. Spinodal-like structures[10] or semi-continuous dimples[11] have been found for the adsorption of end-functionalized polymer chains from poor−solvent conditions on a surface. The microphase separation was found to be restricted to an intermediate range of grafting densities. At the early stages of adsorption dimples were observed, at the intermediate stage, spinodal patterns, while at long adsorption time a uniform layer. There, phase separation required a critical amount of polymeric material for long wavelength fluctuations to percolate while, at high grafting densities it was energetically unfavorable to form concentration variations in the plane of the brush.

In addition, the situation of polymer chains grafted onto strongly adsorbing surfaces in poor−solvent conditions has been studied, using an analytical theory and computer simulations. It was observed that strongly adsorbing chains do not form

octopus "micelles", instead they fuse into compact islands, which in the limit of high grafting density can form a continuous network.[12]

The films formed from the non-micellar solutions did not show the salient structural features observed for films from micellar solutions (figure 3.IV.1). A possible explanation is the high and homogenous surface coverage from the early stage of adsorption, in the former case, which may have hindered the transformations observed for the micellar films.

3.IV.5 CONCLUSIONS

Summarizing, we have investigated the conformations of adsorbed P2VP/PS diblock copolymer monolayers at long incubation/adsorption times. For films formed from the micellar solution, distinct morphologies were observed with increasing exposure time of the substrate in the solution. For long incubation times, spinodal-like patterns were observed, reminiscent of spinodal decomposition of unstable binary mixtures[13]. We attributed the formation of heterogeneous morphologies to the interplay between attractive interactions between adsorbed P2VP chains and repulsion interactions between grafted PS chains. For films formed from a non-micellar solution, the morphology did not show any peculiar features.

REFERENCES

[1] Israelachvili, J.N. "*Intermolecular and Surface Forces*" **1992**, Academic Press: New York.
[2] a) Huguenard, C.; Varoqui, R.; Pefferkorn, E. *Macromolecules* **1991**, 24, 2226
b) Pefferkorn, E.; Elaissari, A.; Huguenard, C.; *Macromolecular reports* **1992**, A29, 147
[3] Sub chapter 3.I
[4] Sub chapter 3.II and references therein
[5] Sub chapter 3.I and references therein
[6] Field, J.B.; Toprakcioglu, C.; Dai, L.; Hadziioannou, G.; Smith, G.; Hamilton, W. *J. Phys. II (France)* **1992**, 2, 2221
[7] Pelletier, E.; Stamouli, A.; Belder, G.F.; Hadziioannou, G.; *Langmuir* **1997**, 13, 1884
[8] Parsonage, E.; Tirrell, M.; Watanabe, H.; Nuzzom R.G. *Macromolecules* **1991**, 24, 1987
[9] Michev, A.; Binder, K. *J. Chem. Phys.* **1997**, 106, 1978
[10] Karim, A.; Tsukruk, V.V.; Douglas, J.F.; Satija, S.K.; Fetters, L.J.; Reneker, D.H.; Foster, M.D. *J. Phys. II France* **1995**, 5, 1441
[11] Koutsos, V. *Physical properties of grafted polymer monolayers studied by scanning force microscopy: morphology, friction, elasticity* Ph.D. thesis, University of Groningen **1997**
[12] Sevick, E.M.; Williams, D.R.M. *Phys. Rev. Lett.* **1999**, 82, 2701

[13] a) Hasimito, T. "*Structure formation in polymer mixtures by spinodal decomposition*" Current Topics in Polymer Science, Volume II, Hahser Publishers, Munich Vienna New York, Chapter 6.1
b) Binder, K. "*Spinodal Decomposition*" Material Science and Technology, Edited by Chan, R.W.; Haasen, P.; Kramer, E.J. Volume 5, Chapter 7
c) Strobl, G.R.; Bendler, J.T.; Kambour, R.P.; Shultz, A.R.; *Macromolecules*, **1986**, 19, 2683

CHAPTER 4

FORCE MEASUREMENTS ON ADSORBED DIBLOCK COPOLYMER MONOLAYERS IN VARIOUS SOLVENT CONDITIONS

ABSTRACT

Surface Forces Apparatus (SFA) and Atomic Force Microscope (AFM) are used to study the forces exerted by adsorbed diblock monolayers (P2VP/PS) in the mushroom regime, in various solvent conditions. The main difference between the AFM and SFA apparatuses is that in the AFM configuration the area of contact is much smaller –the dimensions of the tip and the dimensions of the polymer chains are of the same order of magnitude.

In toluene (good solvent for PS), the SFA force profile is a long-range reversible monotonic repulsion. The AFM approach force profiles exhibit an attractive minimum at small distances, within the otherwise long-range monotonic repulsion. This minimum is attributed to the theoretically predicted escape transitions; the polymer chains, trapped underneath the tip, escape to avoid compression. The force profiles are compared with theoretical models.

In cyclohexane at temperatures near-theta conditions for PS, the AFM force profiles exhibit a long-range reversible monotonic attraction, which is attributed to bridging. At lower temperatures, when the solvent is a poor one for PS, the approach force profiles exhibit a long-range monotonic attraction, while the retract force profiles exhibit multiple attractive peaks, due to strong adsorption of PS chains on the AFM tip. The magnitude of attraction decreases with increasing temperature i.e., increasing solvent quality.

4.1 INTRODUCTION

The physical origin of forces exerted among polymer molecules is twofold: the forces that arise from the chemical nature of the system (van der Waals, electrostatic, hydrogen bonding, etc.) and those due to the chain-like character of the macromolecules[1]. The Surface Forces Apparatus (SFA) has been a useful tool to explore these forces, giving much insight into polymer-modified surface interactions.[2] Direct measurements have proven the existence of three types of interactions: the osmotic repulsion in good-solvent conditions, the osmotic attraction in poor-solvent conditions, and the bridging attraction, due to polymer chains simultaneously adsorbed on both surfaces. With the introduction of the Atomic Force Microscope (AFM), local force measurements in polymer systems have started to be explored.[3, 4, 5, 6, 7] The main difference between the two apparatuses is the area of contact between the probe and the molecules. In the SFA configuration the deformation of polymer chains is achieved with practically infinite probes, while in the AFM configuration the probe has dimensions similar to the size of polymer chains, and offers the advantage of addressing single molecule interactions.

The theoretical aspects of the deformation of polymer layers by finite-size objects have received considerable attention in recent years.[8, 9, 10, 11, 12, 13, 14] An isolated end-grafted polymer chain in theta-solvent conditions confined under various geometrical types of objects has been theoretically studied. A conformational transition of the grafted polymer chain from a confined to an escaped state was predicted.[10, 12] The force profile of a polymer brush in poor-solvent conditions has been constructed. A plateau region, where the force does not depend on the degree to which the polymer layer is deformed, was predicted.[13] Recent Molecular Dynamics Simulations showed that the force between a polymer brush, in good-solvent conditions, and a small AFM tip is much smaller than that found when the brush is compressed by an infinite plate or an identical brush, due to lateral motion of the chains.[8] Predictions of the deformation behavior of grafted polymer chains compressed by finite-size particles, in good-solvent conditions, were made based on self-consistent mean field calculations. A variety of behavior was observed depending on the grafting density of the chains on the surface and on whether the chains-tethers were mobile. Under certain conditions chains could undergo escape transitions to avoid compression.[8] It was argued[12] that escape transitions only occur in poor and theta solvent conditions, while in good-solvent conditions transitions are completely eliminated by statistical fluctuations. This contradiction was resolved[14] by Monte Carlo simulations that confirmed the existence of escape transitions of grafted polymer chains in good-solvent conditions. In the limit of $N \to \infty$ the transition is sharp, but for finite N the transition is gradual. Hence, by considering short chains one can fail to detect this transition. Experimental evidence on the theoretical predicted escape transitions is still lacking.

In conclusion, one can expect that the force profiles obtained by an AFM will be rich, but also sensitive to the solvent quality, the grafting density and the chemical nature of the tip, substrate and polymer.

The objective of the present chapter is to investigate the force profiles of a grafted polymer monolayer in the mushroom regime, in various solvent conditions. For

this purpose a diblock copolymer (P2VP/PS) monolayer having a large anchoring P2VP block was utilized.

In good-solvent conditions (toluene), the compression of the polymer monolayer by means of the SFA and the AFM is demonstrated. With the SFA, the force profiles were reversible, while with the AFM the grafted polymer chains exhibited escape transitions. The AFM force profiles are compared with various theoretical models. In near theta and poor-solvent conditions (cyclohexane), escape transitions during the compression of the monolayer were not observed, due to bridging. In poor-solvent conditions, the extrusion of chains from a collapsed polymer layer is recorded, giving rise to friction and enthalpic effects, with possible formation of fibrils. The extrusion of whole diblock copolymers from the layer, leading to irreversible effects, is suggested.

4.2 EXPERIMENTAL SECTION

The material used was the $P2VP_{102}PS_{75}$ diblock copolymer. Due to the slow adsorption kinetics of this diblock copolymer (see sub chapter 3.II), studies of grafted polymer monolayers in the close to the mushroom regime can be performed.

SFA MEASUREMENTS

Sheets of mica were cleaved and cut with a hot platinum wire. The thickness and surface area were 1–3 μm and ~1 cm^2, respectively. One side of the mica sheets was silvered with a thickness of 50 nm, by an evaporation technique (rate ~0.1 $nm \cdot s^{-1}$ and pressure ~10^{-6} Mbar). The mica sheets were then glued -silvered side down- on cylindrical lenses (R = 2 cm). The zero position of distance was first recorded as the contact between the two mica surfaces in argon. 10 ml of toluene (Merck) was brought into the liquid cell, and a force profile was recorded to check for possible contamination. 1 ml of the toluene solution of the diblock copolymer was then injected, reaching a final polymer concentration of 0.045 $mg \cdot ml^{-1}$. Several force profiles were recorded, after an incubation time of several hours.

AFM MEASUREMENTS

TOLUENE¾ Force measurements were obtained using a commercial Atomic Force Microscope (AFM) from Molecular Imaging. The experimental set-up employs a closed cell that protects the sensitive parts of the apparatus from hazardous solvents. Commercially available V-shaped Si_3N_4 cantilevers (Park Scientific) were used with pyramidal probe tips (radius of curvature of 30 nm; spring constant of 0.1 $N \cdot m^{-1}$). A piece of mica 1 × 1 cm^2 was cleaved and immediately placed in the liquid cell. The polymeric solution (0.05 $mg \cdot ml^{-1}$) was then injected and adsorption of the polymer on the mica substrate took place. Around 50 force profiles were taken after the elapse of 1 hour from injection.

CYCLOHEXANE¾ A mica substrate was incubated in a toluene solution of the diblock copolymer (0.05 $mg \cdot ml^{-1}$) for a period of one day. It was taken out, washed with pure

solvent and dried under a stream of argon. It was then placed in the AFM and the cell was filled with cyclohexane. The temperature of the system was varied by means of a heating plate (underneath the sample) from room temperature up to 38°C. This was done in a continuous fashion, with a rate of 1 °C·min^{-1}. During this time, force profiles were obtained using V-shaped Si_3N_4 cantilevers (Park Scientific) were used with pyramidal probe tips (radius of curvature of 30 nm; spring constant of 0.06 N·m^{-1}). An average of 10 force profiles were collected for every 0.5 °C step increase.

CONVERSION OF RAW AFM DATA TO FORCE VS. DISTANCE PROFILES

The distance between the two surfaces, probe and substrate, was varied using a piezoelectric crystal. The total force acting on the AFM tip was measured by detecting the deflection of the cantilever attached to the tip. A laser beam reflected from the back of the cantilever was directed onto a segmented photodiode, which detects small changes in the deflection of the cantilever. Force data were captured as diode output (nA) versus expansion of piezo (nm).

In a typical force–distance measurement, the probe moves towards the surface, recording the approach curve. When the two surfaces are "in contact", the tip continues to compress the surface further until it reaches several nN. In this regime the photodiode signal is linearly proportional to the expansion of the piezo. Data were converted to force (nN) using Hooke's law for a linear elastic spring, k. The linear regime of the force curve serves also to define the zero separation distance. The change in z-position is equal to the change in tip-mica separation plus the change in the cantilever's deflection: $Dz = DD + Dd$. Rearranging, we obtain $DD = Dz - Dd$ and need only to set an actual tip-mica separation distance, D. The point of intimate contact with mica, $D = 0$, is defined as the point where the approach force curve first becomes linear in the high force regime. Linear extrapolations of the baseline were made to find this zero position. The piezo then changes direction and the probe is retracted from the surface and a retract force profile is obtained.

4.3 RESULTS AND DISCUSSION

4.3.1 SFA FORCE PROFILES IN TOLUENE

Hadziioannou at al.[15] were the first to show diblock copolymers (P2VP/PS) adsorbed from toluene solutions on mica exhibit an ideal amphiphile behavior: from toluene solutions the diblock copolymer forms a polymer monolayer. The surface force measurements reveal purely long-range forces and the absence of any bridging.

Figure 4.1 (circle symbols) shows interaction of two mica surfaces covered with the $P2VP_{102}PS_{75}$ diblock copolymer in toluene, in crossed cylinder configuration. It is a monotonic reversible repulsive force, from which one can measure the layer thickness, L_o = 44 nm; as the distance where the force first deviates from zero.

A theoretical description of the experimental force-distance profile can be performed using the Milner Witten Cates model (MWC)[16], which is an exact solution of

self-consistent field equations, and has been used to quantify force profiles of highly dense polymer brushes obtained by SFA. However, the adsorbed monolayer of the $P2VP_{102}PS_{75}$ diblock copolymer cannot be successfully described by the MWC model.[17] It has been found that for block copolymers with sufficiently large P2VP blocks, physical properties of the adsorbed layers are better described by mushroom-type profiles rather than brush-type profiles.[18, 19, 20] A detailed description is presented in ref. 17 and hence not reported here.

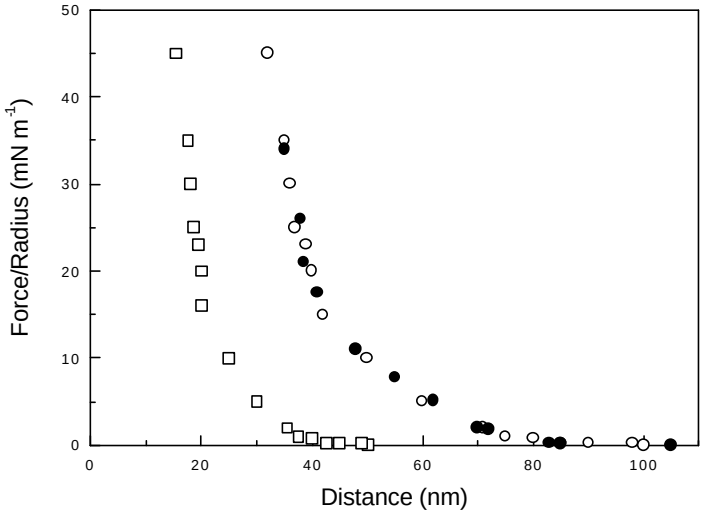

Figure 4.1: *Force-distance profiles for $P2VP_{102}PS_{75}$ in toluene solution, obtained by SFA. The force is normalized by the mean radius of curvature of the cylinders. The circle symbols represent a PS/PS profile, while the square symbols represent a PS/mica profile. Open symbols correspond to the approach curve, solid ones to the retract curve.*

In the following section we are going to compare force profiles obtained by SFA with force profiles obtained by AFM. SFA profiles show the interaction between two surfaces covered with the adsorbed monolayer while AFM profiles show the interaction between the adsorbed monolayer and a bare surface. It has been found[17] that the interactions between two polymer monolayers (PS/PS) (1) and a polymer monolayer with a mica surface (PS/mica) (2) are identical to those between (1) and (2) if the PS/mica profile is scaled by a factor of 2, in order to account for the monolayer's height (square symbols in figure 4.1). The same conclusion was reached using Monte Carlo simulations[8]. Hence, a direct comparison with force measurements obtained with AFM can be made.

4.3.2 AFM FORCE PROFILES IN TOLUENE

Figure 4.2 shows a typical, approach/retract, Force vs. Distance profile obtained by AFM. A bare tip approaches a monolayer-coated surface (formed by a diblock copolymer), in toluene and then retracts. Distinct regimes are labeled. At large distances, there is no interaction between the tip and the sample (I). As the tip is approaching the sample a nonlinear repulsive force is observed (II). A few nm away from the mica substrate the force-profile exhibits an attractive minimum (III). As the piezo continuously pushes the tip towards the sample, the cantilever bends (IV).

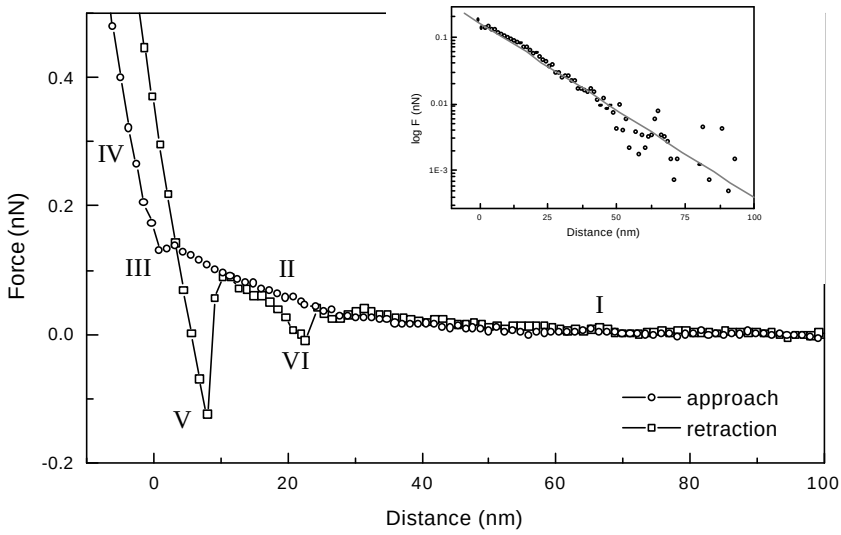

Figure 4.2: *Typical force-distance profiles for the $P2VP_{102}PS_{75}$, in toluene obtained by AFM. Distinct regimes are labeled and discussed in the text. The insert, log(F) vs. D of the approach.*

At some point, the voltage applied to the piezo is reversed, and the tip starts to retract from the sample. A hysteresis is observed, due to piezo artifacts, when the voltage is reversed. With continuing retraction, the tip exhibits a large adhesive force (V). At some point the tip jumps from the surface. Mechanically, instabilities occur when the first derivative of the force to the distance becomes equal to the spring constant. After the jump, the force returns to the value of the approach trace. Some traces also showed single or multiple attractive peaks[21], during which the force increased nonlinearly with the distance (VI), due to physiadsorption of a polymer chain on the AFM tip.

In this section, the forces exerted due to the compression of a polymer monolayer by means of an AFM tip will be compared with SFA force profiles. It will be shown that polymer chains can escape from underneath the tip to avoid compression. We will attempt to relate the experimental data to theoretical predictions.

During the approach of the tip to the polymer monolayer the force increases, due to steric crowding of polymer chains upon tip-polymer contact (~ 40 nm), similar to the profiles obtained by the SFA (figure 4.1). However, several features are different:

(a) Using SFA, the retract force profile followed the same trace as the approach one and both were monotonically repulsive until a distance of around 15 nm (distance of closest approach). Beyond this distance the polymer monolayer could not be compressed further. Using AFM, an attractive peak is superimposed at small separations on the repulsive approach force profile. The minimum of the peak is located at a distance, D_{peak}, of 2.57 ± 0.80 nm and at a force value, F_{peak}, of 0.12 ± 0.02 nN. Furthermore, the retract force profile first exhibits a large adhesion ($F_{adhesion}$ = 0.18 ± 0.01 nN), due to the adhesion of the tip to the substrate, and then follows the trace of approach curve, due to decompression of the polymer monolayer. Finally, in some profiles attractive peaks are evident at large distances, which will be discussed separately.

(b) The repulsive force measured in SFA is much larger than the one measured with AFM. In the SFA measurements a value of F_{max}/R = 50 mN·m^{-1} could be reached. The maximum force reached in AFM is around 0.12 nN. Normalization of the force with the radius of curvature of the tip gives a value F_{max}/R = 4 mN·m^{-1}; an order of magnitude lower than in SFA.

The differences between AFM and SFA data arise because in AFM the polymer monolayer is compressed by a surface with a small radius (~30 nm). Only a few molecules are in direct contact with the tip, compared to SFA where the area of contact is several μm^2. In AFM experiments a "large proportion" of the compressed chains are at the border of the tip and can move and bend laterally. In SFA we still have this phenomenon but the proportion of the chains at the border of the contact zone is very small (since the total area of contact is very large). Thus, the effect of the chain bending and lateral displacement is negligible.

The AFM data (attractive minimum on the approach curves and large adhesion with the substrate on retract curve) suggest that the grafted polymer chains, in order to avoid compression, escape from underneath the tip. Either PS parts of the block chains are displaced laterally with the P2VP being stationary -solid regime- (figure 4.3 b1), or the whole diblock copolymer is moved along the substrate -liquid regime- (figure 4.3 b2).

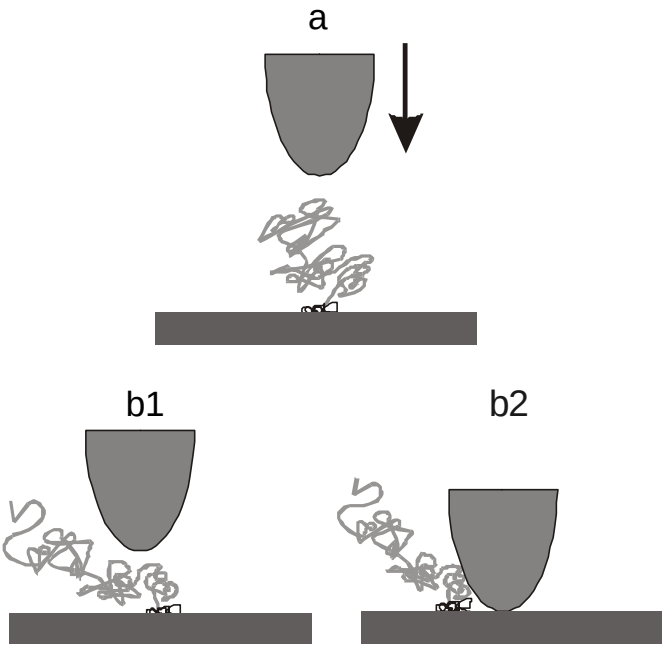

Figure 4.3: *Schematic representation of the compression of an adsorbed diblock copolymer on a surface, in a selective solvent, by an AFM tip.* a) *Tip approaching the polymer chain.* b1) *The adsorbing block is immobile and part of the polymer chain escapes from underneath the tip (solid regime).* b2) *The adsorbing block is mobile and the chain can move laterally on the surface, to avoid compression (liquid regime).*

In the remaining part of the section we will attempt to compare our data with theories presented in literature, concerning the compression of grafted chains with surfaces. A brief review of the theoretical predictions will be presented.

ALEXANDER-DE GENNES MODEL.

Theoretical background: The height of a polymer brush, in good solvent conditions, has been derived by Alexander[22] as $L_o = s^{1/3}R_F^{5/3}$. de Gennes[23], using simple scaling laws, based on the results of Alexander calculated the energy per unit area, *f*, between two parallel surfaces each coated with a polymer brush as a function of their separation, *D*:

$$f \approx \frac{k_B T}{d^3}\left[\left(\frac{2L_o}{D}\right)^{9/4} - \left(\frac{D}{L_o}\right)^{3/4}\right] \qquad \text{for } D < 2L_o \qquad [4.1]$$

where k_B is the Boltzmann constant, T the absolute temperature, d the grafting distance and L_o the equilibrium brush height.

The first bracket term accounts for the osmotic repulsion due to increasing polymer concentration as the surfaces are pushed together. The second bracket term represents the decrease in elastic energy of the chains, as they are compressed. One can essentially neglect the strong osmotic repulsion, at strong compressions[24, 3], for the AFM configuration. This situation occurs with AFM due to the small size of the tip. Furthermore, the polymer chains get laterally displaced, if the external forces become too high. In this case, *f* is given by a simple exponential:

$$f \approx 100\frac{k_B T}{d^3}\exp(-\frac{pD}{L_o}) \quad 0.2 < D/L_o < 0.9 \qquad [4.2]$$

Alexander–de Gennes theory can account for the situation of a polymer brush interacting with a bare surface, by normalizing the displacement, by the separation at which the repulsion first appears:

$$f \approx 50\frac{k_B T}{d^3}\exp(-\frac{2pD}{L_o}) \qquad [4.3]$$

The interaction energy per unit area, *f*, between two parallel plates can be related to the force, *F*, between a flat surface and a sphere of radius *R*, using the Derjaguin approximation $-F(D) = 2pRf(D)$. This approximation can be used when $R >> D$. Hence, equation [4.3] can be written as:

$$F(D) \approx 100\frac{RL_o k_B T}{d^3}\exp(-\frac{2pD}{L_o}) \qquad [4.4]$$

Equation [4.4] describes the interaction of polymer chains with a spherical object, but in AFM measurements the polymer chains are interacting with a tip that has a parabolic shape. A parabola can be described by $z - D = \frac{x^2}{2R}$ where *x* is the radius of the tip at a certain distance *z* from the substrate and *R* is the radius of a sphere inscribed at the end of the tip with the same radius of curvature (figure 4.4).

Thus, to derive a more accurate expression for the total force, the force per unit area has to be integrated over the whole tip surface. The total force is[7]:

$$F \approx 2p\int_0^\infty f(x)xdx = 2p\int_D^\infty f(z)x\frac{dx}{dz}dz = 2p\int_D^\infty f(z)Rdz \Rightarrow$$

$$F = 50k_B T\frac{RL_o}{d^3}\exp(-\frac{2pD}{L_o}) \qquad [4.5]$$

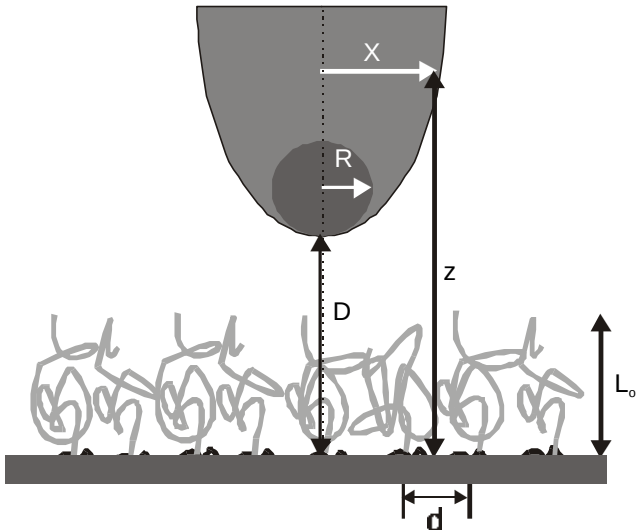

Figure 4.4: *Schematic drawing of an AFM tip and a polymer brush formed by diblock copolymer (P2VP/PS) on a substrate –black lines represent the P2VP blocks and gray lines the PS. The symbols are explained in the text (note that R >> D in reality).*

Comparison: Equations [4.4] and [4.5] are exponentially decaying functions. The fit of these equations (solid gray line of figure 4.5), gives a height of the polymer brush equal to $L_o = 106.2 \pm 14$ nm, and grafting distances of d = 20.8 ± 1.3 nm and d = 16.5 ± 1.2 nm, for eq. [4.4] and [4.5], respectively. The grafting distances correspond to average grafting densities of $s = (0.23 \pm 0.03) \cdot 10^{-16} \mathrm{m}^{-2}$ and $s = (0.37 \pm 0.05) \cdot 10^{-16} \mathrm{m}^{-2}$, respectively. The values obtained for the grafting density agree well with the value obtained by the kinetics experiments, reported in sub chapter 3.II — $s = (0.234 \pm 0.03) \cdot 10^{-16} \mathrm{m}^{-2}$, for the same adsorption time. However, the height of the brush is overestimated, even taking into account the shape of the tip. This observation has been reported also by others[3, 5, 7]. Most probably due to the scaling nature of the model, assumptions that were made, and uncertainties in determining the tip's radius and cantilever's spring constant.

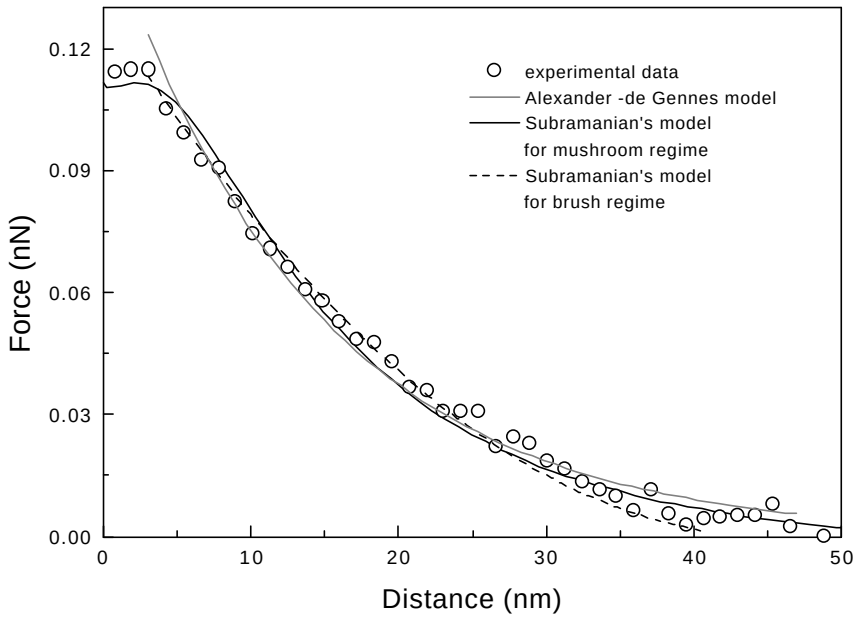

Figure 4.5: *Approach force–distance profile. The profile is fitted with various distance dependencies described in the text.*

SUBRAMANIAN'S MODEL.

Theoretical background: We shall briefly review the scaling predictions of Subramanian et al.,[8] who studied the interaction of a finite object with a grafted polymer layer, in good-solvent conditions. Several cases have been considered.

For polymer chains on a surface, two regimes were examined, the solid (figure 4.3 b1) and the liquid regime (figure 4.3 b2). In the solid regime, the polymer chains are laterally immobile, and this regime is applicable to polymer chains that are covalently bonded to the surface. In the liquid regime, the polymer chains are mobile on the surface, and this is applicable to polymer chains at a liquid interface or chains physically adsorbed on the surface. Force-distance dependencies were given only for the liquid regime.

For a polymer monolayer with a high grafting density -brush regime-, polymer chains are compressed by the tip but cannot exhibit any escape transitions, due to the high coverage. However, the polymer chains can splay.

For a polymer brush in the liquid regime, the force profile scales with the distance as:

$$F \propto (L_o - D)^2 \qquad [4.6]$$

For a polymer monolayer with a low grafting density -mushroom regime-, the force exerted by the polymer chains can be recognized as the force needed to compress a

solid mushroom system with a prefactor, which accounts for the escape of the mushrooms from under the tip.

$$F \approx k_B T s_o AN \left(\frac{a^{5/3}}{D^{8/3}} \right) \exp\left(-N \left(\frac{a}{D} \right)^{5/3} \right) \qquad [4.7]$$

with σ_o the grafting density, A the area of the tip (pR^2), N the polymerization index and a the monomer size (0.546 nm —calculated from bulk polymer density). The predicted force, thus, will show a maximum and will get smaller with decreasing D.

Comparison: We fitted the data to eq. [4. 6] dashed black line in figure 4.5 and found a layer height, L_o, of 45 ± 5 nm, which is consistent with the expected value.

Our force profiles showed the same features as described in eq. [4.7]: at small separations, a local minimum on the repulsive curve is evident. The experimental data fitted with equation [4.7] (black solid line in figure 4.7). Direct application gave a grafting density, $s_o = (2.7 \pm 0.4) \cdot 10^{-16} \mathrm{m}^{-2}$. The calculated grafting density is clearly overestimated. This discrepancy is not surprising, taking into account that numerical prefactors have been ignored in deriving equation [4.7][9], and the experimental uncertainties discussed above. Furthermore, it has been argued that the escape transitions are rate-dependent.[14] The model that we have employed is based on scaling laws, which do not take into account possible time effects.

4.3.3 AFM FORCE PROFILES IN CYCLOHEXANE

We have measured the forces between the adsorbed diblock copolymer monolayer and the AFM tip in cyclohexane. These measurements were done at temperatures ranging from 22 °C up to 38 °C. With change of temperature, the solvent quality is changed from a poor to a near-theta solvent for PS; the theta-temperature of PS in cyclohexane in the bulk, is 34.5 °C.

In figure 4.6 typical force profiles are shown for poor-solvent conditions (a) and near-theta-solvent conditions (b). On the approach curves a long-range attraction is evident. Deviations from the zero force start at around 100 nm, much further than the equilibrium height of the monolayer. Whereas at near-theta conditions the approach and retract curves are almost identical, at poor-solvent conditions the retract curves are full of attractive peaks.

The maximum attractive force measured from the force profiles is plotted as a function of the reduced temperature $t = (T-T_q)/T$ for the approach force profiles (figure 4.7 a) and the retract force profile (figure 4.7 b). For the retract curves, two sets of data are depicted, circles and squares; circles correspond to the maximum long-range attraction and squares to the maximum attractive force of the peaks. By increasing the temperature we observe a smooth decrease of F_{max} for both approach and retract force profiles. A

smooth change of relevant physical properties of polymer monolayers, with no abrupt changes have also been observed by others[25].

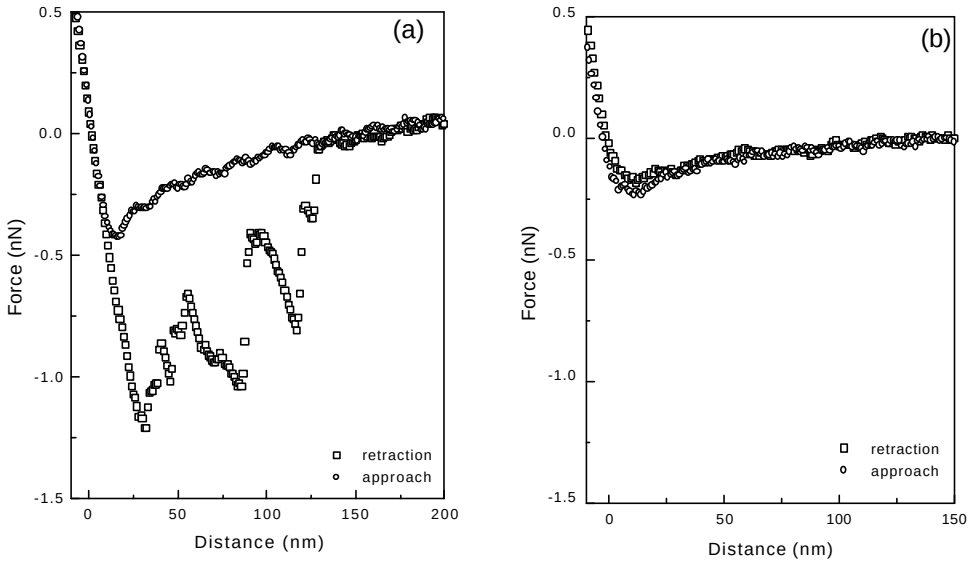

Figure 4.6: *Typical force-distance profiles for the $P2VP_{102}PS_{75}$ diblock copolymer adsorbed on mica, in cyclohexane* a) *at 22 °C and* b) *at 37.7 °C.*

At poor-solvent conditions an attraction is expected, due to osmotic interactions. The PS chains are in a poor-solvent and prefer to be in contact with each other rather than in contact with the solvent. Another source of attraction is the formation of polymer "bridges" between the substrate and the tip (the chain is attached to both surfaces at the same time). This force is also attractive, due to the tension of the bridge, which is of entropic origin. As the temperature increases, and the solvent becomes a near-theta one, the osmotic interactions become zero-to-positive, while bridging still exists. Hence, the maximum attractive force should decrease with increasing temperature. Such a trend is indeed observed in figure 4.7 a.

Due to the strong adsorption of PS on the tip (bridging) at near-theta and poor-solvent conditions we do not observe any escape transitions like the one observed in good-solvent conditions.

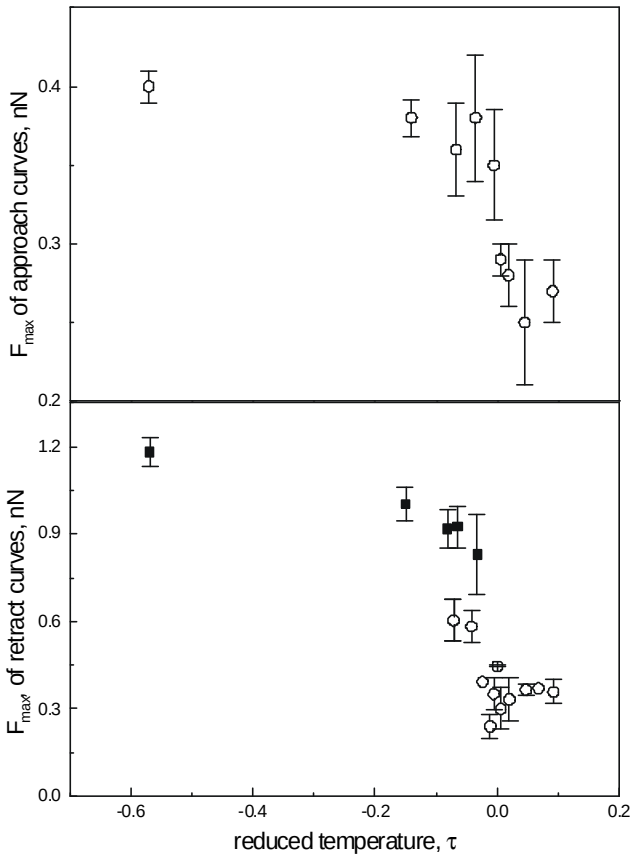

Figure 4.7: *F_{max}, measured from the force-distance profiles, versus the reduced temperature, $t = (T-T_q)/T$.* a) *Measured from approach profiles.* b) *Measured by retract profiles. Symbols are explained in the text. The error bars were obtained from the various attractive peaks and from different force profiles.*

On the retract curves, at poor-solvent conditions, multiple attractive peaks were observed. Due to solvophobic interactions, the grafted chains on the surface aggregate into surface octopus "micelles" (sub chapter 3.II). During the retraction of the tip from the surface, parts of chains that have adsorbed on the tip and get stretched, altering thus the structure of the collapsed chains. At a critical extension, chains or parts of chains get extruded from the entangled polymer matrix.[26] This leads to frictional forces and exposure of monomers to the poor-solvent. In addition, the extruded monomers can form aggregates, in the form of strands, to minimize the contact with the solvent. These phenomena could explain the high forces measured on the retract curves.

At high extensions, we cannot exclude the possibility of extrusion of whole diblock copolymer from the adsorbing layer. A number of communications[27] have reported the force required to detach a chain from an adsorbing surface. The force versus extension profile exhibits sharp discontinuities, which have been interpreted in terms of

desorption of adsorbed monomers. This phenomenon could create irreversible effects and explain the large distance at which the forces were first detected.

Force measurements of adsorbed diblock monolayers in cyclohexane have been performed with the SFA[15]. Attraction was found at poor-solvent condition, and repulsion at near-theta conditions. A comparison is hard though to be performed, due to a) the different experimental conditions (in SFA both surfaces were covered with molecules) and b) to the possible effects, discussed above, happening during the AFM experiments.

4.4 CONCLUSIONS

We have directly measured the force versus compression profiles of a polymer monolayer in the mushroom regime with AFM and SFA, in good-solvent conditions. We observed different responses of the force at high compressions, due to differences in the area of confinement, with respect to the size of the molecules. In SFA configuration, we observe a collective response involving many chains in the monolayer while, in the AFM configuration only a few chains are involved.

The force profiles obtained with AFM in good-solvent confirm recent theoretical predictions that polymer chains grafted on a surface can exhibit escape transitions when the chains are compressed by a surface with a small radius. We have attempted to quantify the experimental data with a recent theory, which takes into account the escape of the polymer chains from underneath the tip. Direct application described our data poorly, primarily due the to scaling nature of the theory and to possible time effects.

For measurements performed in poor and near-theta-solvent conditions, the force profiles were difficult to quantify. Escape transitions were not observed, due to the strong adsorption of PS chains on the AFM tip. Attractive forces were measured mainly due to bridging under compression. Stretching of the bridging chains, on decompression, lead to frictional forces, exposure of polymer chains in poor-solvent, and possible extrusion of whole diblocks, creating irreversible effects.

REFERENCES

[1] Flory, P. J. *Principles of Polymer Chemistry* Cornell University Press (Ithaca N. Y.) **1953**

[2] a) Israelachvili, J. N. *Intermolecular and Surface Forces*: Academic Press; London, **1992**

b) Patel, S.S.; Tirrell, M. *Annu, Rev. Phys. Chem.* **1989**, 40, 597

c) Luckham, P.F. *Polymer Surfaces and Interfaces*: Edited by Feast, W.J. and Munro, H. S. **1987** John Wiley & Sons Ltd

[3] O'Shea, S.J.; Welland, M.E.; Rayment, T. *Langmuir*, **1993**, 9, 1826

[4] Overney, R.M.; Leta, D.P.; Pictroski, C.F.; Rafailovich, M.H.; Liu, Y.; Quinn, J.; Sokolov, J.; Eisenberg, A.; Overney, G. *Phys. Rev. Lett.* **1996**, 76, 1272

[5] Koutsos, V. *Physical properties of grafted polymer monolayers studied by scanning force microscopy: morphology, friction, elasticity* Ph.D. thesis, University of Groningen **1997**
[6] Kelly, T.W.; Schorr, P.A.; Johnson, K.D.; Tirrell, M.; Frisbie, C.D. *Macromolecules* **1988**, 31, 4297
[7] Butt, H-J.; Kappl, M.; Mueller, H.; Raiteri, R. *Langmuir* **1999**, 15, 2559
[8] Murat, M.; Grest, G.S. *Macromolecules* **1996**, 29, 8282
[9] Subramanian, G.; Williams, D.R.M.; Pincus, P.A. *Europhys. Lett.* **1995**, 29, 285
[10] Guffond, M.C.; Williams, D.R.M.; Sevick, E.M. *Langmuir* **1997**, 13, 5691
[11] Williams, D.R.M.; MacKintosh, F.C. *J. Phys. II* **1995**, 5, 1407
[12] a) Jimenez, J.; Rajagopalan, R. *Eur. Phys. J. B* **1998**, 5, 237
b) Jimenez, J.; Rajagopalan, R. *Langmuir* **1998**, 14, 2598
[13] Zhulina, E.; Walker, G.C.; Balazs, A.C. Langmuir **1988**, 14, 4615
[14] Milchev, A.; Yamakov, V.; Binder, K. *Europhysic letters* **1999**, 47, 675
[15] Hadziioannou, G.; Patel, S.; Granick, S.; Tirrell, M. *J. Am. Chem. Soc.* **1986**, 108, 2869
[16] a) Milner, S.T.; Witten, T.A. Cates, M.E. *Macromolecules*, **1988**, 21, 2610
b) Milner, S.T. *Europhys. Lett.* **1988**, 7, 695
[17] Belder, G. *Surface forces and nanorheological properties of adsorbed polymer monolayers* Ph.D. thesis, University of Groningen **1995**
[18] Field, J.B.; Toprakcioglu, C.; Dai, L.; Hadziioannou, G.; Smith, G.; Hamilton W. *J. Phys. II France* **1992**, 2, 2221
[19] a) Kent, M.S.; Lee. L.T.; Farnoux, B.; Rondelez, F.; *Macromolecules* **1992**, 25, 6240
b) Kent, M.S.; Lee. L.T.; Farnoux, B.; Rondelez, F.; Smith, G.S. *J. Chem. Phys.* **1995**, 103, 2320
[20] Baranowski, R.; Whitmore, M.D.; *J. Chem. Phys.* **1995**, 103, 2343
[21] Not all force profiles recorded showed these attractive peaks.
[22] Alexander, S. *J. Phys. (Paris)* **1977**, 38, 983
[23] de Gennes, P.G. *Adv. Colloid Interface Sci.* **1987**, 27, 789
[24] Israelachvili, J.N. *Intermolecular and Surface Forces*: Academic Press; London, **1992**
[25] a) Karim, A. S.K.; Satija, S.K.; Douglas, J.F.; Anker, J.F.; Fetters, L.J. *Phys. Rev. Lett.* **1994**, 73, 3407
b) Webber, R.M.; van der Linden, C.C.; Anderson, J.L. *Langmuir* **1996**, 10, 1040
c) Habicht, J.H.; Schmidt, M.; Ruhe, J.; Johannsmann, D. *Langmuir* **1999**, 15, 2460
d) Kent, M.S.; Majewski, J. Smith, G.S.; Lee, L.T.; Satija, S. J. *Chem. Phys.* **1999**, 110, 3553
[26] Brochard-Wyart, F.; de Gennes, P.G.; Leger, L.; Marciano, Y.; Raphael, E. *J. Phys. Chem.* **1994**, 98, 9405
[27] Haupt, B.J.; Ennis, J.; Sevick, E.M. *Langmuir* **1999**, 15, 3886 and references therein

CHAPTER 5

NANORHEOLOGY OF ADSORBED DIBLOCK COPOLYMER MONOLAYERS

ABSTRACT

The mechanical properties of P2VP/PS block copolymer monolayers are investigated by means of a Surface Forces Apparatus adapted to operate as a rheometer at the near-molecular level. Nanorheological experiments to determine the complex shear modulus have been performed as a function of the separation and the frequency, in the linear regime of deformation. The experimental data are compared with a model relating the complex shear modulus to the structure of the confined adsorbed monolayers.

5.1 INTRODUCTION

The determination of ultra-thin film properties is crucial for understanding the behavior of complex materials, and processes such as adhesion and lubrication. The Surface Forces Apparatus has been very helpful in studies of static and dynamic properties of thin layers confined between two surfaces.[1] Rheological measurements on ultra-thin layers can be performed using a modified SFA, adapted to operate as a rheometer at the near-molecular level.

Various methods have been developed to study the rheological properties of thin films. Drainage experiments[2] —the two surfaces are brought together at a constant speed— give information on the position of the shear plane. Relaxation measurements[3] determine the variation of the viscosity and the relaxation time as a function of the surface separation. Small amplitude oscillatory motions around an average distance measure the variation of the viscosity[4] or the complex shear modulus[5] as a function of the confinement level. These methods are based on normal displacements of one of the two surfaces, and determination of the viscoelastic properties of the interface can be performed, through the lubrication approximation. In contrast, tangential experiments —where two surfaces are moved parallel to each other— should give more direct information about the viscoelastic properties. Only a few experiments have been performed with an SFA adapted to impose tangential displacements on one of the surfaces at a constant separation. Most of these have been performed with polymer melts[6], while dynamic experiments on adsorbed polymer layers in solution [7, 8, 9] are limited in number.

In the case of two highly stretched polymer brushes sheared against each other, in good-solvent conditions, it has been shown that measurable shear forces emerge only at high compressions and high shear velocities.[9] This was attributed to the small interpenetration zone between the opposite polymer brushes. Scaling[10] and self-consistent field theories[11] to describe physical properties of polymer brushes are based on the assumption of no interpenetration in the limit of infinitely high molecular weight. However, computer simulations[12, 13] show that polymer brushes indeed do interpenetrate.

The objective of the present chapter is to study the linear shear response of two adsorbed diblock copolymer monolayers, close to the mushroom regime. The Experimental section gives a brief technical description of the apparatus and explains how to extract the complex shear modulus from the raw data. In the Results section the experimental data obtained by shearing two monolayers of diblock copolymer against each other in the linear regime of deformation are shown. Finally, the results are compared with a theoretical model.

5.2 EXPERIMENTAL SECTION

APPARATUS¾ The lower surface is supported by a leaf spring ($k_v \cong 1000$ N·m^{-1}), attached to the inside of the liquid cell, rigidly connected to a piezo-block. The lateral

expansion of the piezo-block is used to displace the lower surface tangentially with respect to the upper surface. The force transmitted through the sample under study is determined from the displacement of the support of the upper surface. This support is suspended from two vertical leaf springs. The deflection of these springs is measured directly by means of a very sensitive two-beam fiber interferometry, originally developed for AFM[14]. The fiber tip is positioned by a piezoelectic tube, which is incorporated in a feedback system designed to maintain a fixed separation between the fiber tip and a small mirror connected to the support of the upper surface. The feedback voltage on the piezoelectic tube is proportional to the displacement of the upper surface. A displacement resolution close to 0.1 nm can be achieved with this system. It gives a force resolution ~10^{-7} N, depending on the stiffness of the spring. A relatively high stiffness ($k_h \cong 3000$ N·m^{-1}) is used to shift the resonance frequency to high values. The mass, m, of the upper surface (lens + support) is around 13 g, giving a resonance frequency of $\sqrt{k_h / m} \cong 390$ Hz.

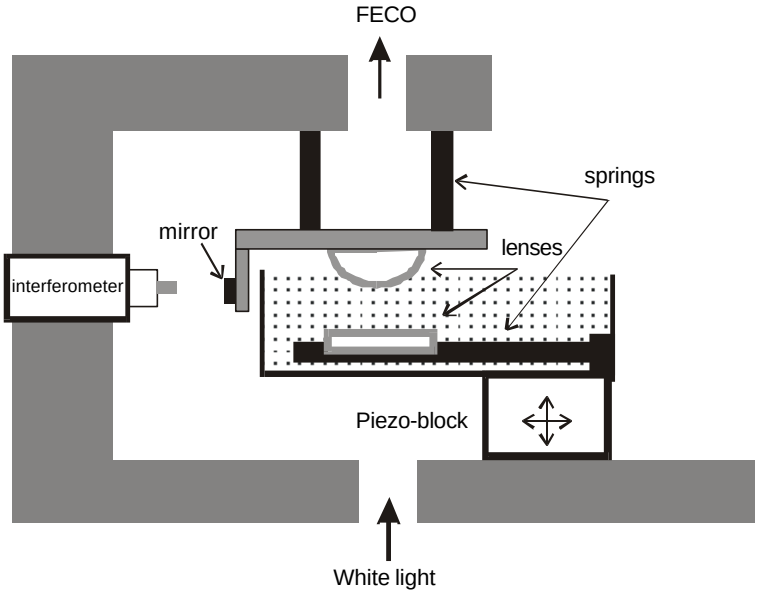

Figure 5.1: *Schematic drawing of the apparatus*

The piezo constant of the fiber positioning tube (≅ 13 nm·V^{-1}) was calibrated against the known wavelength delivered by the laser diode of the interferometer (λ = 846 nm). The voltage needed to expand the piezo between two successive peaks, λ/4, of the reflected light was measured when the fiber was displaced normally to the mirror (the feedback loop, to maintain a constant separation between the fiber tip and the mirror, was open). The same procedure was applied to calibrate the tangential expansion (≅ 62 nm·V^{-1}) of the piezoelectric block. In this case a mirror was connected to the piezo-block and the piezo-block was moved instead of the fiber.

The transfer function between the input sinusoidal voltage, $x_1(t) = x_1^o \sin(\omega t)$, applied to the piezo-block and the output voltage, $x_2(t) = x_2^o \sin(\omega t + \varphi)$, (where φ is the phase shift between the input and the output voltage) applied by the feedback system to the piezo tube, was measured in the frequency regime (0.1–50 Hz). Typical signal curves are presented in figure 5.2. Lower frequencies can be reached but then thermal drifts can no longer be neglected. The amplitude ratio of the measured voltages $x_1^o / x_2^o \cong$ 0.2, shows no variations with frequency and there is no significant phase shift. In addition, the ratio of the voltage amplitudes is in agreement with the distance calibrations based on the known wavelength of the laser diode used in the interferometer (13/62 ≅ 0.2).

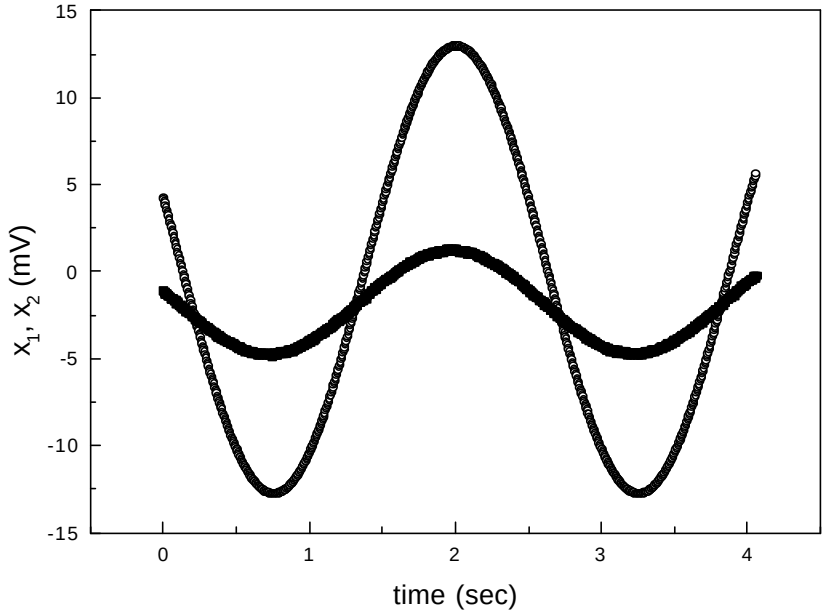

Figure 5.2: *Input oscillatory signal imposed to the piezo-block (open) and output voltage (solid) needed to expand the piezotube supporting the fiber as a function of time. The amplitude of the input signal represents a displacement of 0.6 nm.*

MODELLING¾ Assume a medium sandwiched between to flat surfaces. When a sinusoidal motion, x_1, is imposed on the lower surface, the resulting motion of the upper surface, x_2, is coupled to the motion of the lower surface through the shear modulus G^* of the viscoelastic medium.

The strain resulting from the motion $x_1(t)$ imposed on the system is given by:

$$\gamma = \frac{x_1(t) - x_2(t)}{D} \qquad [5.1]$$

where D is the surface separation.

The resulting stress is:

$$s = G^* g = \frac{F_{shear}}{A} \qquad [5.2]$$

where A is the area of the plates in contact with the sheared medium.

In order to calculate G^*, we apply the motion equation to the upper surface:

$$F_{shear} + F_{spring} = m\frac{d^2 x_2}{dt^2} \qquad [5.3]$$

where F_{spring} is the restoring force due to the leaf springs, k_h, supporting the upper surface. By combining the above equations, we obtain the complex shear modulus G^* as a function of known parameters:

$$G^* = \left(k_h - m\omega^2\right)\frac{D}{A}\left(\frac{x_1^o}{x_1^o e^{j\varphi}} - 1\right)^{-1} \qquad [5.4]$$

The inertial term can be neglected since we work at low frequencies ($k_h >> m\omega^2$).

The above analysis applies rigorously for flat and parallel surfaces. The surfaces of interest bear polymer layers extending to distances of $L_o \sim 40$ nm. When the closest separation between the mica surfaces is less than the sum of the layer thickness, $2L_o$, a circular area of contact is formed. Its radius is given by:

$$r = \left(2R\left(2L_o - D\right)\right)^{1/2} \qquad \text{with } D < 2L_o << R \qquad [5.5]$$

where R is the radius of curved surfaces on which the mica surfaces are glued.

This relationship indicates that r is much larger than D. An example of numerical application of eq. [5.5] with R = 1 cm, L_o = 100 nm, D = 50 nm gives $r \sim 31$ μm. Thus, for tangential oscillations with amplitude smaller than D, the geometry of the system can be approximated as plane-plane, simplifying the rheological analysis considerably.

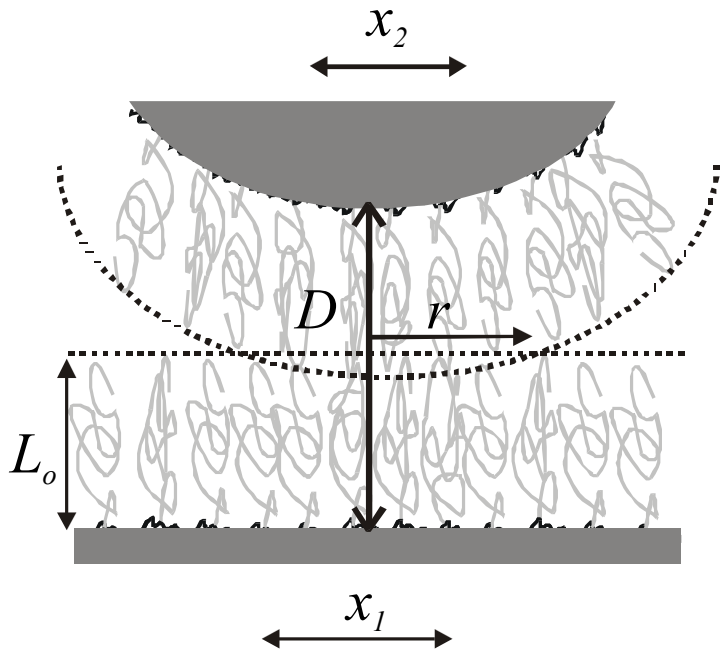

Figure 5.3: *Modelization of the interfacial area. D is the smallest separation between the solid surfaces; r is the radius of contact area between the layers the solid surfaces; L_o is the thickness of one layer and x_1 and x_2 are the displacement of the lower and the upper surfaces, respectively.*

SAMPLES¾ Freshly cleaved muscovite rudy mica (grade 4) is used as a substrate for the experiments. The P2VP/PS block copolymer employed has a molecular weight of 102 000 g·mol^{-1} and 75 000 g·mol^{-1} for the P2VP and PS block, respectively. Analytic grade toluene is used as a solvent. PS is well solvated by toluene, while P2VP is non-solvated. Monolayers on mica having an anchor layer of P2VP and a buoy layer of PS chains are formed via adsorption from a toluene solution.

PROCEDURE¾ Mica sheets (thickness ~ 2 μm) are coated by evaporating a 45 nm layer of silver on one side. The sheets are glued on cylindrical lenses (R ~ 2 cm), with the silvered side facing the lenses, with a mixture 50/50 by weight of dextrose and galactose. The apparatus is flushed with argon for more than half an hour prior to the experiments. The contact position is defined by the adhesive contact between the two mica surfaces in argon. All distances between the mica surfaces refer to this contact point.

Surface forces are first recorded in pure toluene, to check for possible contamination. Then 1 ml of the diblock copolymer solution is added to the liquid cell leading to a final polymer concentration of 0.045 mg·ml^{-1}, which is below the cmc. The

surfaces are kept well separated (~1 mm) in order to allow the polymer chains to diffuse and adsorb on the mica surfaces.

Dynamic measurements were carried out by varying the frequency. For each change in frequency, the surfaces were brought together in small steps. After each step sufficient time was allowed to elapse, to obtain a steady-state response. The normal force was then collected and the amplitude and phase shift of the shear response were recorded. Care was taken to keep the input signal small enough to stay in the linear regime.

The experiments have been performed at a constant temperature of 20 ± 0.5 °C.

5.3 RESULTS

The compression of the diblock copolymer layers results in a monotonic repulsive force (figure 5.6), whose range reflects the extension of the layers normal to the surfaces. The threshold of the repulsive forces, $2L_o$ = 80 nm, is used to define the area of contact needed to calculate the complex shear modulus when the layers are sheared.

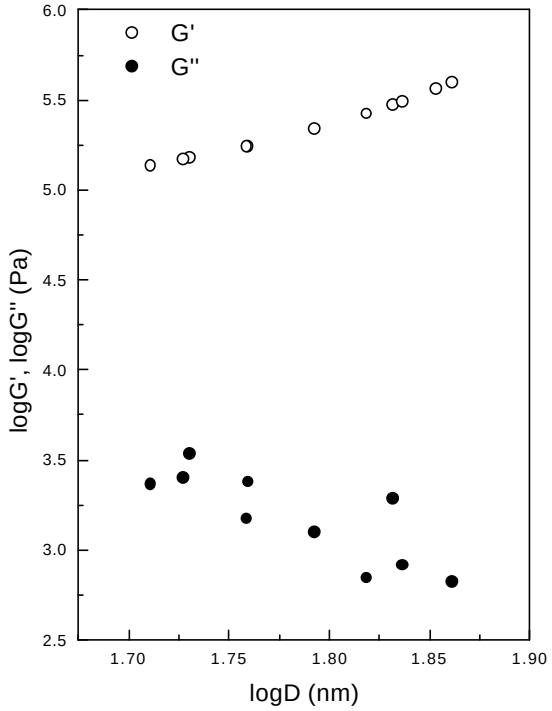

Figure 5.4: *Log-Log graph of storage G' and loss G'' modulus as a function of distance D, at a constant frequency of 5.43 Hz.*

Shear experiments between two adsorbed monolayers of diblock copolymer in toluene have been performed. Figure 5.4 shows the storage modulus G', and the loss modulus G'', as a function of the closest separation D between the mica surfaces. The measurements have been performed at a constant frequency of 5.43 Hz and a strain lower than unity. The shearing has been performed at distances below the first contact of the adsorbed layers, $2L_o$. At distances beyond the threshold of the static force, we have not been able to measure any tangential forces. Figure 5.4 shows that G' increases as the separation increases, while the experimental data of G'' show an decrease, however there is a lot of scatter. Furthermore, G' is larger than G'' at all measured distances. Hence, the viscoelastic behavior is dominated by the elastic component.

Figure 5.5 shows the variations of the in-phase, G', and out-of-phase, G'', components of the shear modulus as a function of the frequency for a fixed distance, 65.9 nm, lower than $2L_o$. G' displays a plateau modulus for all frequencies employed while G'' decreases as $w^{-1/2}$.

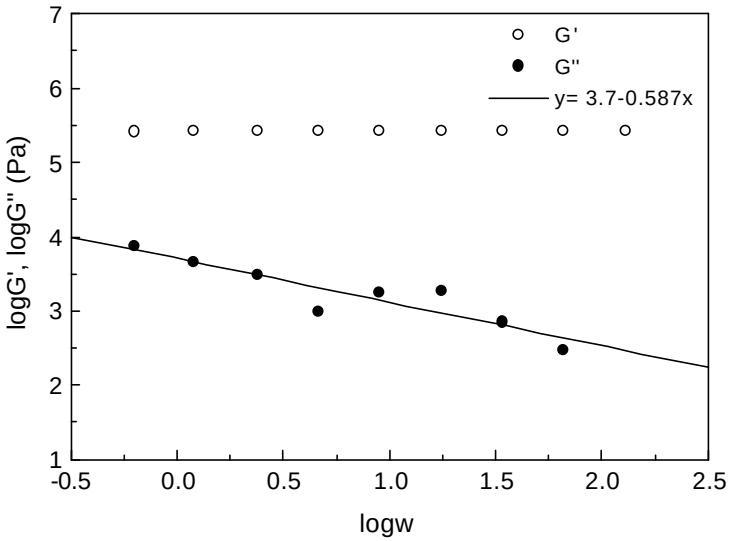

Figure 5.5: *Log-Log graph of storage G′ and loss G″ modulus as a function of frequency w, at a separation of 66 nm. The straight line shows a slope of a -0.587.*

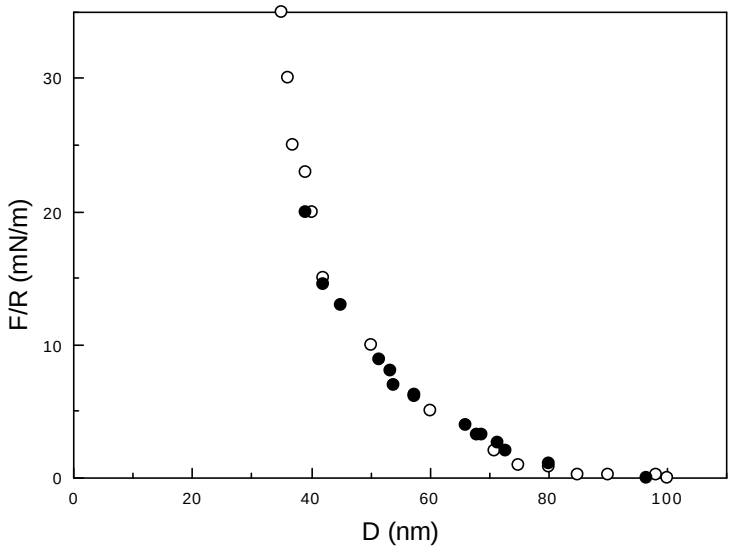

Figure 5.6: *Plot of normalized force F/R as a function of distance D; before (open) and during shearing experiments (solid).*

In order to check for any influence of the tangential displacement on the structure of the layer, the normal force is also measured during the shear experiment. The resulting force profile is compared with the force profile measured before the shear displacements (figure 5.6). There is no distinguishable change. This indicates that the structure is not altered by the tangential displacement of the surfaces.

5.4 DISCUSSION

When two brushes are compressed against each other, they interpenetrate weakly[15]. The interpenetration layer controls the shearing properties of the brushes[15, 16]. Its thickness increases as the grafting density is reduced.[12] The friction coefficient between real brushes (high grafting density) has been reported to be weak[7, 9]. The case that we are dealing with is different, since we do not have real brushes but adsorbed layers of slightly asymmetric copolymers. The structure of these layers is intermediate between the mushroom and the brush regime (sub chapter 3.II).

The interface between the mica surfaces can be approximated by a layered system (figure 5.7), symmetric about the middle of the gap. The layers that are considered are: the interpenetration layer (thickness d), the P2VP layer (thickness d_{P2VP}) and the part of PS layer that is not interpenetrating.

The viscoelastic properties of such a layered structure can be described by the relationship:

$$\frac{D}{G^*} = \frac{d}{G^*_{\text{int}}} + \frac{d_{P2VP}}{E_{P2VP}} + \frac{D - d - d_{P2VP}}{E_{PS}} \qquad [5.6]$$

where G^* is the global complex modulus characterizing the interface, G^*_{int}, E_{P2VP} and E_{PS} are the moduli of the interpenetration layer, the P2VP layer and the non–interpenetrated part of the PS layer, respectively.

Figure 5.7: *Scheme of the area of contact between the layers: d is the interpenetration layer thickness, d_{P2VP} is the thickness of the P2VP layer and D is the separation between the solid surfaces.*

d_{P2VP}/E_{P2VP} can be neglected in comparison with the other terms in eq. [5.6]. d_{P2VP} amounts to a 15 Å[17], which is much smaller than the thickness of the PS layer. In addition, the P2VP is immersed in a poor-solvent, and its bulk melt glass temperature, $T_g \approx 105$ °C, is higher than the experimental temperature, 20 °C. Its modulus should be close to a glassy modulus and thus much higher than the other modulus considered in eq. [5.6].

Equation [5.6] can be reduced to the contributions of the interpenetration layer and the non-interpenetrating part of the PS layer. We will now focus on the interpenetration layer. We make the assumption that d is small in comparison to D, and nearly independent of the degree of confinement of the layers. The complex modulus, G^*_{int}, characterizing the behavior of the chains within the interpenetration layer, can be described by the Rouse model, if no entanglements are present within the layer. Hence, for high frequencies[18] $wt > 1$, the modulus of the interpenetration layer should vary as

$G'_{\text{int}} \sim G''_{\text{int}} \propto \omega^{1/2}$, where τ is the relaxation time accounting for the response of the interpenetration layer.

We consider the non-interpenetrating part of the PS layer. This part can be characterized by an elastic modulus E_{PS} accounting for the stretching of the chains due to the shearing. Calculations to obtain such a modulus have already been presented in the case of a brush/wall system.[7]

$$E_{PS} \propto D^{3/4} \qquad [5.7]$$

Considering $G'_{\text{int}} > E_{PS}$ for high frequencies, equation [5.6] can be written as:

$$\left\{ \begin{array}{l} G' \approx \dfrac{E_{PS} D}{(D - d - d_{P2VP})} \propto \dfrac{D^{7/4}}{(D - d - d_{P2VP})} \\ G'' \approx \dfrac{E_{PS}^2 d D}{2(D - d - d_{P2VP})^2 G'_{\text{int}}} \propto \dfrac{D^{5/2} d \omega^{-1/2}}{2(D - d - d_{P2VP})^2} \end{array} \right\} \qquad [5.8]$$

This model can be compared with the experimental data presented in figure 5.4 and 5.5. At a constant separation between the mica surfaces, the value of G' is independent of the frequency throughout the range of measurements. In addition G'' decreases as $\omega^{-1/2}$ (figure 5.5). These dependencies are in agreement with the proposed model.

Equations [5.8] show the increase of G' and G'' as D increases. Figure 5.4 shows the same dependence for G'. For G'' we do not obtain the same dependence, in figure 5.4 we found a decrease with D. This discrepancy can be due to the dependence of the interpenetration layer on D, which in the model was assumed to be independent. Furthermore equation [5.7] has been derived for a brush system, and our system can not be considered as a real brush.

An estimation of the average force F_{str}, of a single chain slightly stretched in a layer is possible. This force is connected to the modulus of the PS layer by the relationship:

$$F_{str} \approx \frac{E_{PS}}{\sigma} \qquad [5.9]$$

where σ is the number of chains per unit area. By combining eq. [5.8] and [5.9], F_{str} can be expressed as a function of the known parameters, if d is neglected.

$$F_{str} \approx \frac{G'(D - d_{P2VP})}{D\sigma} \qquad [5.10]$$

The thickness of the P2VP layer can be considered to be around 15 Å[17] and $\sigma \approx 0.8\times10^{16} m^{-2}$ [19]. Numerical application of equation [5.10] leads to $F_{str} \approx 3\times10^{-11}$ N. This value is in the range expected for a stretched chain in the linear regime of deformation.

5.5 CONCLUSIONS

Shear measurements between two adsorbed diblock copolymer monolayers in the mushroom regime have been presented, as a function of the frequency and the confinement. The storage modulus is independent of the frequency, while the loss modulus scales as $\omega^{-1/2}$. The storage modulus decreases with confinement and the loss modulus increases with confinement. The results are interpreted in terms of a quantitative model that describes the variation of the complex shear modulus as a function of the confinement level and frequency. The model was partially inadequate to describe the variation of the loss modulus with separation, possibly due to variation of the interpenetration layer on the separation.

REFERENCES

[1] Israelachvili, J.N. *Intermolecular and Surface Forces*: Academic Press; London, **1992**
[2] a) Chan, D.Y.C.; Horn, R.G. *J. Chem. Phys.* **1985**, 83, 5311
b) Georges, J.M.; Millot, S.; Loubet, J.L.; Tonck, A. *J. Chem. Phys.* **1993**, 98, 7345
[3] a) Horn, R.G.; Hirz, S. Hadziioannou, G.; Franck, C.W.; Catala, J.M. *J. Chem. Phys.* **1989**, 90, 6767
b) Pelletier, E.; Monfort, J.P.; Loubet, J.L.; Tonck, A.; Georges, J.M. *J. Polym. Sci. B* **1996**, 34, 93
[4] a) Israelachvili, J.N. J. *Colloid Interface Sci.* **1986**, 110, 263
b) Israelachvili, J.N.; Kott, S.J.; Fetters, L.J. *J. Polym. Sci. B* **1989**, 27, 489
[5] a) Monfort, J.P.; Hadziioannou, G. *J. Chem. Phys.* **1988**, 88, 7187
b) Pelletier, E.; Monfort, J.P.; Loubet, J.L.; Georger, J.M. *Macromolecules* **1995**, 8, 1990
[6] a) Peachley, J.; Alsten, J.V.; Granick, S. *Rev. Sci. Instrum.* **1991**, 62, 463
b) Granick, S.; Hu, W. *Langmuir* **1994**, 10, 3857
c) Peanasky, J.; Cai, L.L.; Granick, S.; *Langmuir* **1994**, 10, 3874
[7] Pelletier, E.; Belder, G.F.; Subbotin, A.; Hadziioannou, G. *J. Phys. II (France)* **1997**, 7, 271
[8] Cai, L.L. *"Nanorheoloy of polymer brushes"* Ph.D. thesis University of Illinois **1997**

[9] a) Klein, J. *Colloids and Surfaces A* **1994**, 86, 63
b) Klein, J.; Kumacheva, E.; Mahalu, D.; Perahia, D.; Fetters. L.J. *Nature* **1994**, 370, 634
[10] a) Alexander, S. *J. Phys. (Paris)* **1977**, 38, 983
b) de Gennes, P.G. *Adv. Colloid Interface Sci.* **1987**, 27, 789
[11] Milner, S.T.; Witten, T.A.; Cates, M.E. *Macromolecules* **1988**, 21, 1610
[12] Murat, M.; Grest, G.S. *Phys. Rev. Lett.* **1989**, 63, 1074
[13] Chakrabarti, A.; Nelson, P.; Toral, R. *J. Chem. Phys.* **1994**, 100, 748
[14] Rugar, D.; Msmin, H. J.; Guthner, P. *Appl. Phys. Lett.* **1989**, 55, 2588
[15] Semenov, A.N. *Langmuir* **1995**, 11, 3560
[16] Joanny J. F. *Langmuir* **1992**, 8, 989
[17] Field, J.B.; Toprakcioglu, C.; Dai, L.; Hadziioannou, G.; Smith, G.; Hamilton, W. *J. Phys. II (France)* **1992**, 2, 2221
[18] Ferry, J.D. *Viscoelastic Properties of Polymers*, **1980**, Wiley editions
[19] a) Pelletier, E.; Stamouli, A.; Belder, G.F.; Hadziioannou, G.; *Langmuir* **1997**, 13, 1884
b) sub chapter 3.II

SUMMARY

Polymer monolayers are important in various areas of technology. They play an important role for example in the stabilization of colloidal particles, (bio)compatibility, adhesion, friction and lubrication.

A specific class of polymers used to modify surfaces is the block copolymers. These copolymers consist of two or more blocks which are covalently bonded together, giving these copolymers their unique properties such as the possibility to phase separate in ordered microstructures, the formation of micelles and the formation of grafted monolayers.

The aim of this thesis was to get a better understanding of the normal and lateral interactions of adsorbed diblock copolymer monolayers. The goal was to couple these interaction with the microscopic structural properties of the polymer layers. Therefore, two instruments were used, the Atomic Force Microscope (AFM) in order to analyze the microscopic morphology, and the Surface Forces Apparatus (SFA) to measure the interacting forces (normal and lateral) between two polymer monolayers. Furthermore, the AFM was also used as a spectroscopic method by obtaining force-distance profiles. The contents of this thesis are summarized for each chapter below.

In **chapter 2** the principles of operation of the instruments used to investigate the subjects of this thesis are discussed. Specific AFM methods in order to visualise the topography of soft samples, such as contact mode in fluid and tapping mode are described in this chapter. The principle of operation of the "classical" SFA, where the distance between two surfaces is measured via an optical interfereometric technique while the force with a mechanical spring, is shortly described. Although the "classical" SFA has contributed tremendously in understanding the behaviour of confined thin polymer films there is still room for improvement of the SFA' s measurement concept. In this chapter the principle of operation of the new SFA with a force feedback system is presented. The most important advantages that the new system offers are: independent control of the force and the distance, reduction in thermal drifts and the possibility to use opaque substrates. Furthermore, measurements of the new system can be fully automated. This increases the reliability and reproducibility of the measurements and increases the speed in which the measurements can be performed. The first attractive and repulsive force-distance profiles obtained with the new SFA are shown in this chapter. It is shown that the principle of operation works, but that the new design needs further modifications, in order to compete with existing apparatuses, with respect to the sensitivity and the feedback system.

In **chapter 3** the microscopic structure of adsorbed P2VP/PS diblock copolymer monolayers are investigated my means of an AFM. Chapter 3 in divided into four sub chapters, which are summarized below.

In **sub chapter 3.I** the organization of P2VP/PS micelles on top of a P2VP/PS monolayer is described. The experiments were performed with a series of well-defined P2VP/PS diblock copolymers consisting of equal length PS-block and P2VP-block which varies in length. P2VP/PS monolayers are formed on a mica substrate by dipping the substrate in a toluene solution of the copolymer above the cmc. The samples were let to dry under ambient conditions in air. In the case of the diblock copolymer with the largest P2VP block spherical objects were observed on top of the adsorbed monolayer. It was argued that these objects are micelles already existing in the solution from which the samples were prepared. The influence of the insoluble P2VP-block on the structure of the top layer of the copolymer film is also studied. By decreasing the size of the P2VP-block the spherical objects on top of the adsorbed monolayer loose their spherical shape and worm-like structures appear. For the copolymer with the shortest P2VP-block a flatten layer with a hole structure is observed. The possible reasons for these morphological changes are discussed on the basic of differences in cmc, unimer amount, and unimer expulsion rates for the micellar solutions.

Similar transformations were observed upon stepwise dissolution of the polymer layer for a film formed with the largest diblock copolymer. It was observed that the micelles deposited on the adsorbed monolayer tend to decompose upon dissolution changing their shape from a spherical to an elliptical one. After several dissolution steps worm-like structures or lamella-like structures appeared. The structures observed upon dissolution are similar to the ones formed upon annealing of diblock copolymer films prepared by spin casting.

In **sub chapter 3.II** the conformations of asymmetric P2VP/PS polymer chains physically adsorbed on a substrate in poor-solvent conditions were investigated. The P2VP/PS monolayers were formed by immersing a mica substrate in a toluene solution of the diblock copolymer. Toluene is a selective solvent (good solvent for the PS-block and poor solvent for the P2VP-block). The P2VP-block adsorbs on the substrate and thus grafts the PS-block, which does not adsorb. The resulting polymer monolayers are imaged in water. Microphase separation of the polymer monolayer in ordered globular clusters (surface octopus "micelles") was observed. A comparison of the experimental data with the theory of Williams, which describes the fusion of grafted polymer chains due to the reduction of solvent quality, has allowed us to directly determine the surface coverage. The time-dependent mass coverages are in agreement with independent measurements reported in literature. In addition, the results have confirmed previously reported data on similar systems showing that a mushroom regime can be expected, in good solvent, rather than a brush one.

In **sub chapter 3.III** the adsorption behavior of P2VP/PS diblock copolymers from a toluene solution on various substrates is investigated. Different adsorption mechanisms are proposed, depending on the chemical nature of the substrate. Special attention is given to the adsorption of micelles on a surface with no chemical affinity for the PS-block of the copolymer. A possible mechanism for this case is presented in this chapter. The mechanism is based on the assumption that the PS corona can

rearrange/deform to allow direct contact between the P2VP blocks and the substrate. The adsorption time obtained experimentally satisfactorily agrees with a theoretical expression, which describes the deformation of the PS-blocks in the micelle corona.

The formation of a stable diblock copolymer monolayer (equilibrium structure) can be a very slow process. This is discussed in **sub chapter 3.IV**, where the morphology of the film is followed as a function of time. It is observed that in the case of the P2VP/PS block copolymer with the longest P2VP-block, the structure of the monolayer continuously changes when the film is stored in the P2VP/PS solution for a long period of time. This implies that the initial structure does not represent an equilibrium state. The evolution of the structure is discussed in terms of desorption/adsorption of the P2VP anchoring blocks on the substrate.

In **chapter 4** the elastic properties of P2VP/PS diblock copolymers in the mushroom regime are investigated in various solvent conditions. In order to study the elastic properties of the monolayers, AFM and SFA force-distance profiles in various solvents were obtained. Force-distance profiles obtained by AFM and SFA differ from each other. These differences are caused by the fact that in AFM the area of contact is much smaller than in the SFA. With the SFA the macroscopic properties of a polymer monolayer are measured whereas with the SFA the miscoscopic properties are measured.

The approaching force-distance profiles of a polymer monolayer obtained with the AFM, in good-solvent confirm recent theoretical predictions that a part of the polymer chains can escape or pushed away in the sideways, under the compression of a small object, such as the AFM tip. As a result "escape transitions" are observed in the force-distance profile. The AFM data obtained in good-solvent conditions can be explained qualitatively and partially quantitatively by theories that describe the compression of a polymer monolayer. For measurements performed at poor-solvent and near-theta-solvent conditions, AFM force-distance profiles were difficult to quantify. This was mainly caused by the physiadsorption of PS segments on the AFM tip, which could have resulted in the extraction of polymer chains from the polymer layer during retraction.

In **chapter 5** the shearing properties between two P2VP/PS monolayers in the so-called mushroom regime are described. The shearing properties are studied by means of a dynamic SFA ("nanorheometer"), where the polymer layers in the lateral direction are sheared with a piezoelectric transducer. Nanorheological measurements in order to determine the complex shear modulus were performed in the linear regime of deformation, as a function of the confinement level of the two monolayers and the frequency. The experimental data are compared with a semi-quantitative model, which describes the variations of the complex shear modulus as a function of the distance between the two monolayers and the frequency.

SAMENVATTING

Monolagen van polymeren vinden hun toepassing op verschillende technologische gebieden. Zij spelen een belangrijke rol op het gebied van bijvoorbeeld de stabilisatie van colloï den, (bio)compatibiliteit, hechting, wrijving en smering.

Een specifieke klasse van polymeren zijn de blokcopolymeren. Deze copolymeren bestaan uit twee of meer chemisch verschillende blokken die covalent aan elkaar gebonden zijn. Dit geeft deze copolymeren unieke eigenschappen zoals b.v. de mogelijkheid tot microfasescheiding in geordende nanostructuren, micelvorming en de vorming van "verankerde" copolymeermonolagen.

Het doel van dit proefschrift was om een beter begrip te krijgen van de normale en laterale interacties van geadsorbeerde diblokcopolymeermonolagen. Het uitgangspunt was om deze interacties te koppelen aan de microscopische structuurkenmerken van de polymeermonolagen. Hiervoor zijn twee meettechnieken gebruikt, namelijk de Atomic Force Microscope (AFM), om de microscopische oppervlaktestructuur van de polymeerlagen te analyseren, en het z.g. Surface Forces Apparatus (SFA), waarmee de interactiekrachten (zowel normaal- als afschuifkrachten) gemeten kunnen worden tussen twee polymeerlagen als functie van hun onderlinge afstand. Tevens zijn er met de AFM ook spectroscopische analyses uitgevoerd in de vorm van kracht–afstandmetingen. Hieronder zal de inhoud van dit proefschrift per hoofdstuk kort samengevat worden.

In **hoofdstuk 2** worden de principes van de meettechnieken die gebruikt zijn voor dit onderzoek nader toegelicht. Specifieke AFM meetmethoden voor het visualiseren van de oppervlaktestructuur van zachte materialen, zoals de "contact mode" in vloeistof en de "tapping mode", worden beschreven in dit hoofdstuk.

Het principe van de "klassieke" SFA, waarbij de afstand tussen de oppervlakken gemeten wordt via een (optische) interferometrische techniek en waarbij een mechanische veer wordt gebruikt als krachtsensor, wordt in het kort toegelicht in dit hoofdstuk. Ondanks het feit dat de "klassieke" SFA een grote bijdrage heeft geleverd aan het begrijpen van het gedrag van ruimtelijk begrensde dunne polymeerfilms is er nog steeds ruimte voor verbetering van het SFA meetconcept. In dit hoofdstuk wordt het principe van een nieuwe SFA met een "force feedback" systeem beschreven. De belangrijkste voordelen die het nieuwe systeem biedt zijn de onafhankelijke controle en meting van de kracht en de afstand tussen de polymeerlagen, de gereduceerde thermische drift en de mogelijkheid om niet-transparante substraten te gebruiken. Tevens kan de meting met het nieuwe ontwerp volledig geautomatiseerd plaatsvinden. Dit bevordert de betrouwbaarheid en reproduceerbaarheid van de metingen en verhoogt de snelheid waarmee de metingen kunnen worden uitgevoerd. De eerste attractieve en repulsieve kracht–afstandcurven verkregen met de nieuwe SFA worden getoond in dit hoofdstuk. Echter, om te kunnen concurreren met bestaande apparaten voor krachtmetingen moeten er nog wel enige aanpassingen met betrekking tot de gevoeligheid en het feedbacksysteem gedaan worden.

In **hoofdstuk 3** wordt de microscopische structuur van geadsorbeerde P2VP/PS diblokcopolymeerlagen onderzocht met behulp van een AFM. Hoofdstuk 3 is opgedeeld in vier deelhoofdstukken die hieronder in het kort worden samengevat.

In **deel 3.I** wordt de organisatie van P2VP/PS micellen op een P2VP/PS monolaag beschreven. De experimenten zijn uitgevoerd met een serie goed gedefinieerde P2VP/PS diblokcopolymeren met dezelfde PS-bloklengte en een P2VP blok dat in lengte varieert. De P2VP/PS monolagen zijn bereid door een micasubstraat te dippen in een tolueenoplossing met een concentratie van de diblokcopolymeren boven de cmc. Na het dippen zijn deze substraten gedroogd aan de lucht. In het geval van het blokcopolymeer met het langste P2VP blok werden monolagen waargenomen die gedeeltelijk bedekt waren met bolvormige objecten. Het is gebleken dat dit micellen uit de polymeeroplossing zijn die zich hebben afgezet op de monolaag tijdens drogen van het substraat aan de lucht. De invloed van de grootte van het onoplosbare P2VP-blok op de structuur van de toplaag van de copolymeerfilm is ook bestudeerd. Bij een afname in de lengte van het P2VP blok raken de sferische objecten die de geadsorbeerde monolaag bedekken hun vorm kwijt en komen daar worm-achtige structuren voor in de plaats. Het copolymeer met het kortste P2VP blok gaf een vlakke laag met een gatenstructuur te zien. De mogelijke oorzaken van deze morfologische verschillen worden besproken in termen van de verschillen in: cmc, de unimeerconcentratie en de unimeeruitdrijvingssnelheid voor de verschillende copolymeren in oplossing. Gelijksoortige morfologische transformaties zijn waargenomen tijdens het stapsgewijs oplossen van een monolaag van het copolymeer met het langste P2VP-blok. Het is gebleken dat de micellen op de geadsorbeerde monolaag tijdens het oplossen de neiging hadden om uiteen te vallen waarbij hun vorm veranderde van bolvormig naar elliptisch. Na meerdere wasstappen verschenen er worm-achtige of lamellaire structuren. De waargenomen structuren verkregen door het oplossen van de geadsorbeerde polymeerlaag lijken op die gevormd na het annealen van een gespincaste diblokcopolymeerfilm.

In **deel 3.II** wordt de conformatie bestudeerd van fysisch verankerde asymmetrische P2VP/PS polymeerketens in een slecht oplosmiddel. De P2VP/PS monolagen zijn bereid door een micasubstraat te dippen in een tolueenoplossing van de diblokcopolymeren. Tolueen is een selectief oplosmiddel d.w.z. een goed oplosmiddel voor het PS-blok van het copolymeer en een slecht oplosmiddel voor het P2VP blok. Het P2VP-blok adsorbeert om deze reden op het micaoppervlak en verankert daarmee het PS-blok, dat zelf niet adsorbeert. De verkregen monolagen zijn afgebeeld met een AFM in water, dat een slecht oplosmiddel is voor PS. Hierbij is microfasescheiding van de polymeerlaag in geordende globulaire clusters (“surface octopus "micelles"”) waargenomen. Een vergelijking van de experimentele meetgegevens met de theorie van Williams, die de samensmelting van geënte polymeerketens in micellen beschrijft, geeft ons de mogelijkheid om een schatting te maken van de bedekkingsgraad van het substraat. De geschatte tijdsafhankelijke bedekkingsgraden zijn in overeenstemming met die uit onafhankelijke metingen die gerapporteerd zijn in de literatuur.

In **deel 3.III** wordt het adsorptiegedrag van P2VP/PS diblokcopolymeren vanuit een tolueenoplossing op verschillende substraten beschreven. Enkele adsorptiemechanismen worden hier gepresenteerd, afhankelijk van het chemische karakter van het betreffende substraat. Speciale aandacht wordt besteed aan de adsorptie van micellen op een substraat dat geen chemische affiniteit heeft voor het PS-blok van het copolymeer. Een mogelijk mechanisme voor dit specifieke geval wordt gepresenteerd in dit hoofdstuk. Het mechanisme is gebaseerd op de aanname dat de PS-corona van de micellen zich kan herschikken/deformeren op het substraat waardoor direct contact mogelijk is tussen de P2VP blokken in de micelkern en het substraat. De experimenteel verkregen adsorptietijden komen goed overeen met die verkregen uit een theoretische expressie die de deformatie van de PS-staarten in de corona beschrijft.

De vorming van een stabiele diblokcopolymeermonolaag (evenwichtstoestand) kan een erg langzaam proces zijn. Dit wordt besproken in **deel 3.IV**, waar de morfologie van een gevormde polymeermonolaag wordt gevolgd in de tijd. Het is gebleken dat in het geval van het P2VP/PS diblokcopolymeer met het langste P2VP blok, de structuur van de monolaag voortdurend verandert als deze wordt bewaard in de P2VP/PS oplossing voor een langere periode. Dit impliceert dat de initieel gevormde monolaag niet een evenwichtstoestand vertegenwoordigt. De evolutie van de structuur van de monolaag wordt besproken in termen van desorptie/adsorptie van de P2VP-“anker”-blokken op het substraat.

In **hoofdstuk 4** wordt het elastisch gedrag beschreven van een geadsorbeerde P2VP/PS diblokcopolymeermonolaag in het z.g. paddestoelregime onder verschillende oplosmiddelcondities. Om het elastisch gedrag van de monolagen te bepalen zijn er met zowel de AFM als de SFA kracht–afstandprofielen opgenomen in verschillende oplosmiddelen. Het is gebleken dat de kracht–afstandprofielen verkregen met de AFM en SFA van elkaar verschillen. Deze verschillen worden veroorzaakt door het feit dat het contactoppervlak (“area of confinement”) bij AFM vele malen kleiner is dan in het geval van de SFA. Met een SFA worden de macroscopische eigenschappen van een dunne polymeerlaag gemeten, terwijl de AFM de microscopische eigenschappen meet. De heenwaartse kracht–afstandprofielen verkregen met de AFM tijdens metingen met de monolaag in een goed oplosmiddel bevestigen de recente theoretische benaderingen dat polymeerketens zijdelings kunnen worden weggedrukt/ontsnappen tijdens compressie van een gedeelte van de polymeerlaag door een klein object zoals een AFM tip. Dit resulteert in een zogenaamde “escape transition” (ontsnappingsovergang) in het kracht–afstandprofiel. De AFM data verkregen in een goed oplosmiddel kunnen zowel kwalitatief als semi-kwantitatief verklaard worden met enkele theorieën die de compressie van polymeermonolagen beschrijven. Daarentegen waren de kracht–afstandprofielen verkregen in een slecht oplosmiddel en onder bijna-theta-condities, moeilijk te kwantificeren. Dit wordt voornamelijk veroorzaakt door de fysische adsorptie van PS-segmenten aan de AFM tip, wat kan resulteren in de extractie van polymeerketens uit de monolaag tijdens de terugwaartse beweging van de AFM tip.

In **hoofdstuk 5** wordt het afschuifgedrag tussen twee P2VP/PS diblokcopolymeermonolagen in het z.g. paddestoelregime beschreven. Het afschuifgedrag is bestudeerd met behulp van een dynamische SFA ("nanorheometer") waarbij de polymeerlagen in laterale richting ten opzichte van elkaar bewogen kunnen worden d.m.v. een piëzo-elektrische translatie-eenheid. De nanoreologische experimenten om de complexe afschuifmodulus te bepalen zijn uitgevoerd als functie van de ruimtelijke begrenzing van de twee polymeerlagen (afstand tussen de micasubstraten) en de afschuiffrequentie, in het lineaire (deformatie)regime. De experimentele data zijn vergeleken met een semi-kwantitatief model dat de variatie van de complexe afschuifmodulus als functie van de afstand tussen de monolagen en de afschuiffrequentie beschrijft.